高能量粒子实验物理

Part-I: Basic experiments of energetic-particles and Alfven waves in fusion plasmas

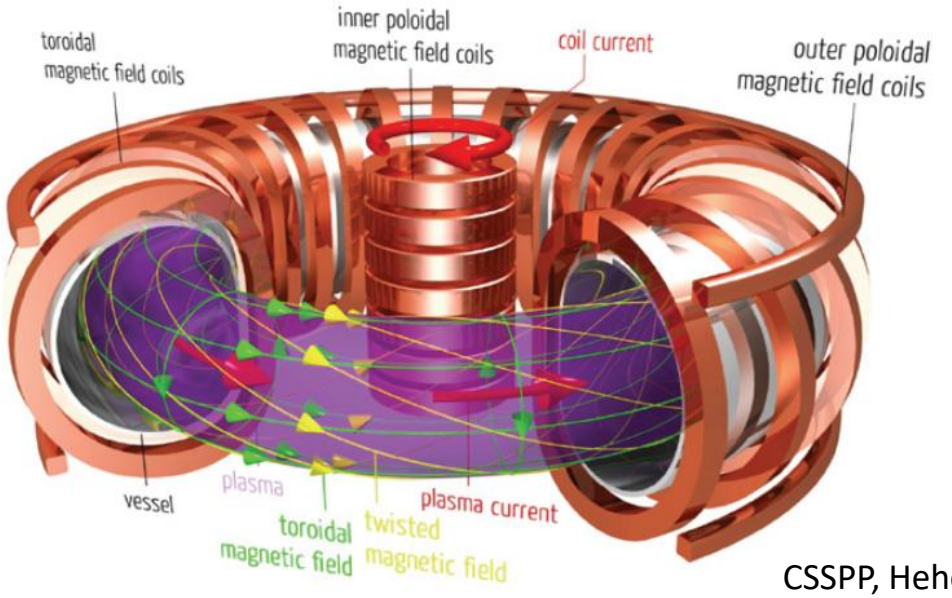

Wei Chen 陳偉

Southwestern Institute of Physics

CSSPP, Hehei, July 10, 2025

Alfven Wave in Space and Lab Plasmas

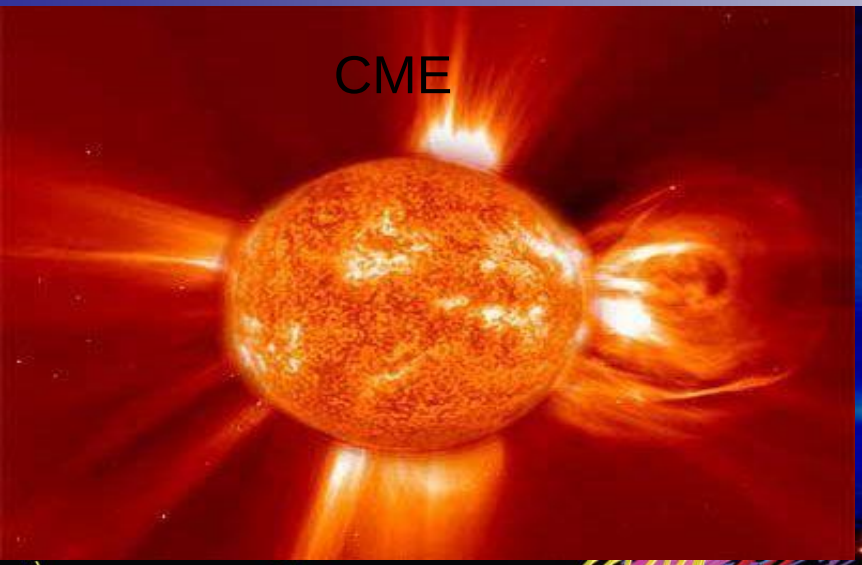

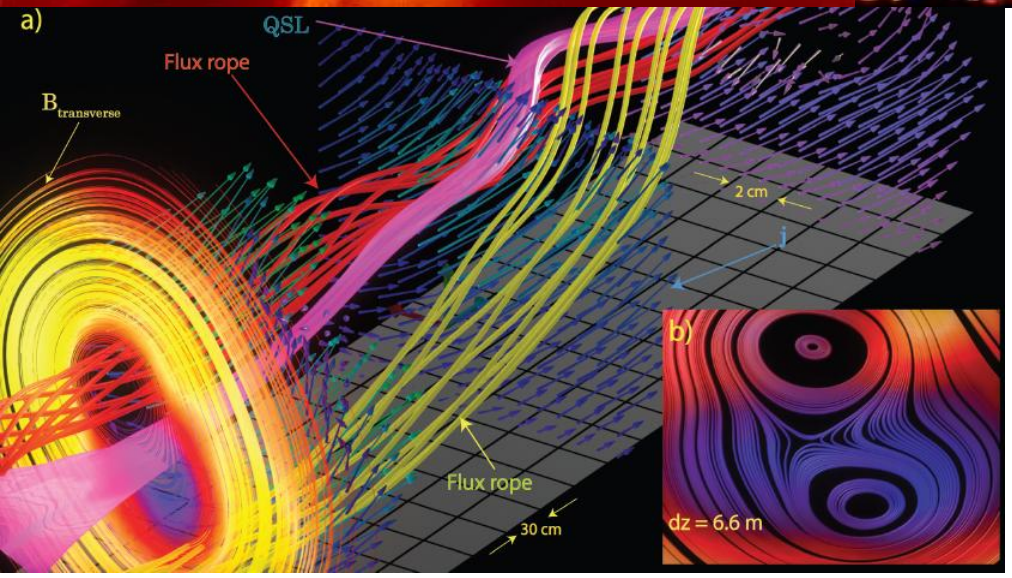

LAPD at UCLA.

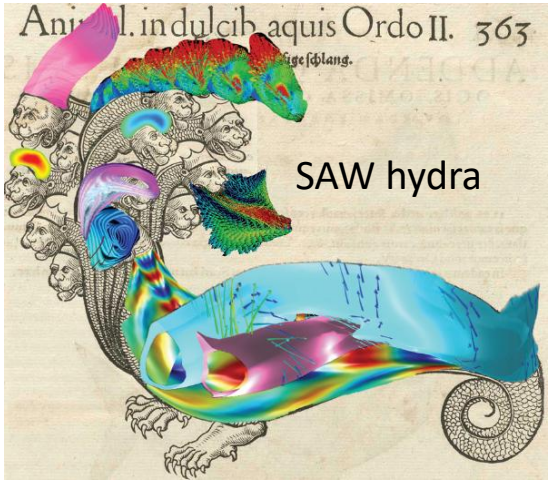

Many faces of SAWs, W. Gekelman et.al PHYSICS OF PLASMAS 18, 055501 (2011)

Outline

- MHD waves and EP sources
- EP motion and confinement
- Roles of EPs in fusion plasmas
- SAW continuum spectrum and gaps
- Discrete Alfven eigenmodes and energetic particle modes
- Destabilization and damping of SAW
- Various Alfvenic modes and observation
- Brief introduction of EP nonlinear physics
- Diagnostic methods of EP phenomena
- EP losses by various MHD activities
- Summary

MHD Waves in Plasmas

- ***CAW and SMW***: the returning force is the magnetic and the kinetic pressure
- ***SAW***: the returning force is the tension of magnetic field lines

SAW: $\omega^2 - k_{\parallel}^2 v_A^2 = 0$ $\quad \vec{v}_{gA} = v_A \dfrac{\vec{B}_0}{B_0}$

CAW: $\omega^2 = (k_{\parallel}^2 + k_{\perp}^2) v_A^2 = k^2 v_A^2$ $\quad \vec{v}_{gF} = v_A \dfrac{\vec{k}}{k}$

SMW: $\omega^2 \approx k_{\parallel}^2 v_S^2$ $\quad \vec{v}_{gS} = v_S \dfrac{\vec{B}_0}{B_0}$

Predicted by H. Alfven; Nature 1942

Nobel prize, 1970

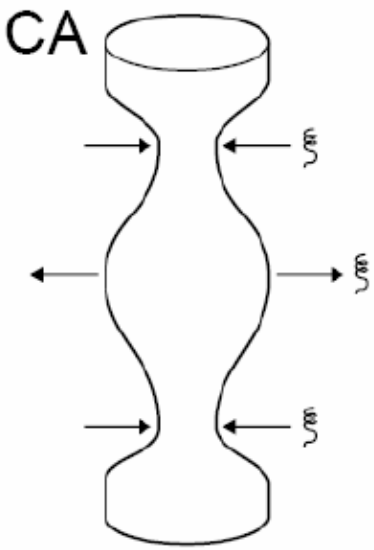

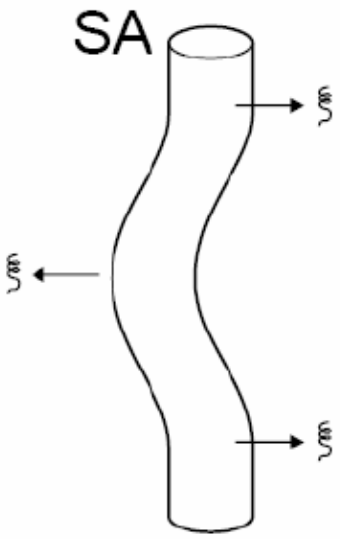

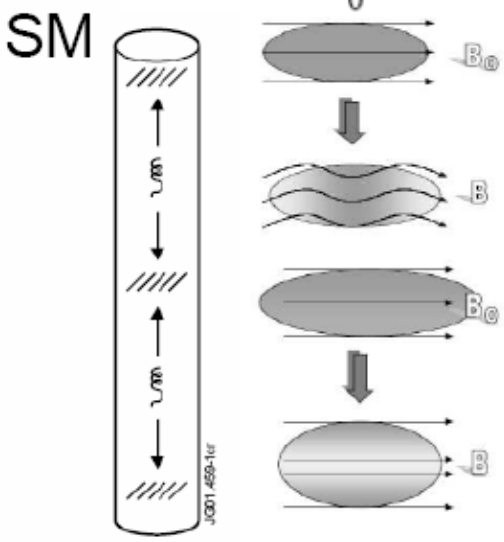

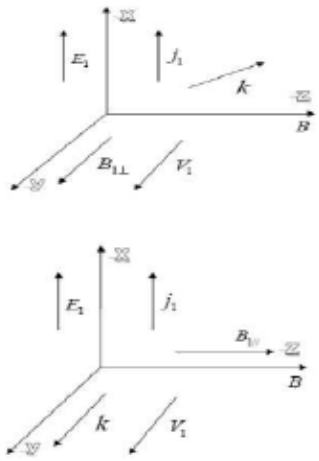

EP sources

Ohmic heating: $\eta \propto T^{-3/2}$ => limited to T~1keV, additional heating needed

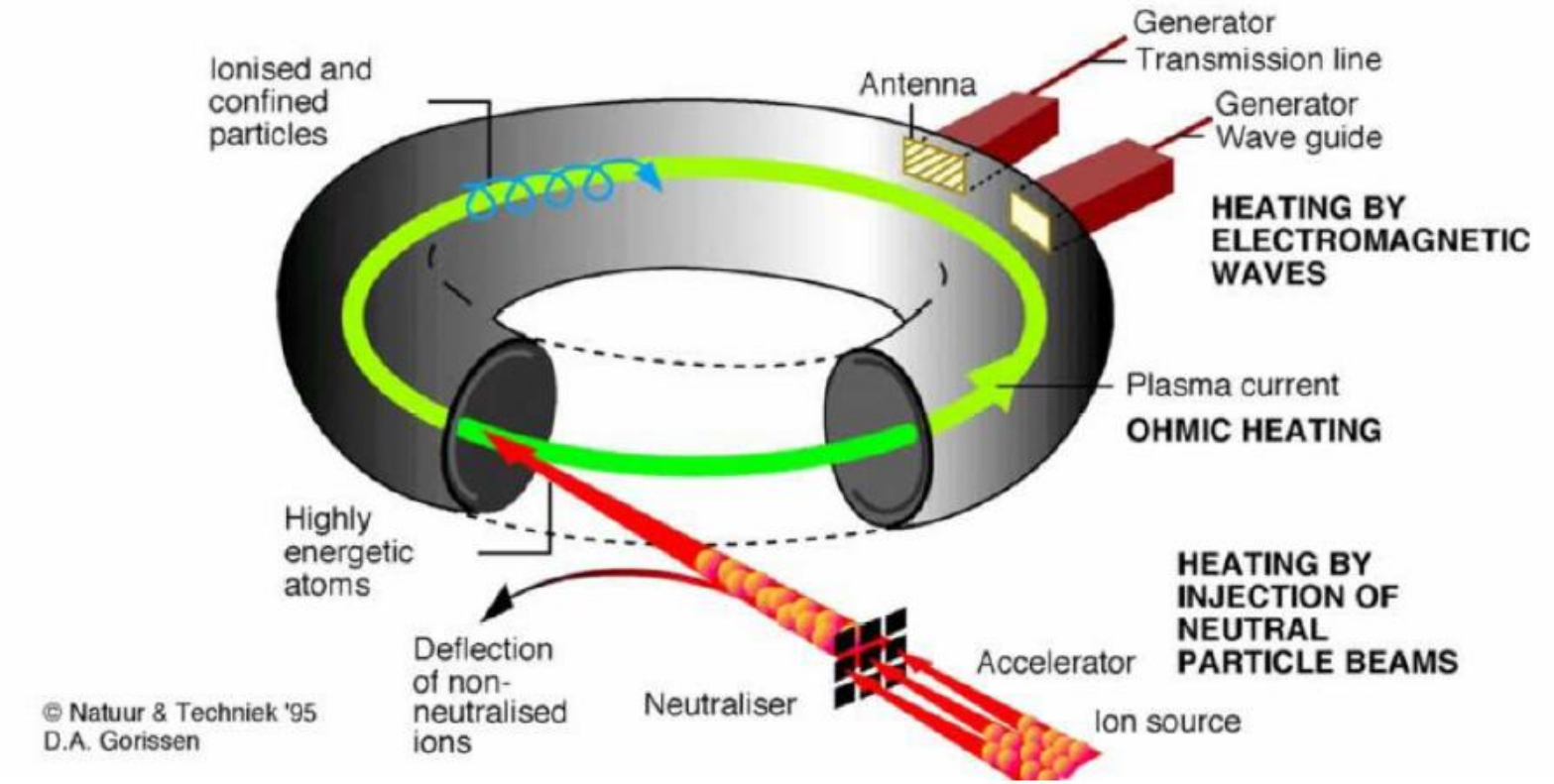

In current fusion devices, EPs are usually introduced by NBI heating or by RF heating. Runaway electrons can be generated during disruptions or sawtooth crashes. E_{NBI}~100kev, E_{RF} ~ 1Mev, $E_{runaway}$ ~10Mev

Alpha particles in burning plasmas

- New physics element in burning plasmas:
  - Plasma is self-heated by fusion alpha particles

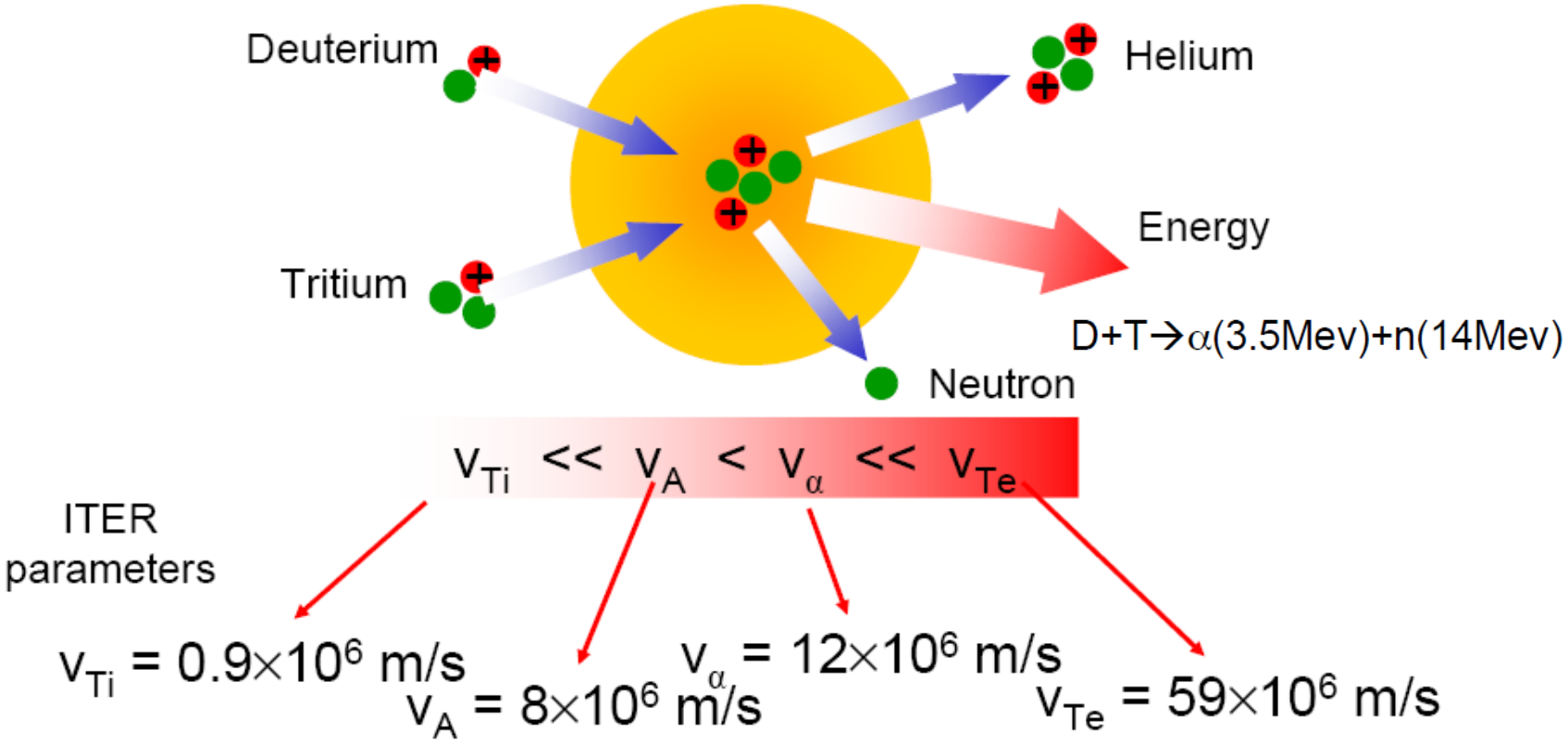

In a fusion reactor, energetic alpha particles are produced by fusion reaction. EPs heat plasmas via Coulomb collisions (mainly heat electrons) and slow down to thermal energy.

EP motions

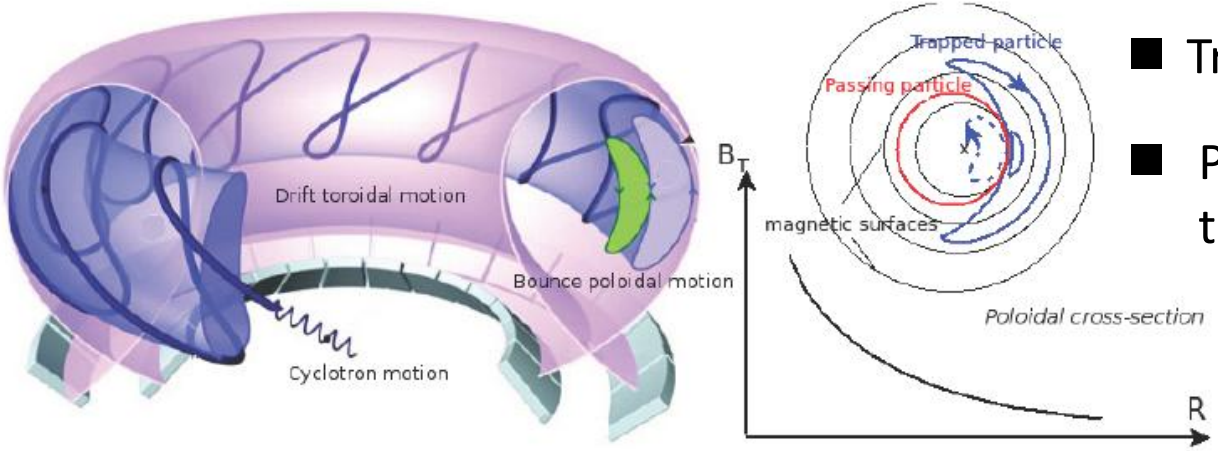

- Trapped & passing particles
- Precession, bounce and transit motions

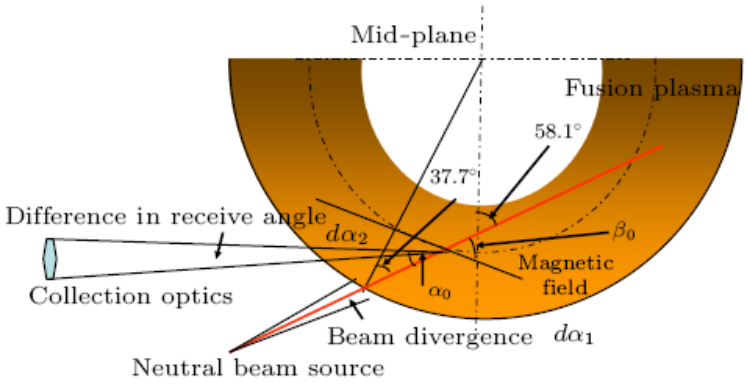

Schematic diagram of NBI system on HL-2A

Neutral beam:

Four positive-ion-sources tangentially co-injected R_{tan}=1.35 m. E~45 keV, P_{nbi}~1.0 MW.

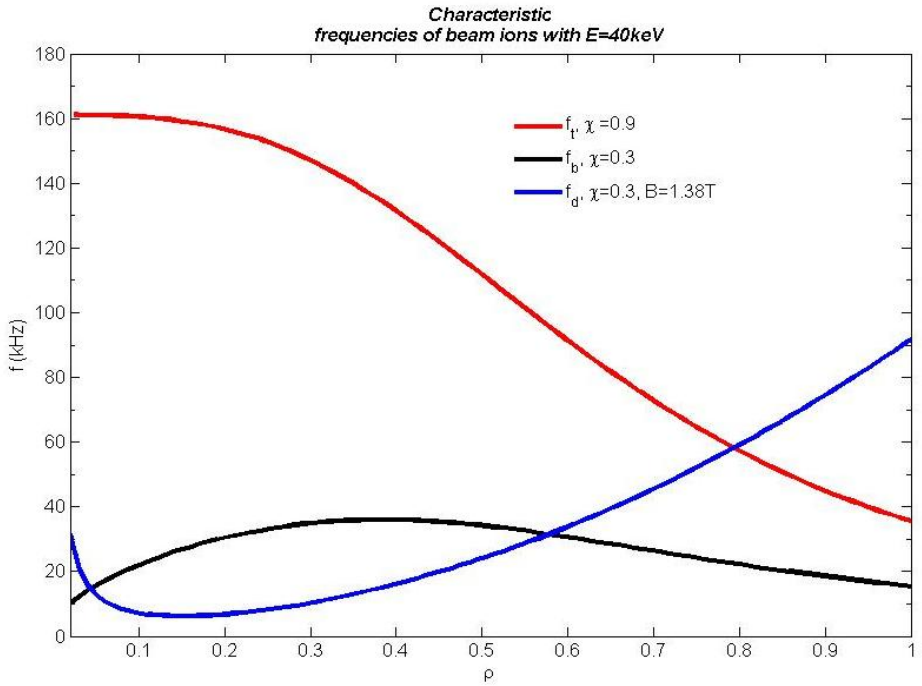

EP confinement

- Constants of motion: energy, magnetic moment and toroidal angular momentum.

$$P_\phi = e\psi + mv_\phi R$$

- For an axisymmetric torus, particles are confined as long as orbit width is not too large. (conservation of P_phi.)

- Toroidal field ripple (due to discrete coils) or other external 3D perturbations can induce stochastic diffusion.

- Symmetry-breaking MHD modes (sawtooth, NTM etc) can also cause EP anomalous transport.

Roles of EPs in fusion plasmas

- Heat plasmas via Coulomb collision
- Influence MHD stability (beta limit, sawtooth, NTM, RWM, ELM, disruption)
- Destabilize Alfven waves via wave-particle resonances (AEs and EPM)
- Affect bulk plasma confinement, degrade plasma heating, and damage reactor wall due to EP redistribution/losses
- Affect wave heating and current drive (equilibrium and control)
- Affect edge stability and confinement
- ……

SAW continuum spectrum

- Shear Alfven wave dispersion relation

$$\omega^2 - k_{\|}^2 v_A^2 = 0$$

- Continuum spectrum

$$\omega^2(r) = \frac{v_A^2}{R_0^2}\left(n - \frac{m}{q(r)}\right)^2$$

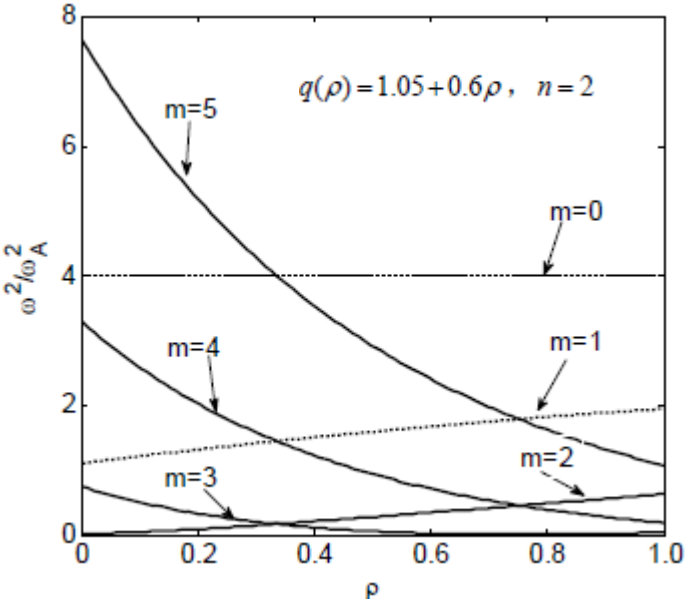

Cylinder geometry, no coupling

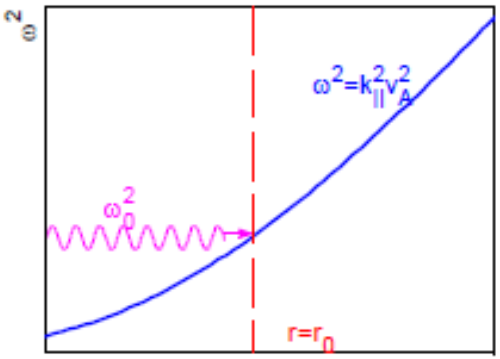

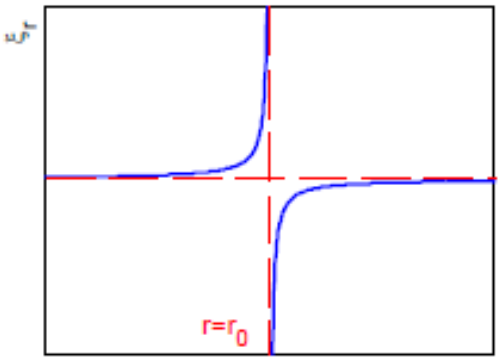

$$\delta\hat{\phi}_{m,n}(r,t) \simeq \frac{1}{t} e^{-i\omega_A(r)t}$$

Driven perturbation at ω is resonantly absorbed at

$\omega = \omega_A(r)$ ⟶ Phase mixing/ continuum damping

Gap and TAE

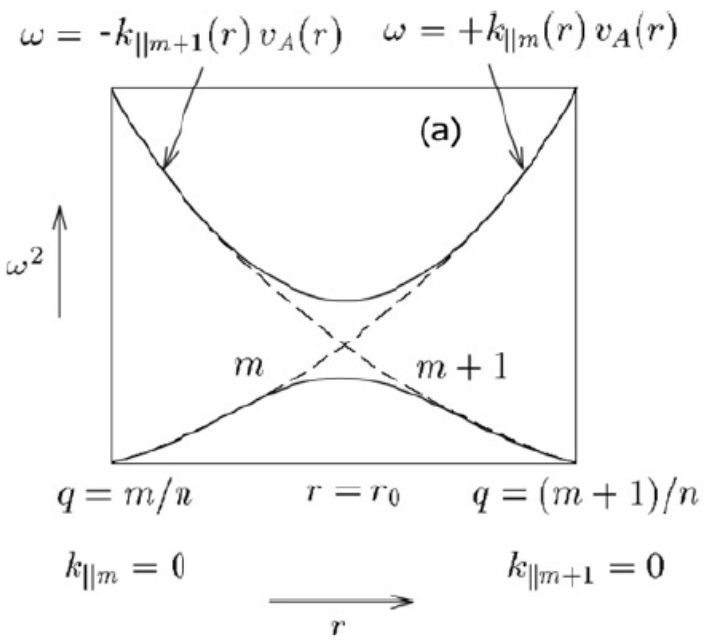

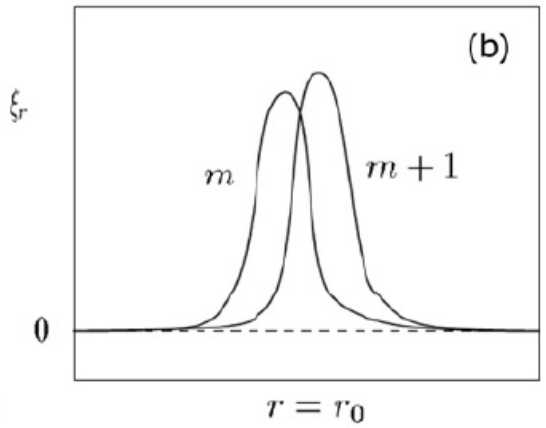

First observation of TAE on TFTR

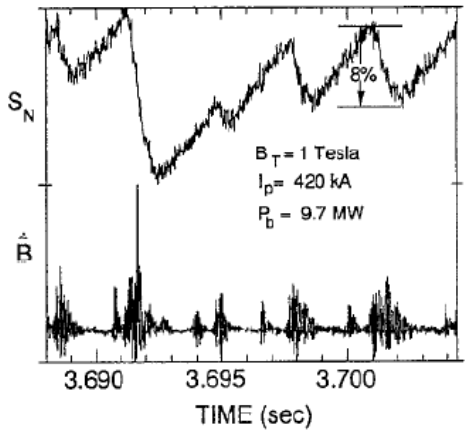

Wong, *et al.* 1991, PRL, **66**, 1874

$$\begin{vmatrix} \dfrac{\omega^2}{\omega_A^2} - k_{\|m}^2 R_0^2 & -\dfrac{r_0}{R_0}\left[\dfrac{n^2}{4(m+1/2)^2} + \dfrac{\omega^2}{\omega_A^2}\right] \\ -\dfrac{r_0}{R_0}\left[\dfrac{n^2}{4(m+1/2)^2} + \dfrac{\omega^2}{\omega_A^2}\right] & \dfrac{\omega^2}{\omega_A^2} - k_{\|m+1}^2 R_0^2 \end{vmatrix} = 0$$

TAE mode frequencies are located inside the toroidcity-induced Alfven gaps; TAE modes peak at the gaps with two dominating poloidal harmonics.

$$k_{\|m}(r_0) = -k_{\|m+1}(r_0) \qquad q(r_0) = \frac{m+1/2}{n}$$

Gap width: $\Delta_{gap} = \dfrac{4\dfrac{r_0}{R_0}}{\dfrac{r_0^2}{R_0^2}} \dfrac{n^2}{(2m+1)^2}$

C.Z. Cheng, L. Chen and M.S. Chance 1985, *Ann. Phys. (N.Y.)* **161**, 21

Fishbone instability (a example of EPM)

Mode structure is of (m,n)=(1,1) internal kink;
Mode is destabilized by energetic trapped particles;
Mode frequency is comparable to trapped particles' precessional frequency

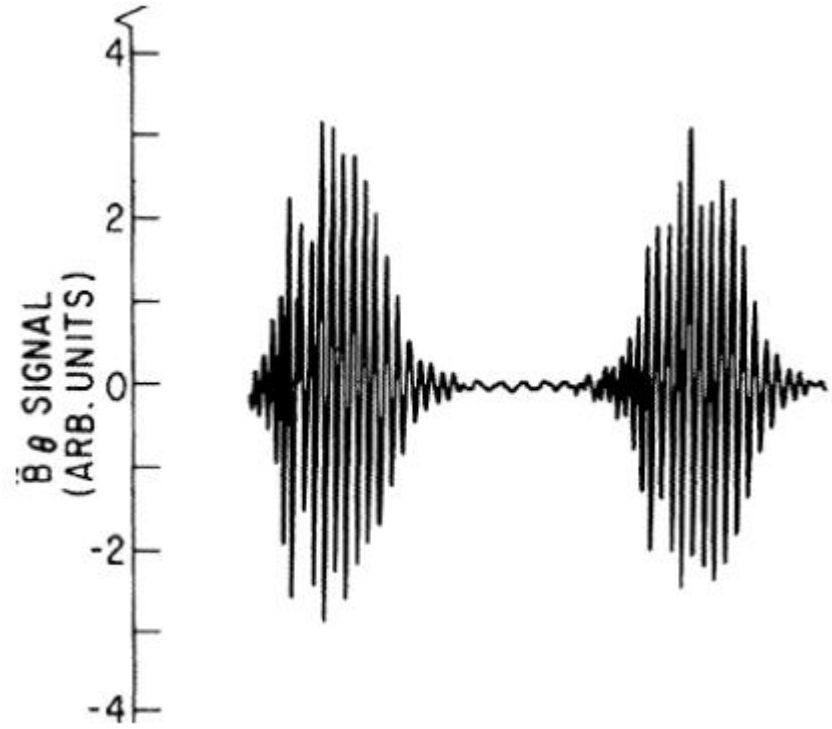

K. McGuire, R. Goldston, M. Bell, *et al.* 1983, *Phys. Rev. Lett.* **50**, 891
L. Chen, R.B. White and M.N. Rosenbluth 1984, *Phys. Rev. Lett.* **52**, 1122

EP instability classification

GFLDR: $-i\Lambda(\omega)+\delta\hat{W}_f+\delta\hat{W}_k=0$

Prof. L. Chen

Frequency gap of SAW given by the condition: $\mathrm{Re}\,\Lambda^2<0$

Discrete Alfvén eigenmode (AE): $\mathrm{Re}\,\Lambda^2<0$

Energetic particle continuum mode (EPM): $\mathrm{Re}\,\Lambda^2>0$

Combined effect of $\delta\hat{W}_f$ and $\mathrm{Re}\,\delta\hat{W}_k$ determines the existence conditions of AE by removing the degeneracy with the SAW accumulation point.

Various effects on $\delta\hat{W}_f+\mathrm{Re}\,\delta\hat{W}_k$ can lead to AE localization in various gaps, i.e. to different species of AE.

Dr. F. Zonca

E.g. for fishbone: $\Lambda=[\omega(\omega-\omega^*_{pi})]^{1/2}$

Fishbone, TAE, RSAE, BAE, EPM

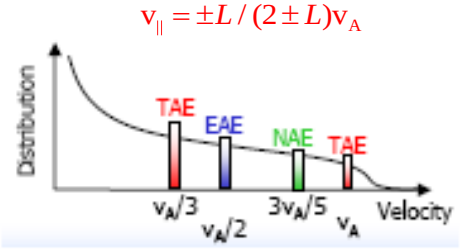

Discrete Alfven eigenmodes and energetic particle modes

Coupling of m and m+k modes breaks degeneracy of Alfven continuum

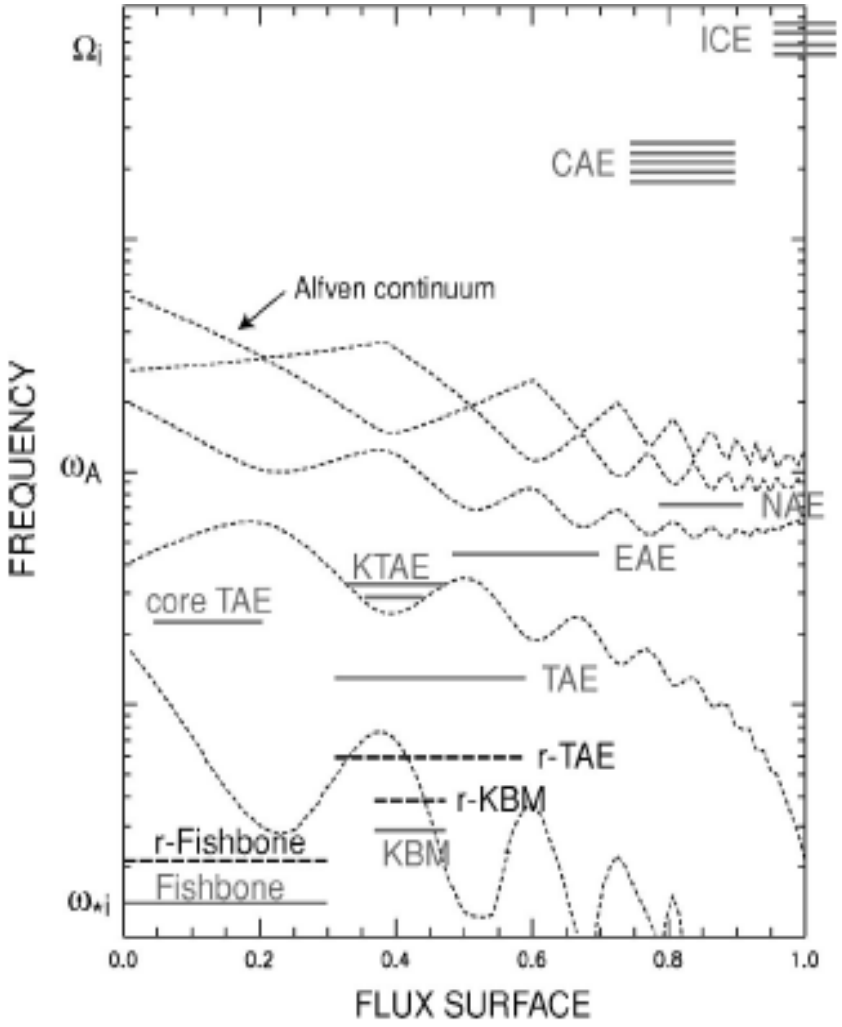

$$|n - \frac{m}{q}| = |n - \frac{m+k}{q}|$$ q=(2m+k)/2n

k=1: toroidicity; k=2: elongation; k=3: triangularity;

- **Discrete Alfven Eigenmodes (AE):**

Mode frequencies located outside Alfven continuum (e.g., inside gaps);
Modes exist in the MHD limit;
EP effects are often perturbative.

- **Energetic Particle Modes (EPM):**

Mode frequencies located inside Alfven continuum and determined by EP dynamics;
EP effects are non-perturbative; Requires sufficient EP drive to overcome continuum damping.

Destabilization of SAW

EP drive

$$\frac{\gamma}{\omega} \propto \beta_h\left[-\frac{n}{\omega}\frac{E_h df}{f dP_\phi} + \frac{E_h df}{f dE}\right]$$

Spatial gradient drive

Landau damping
Due to velocity space gradient

$$\frac{dP_\phi}{dt} = -\frac{n}{\omega}\frac{dE}{dt}$$

$$P_\zeta = mRv_\zeta - Ze\Psi$$

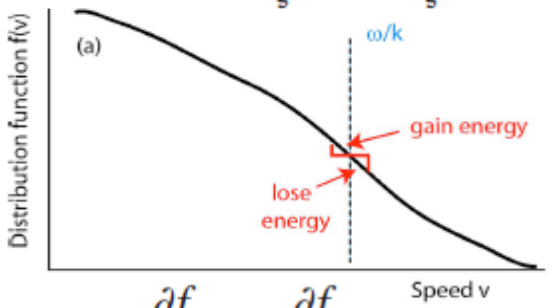

$$\gamma \propto \omega\frac{\partial f}{\partial W} + n\frac{\partial f}{\partial P_\zeta}$$

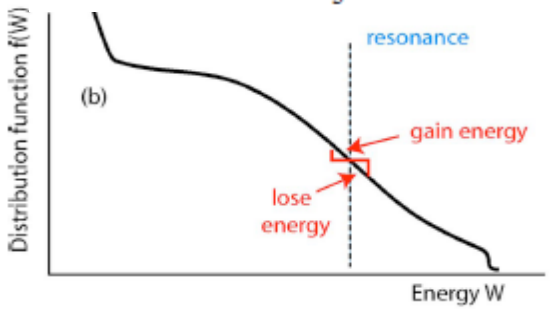

Particles lose energy going outward
Particles gain energy going inward
particles lose energy to waves due to density gradient (free energy!)

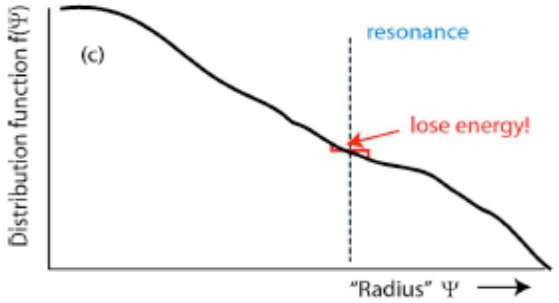

Heidbrink, PoP ***15****, 055501 2008* ← Toroidal Angular Momentum P_ζ

Damping of SAW

- Ion Landau damping
- Electron Landau damping
- Continuum damping
- Collisional damping
- Radiative damping due to thermal ion gyroradius

---The damping comes from coupling to kinetic Alfven waves due to thermal ion gyroradius effects.

G.Y.Fu and J.W. Van Dam, Phys. Fluids B1, 1949 (1989)
R. Betti et al, Phys. Fluids B4, 1465 (1992).
F. Zonca and L. Chen 1992, *Phys. Rev. Lett.* **68**, 592
M.N. Rosenbluth, H.L. Berk, J.W. Van Dam and D.M. Lindberg 1992, *Phys. Rev. Lett.* **68**, 596
R.R. Mett and S.M. Mahajan 1992, *Phys. Fluids B* **4**, 2885

Various Alfvenic modes

Cylindrical limit: Global Alfven Eigenmode (GAE)

Toroidicity: TAE, m&m+1

Elongation: EAE, m&m+2

Triangularity: NAE, m&m+3

q_min: RSAE

Compression: BAE

FLR effects: Kinetic AEs

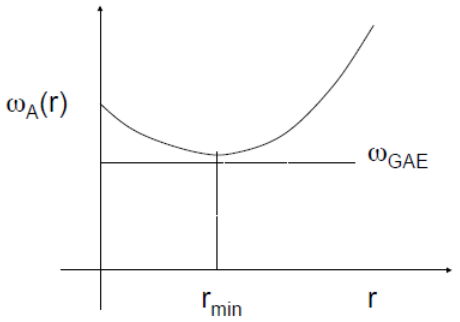

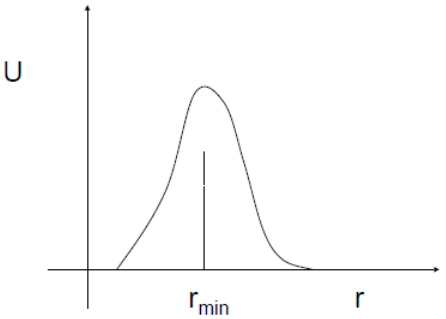

GAE can exist below shear Alfven continuum due to magnetic shear

$$\frac{d}{dt}\omega_{RSAE}(t) \approx m\frac{v_A}{R}\frac{d}{dt}q_{\min}(t)$$

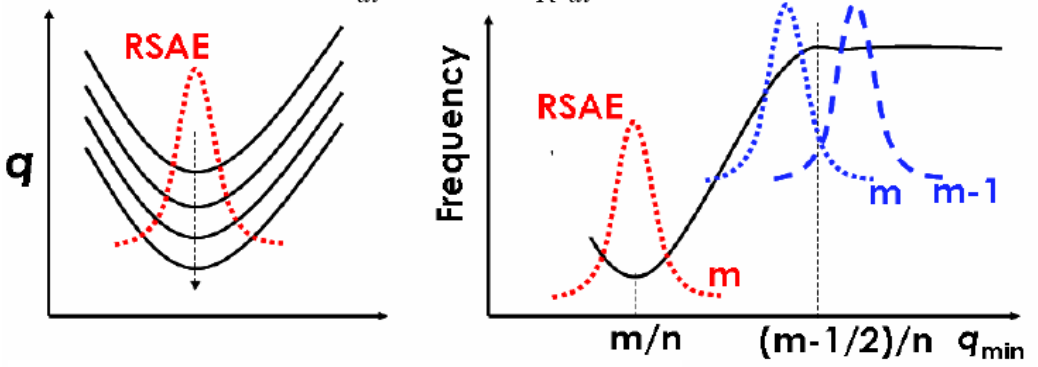

RSAE can exist above maximum or below minimum of Alfven continuum at q=q_min

$$\omega^2 = \omega_0^2 \equiv \frac{V_A^2}{R^2}\left(n - \frac{m}{q_{\min}}\right)^2 + \omega_G^2 + \omega_{PG}^2 + \omega_F^2$$

$$\omega_G^2 \equiv \frac{2}{m_i R^2}\left(T_e + \frac{7}{4}T_i\right)$$

$$\omega_{PG}^2 \equiv -\frac{2}{m_i R^2} r\frac{d}{dr}(T_e + T_i)$$

$$\omega_F^2 \equiv -\frac{\omega}{m}\left|\frac{eB}{m_i c}\right|\frac{r}{n_e}\frac{d}{dr}\langle n_F \rangle$$

Various Alfvenic modes

Frequencies of AEs lie in the Alfvén-continuum gap induced by poloidal mode coupling due to toroidicity, ellipticity and other effects.

TAE/EAE/NAE

$$\omega_{TAE} = v_A / 2qR, \omega_{EAE} \simeq 2\omega_{TAE}, \omega_{NAE} \simeq 3\omega_{TAE}$$

Alfvén velocity $v_A = B/(4\pi n_i m_i)^{1/2}, q = (2m+k)/2n$

Beta induced Alfvén eigenmode (BAE):

$$\omega_{BAE} = (\frac{7}{4} + \frac{T_e}{T_i})^{1/2} q\omega_{ti} = \frac{B(\frac{7}{4}\beta_i + \beta_e)^{1/2}}{(\mu_0 n_e m_i)^{1/2} R} \propto v_A$$

Ion transit frequency $\omega_{ti} = (2T_i / m_i)^{1/2} / qR$

Reversed-shear Alfvén eigenmode (RSAE):

$$f_{HRAE} \sim (n - m/q_{\min}) v_A / 2\pi R$$

$$f_{LRAE} \sim [(m+1)/q_{\min} - n] v_A / 2\pi R$$

$$m/n < q_{\min} < (m+1/2)/n + c, c \sim r_{\min}/nR$$

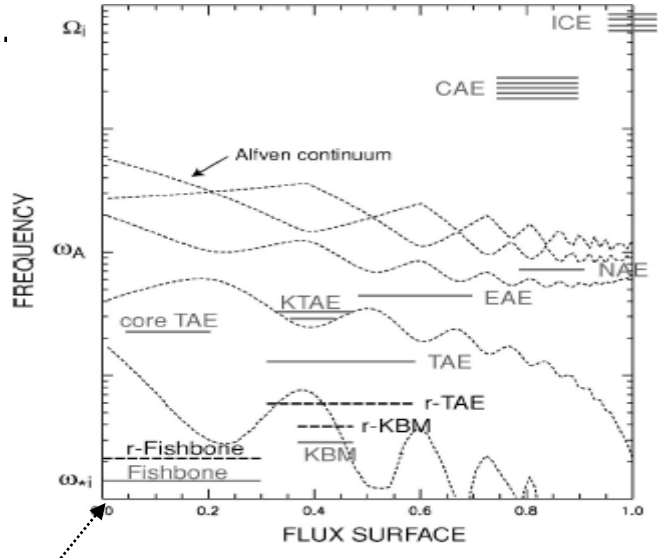

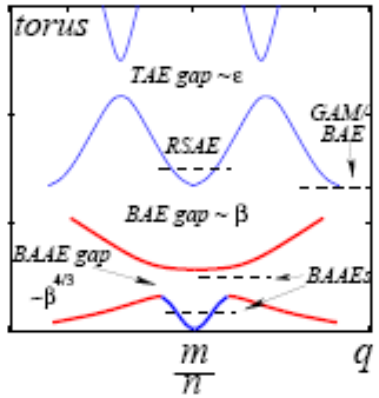

Energetic particle instability Zoo

Heidbrink W W 2002 PoP

Corelenkov N N 2008 IAEA

Observation of various Alfvenic modes

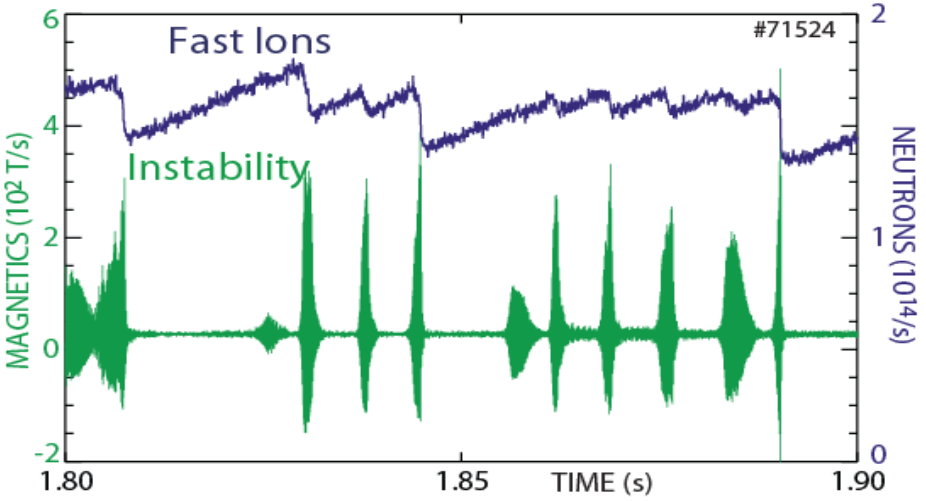

Ion fishbone on DIII-D

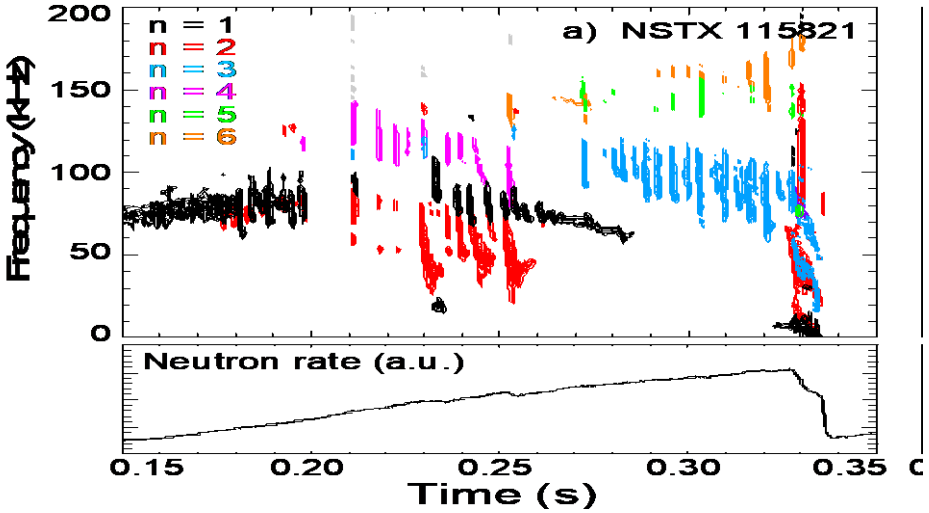

EPM on NSTX

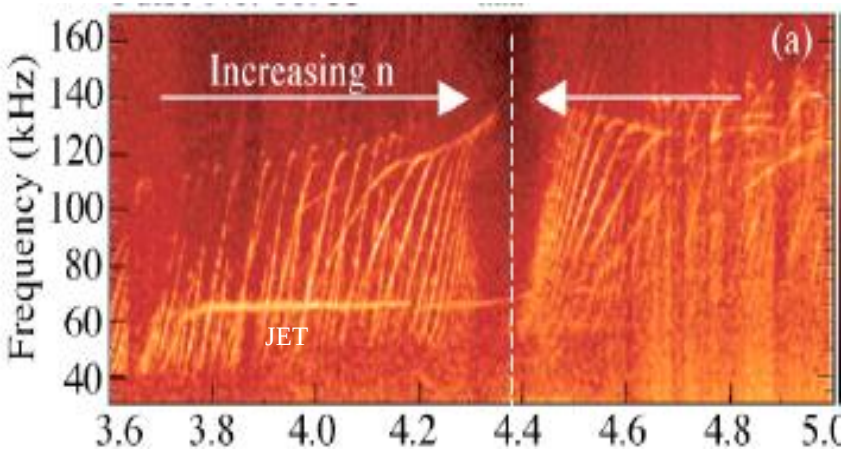

TAE and AC on JET

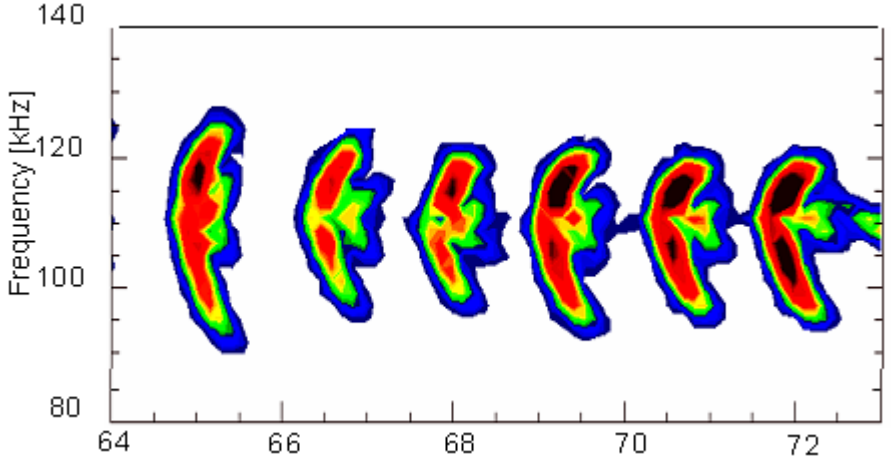

Pitch-fork phenomena on MAST

Observation of various Alfvenic modes

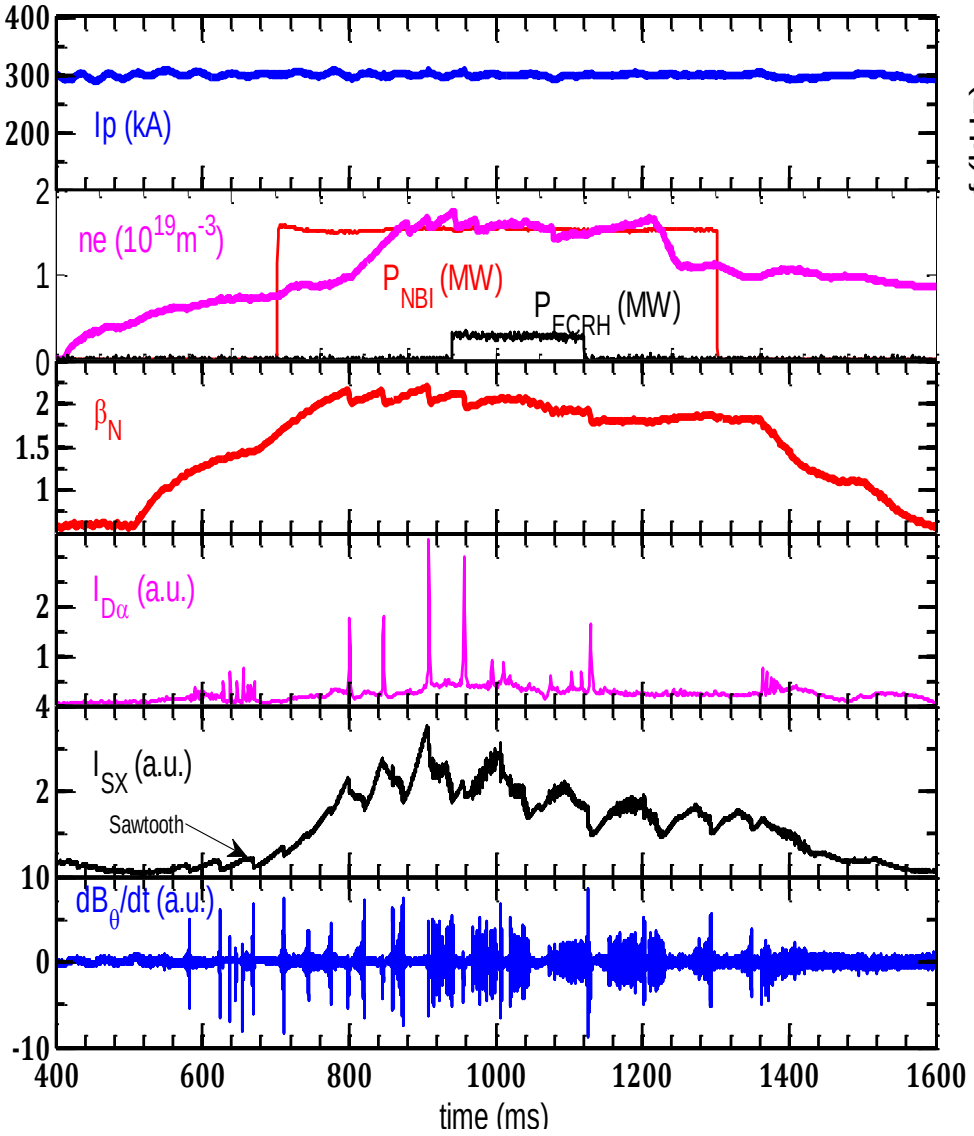

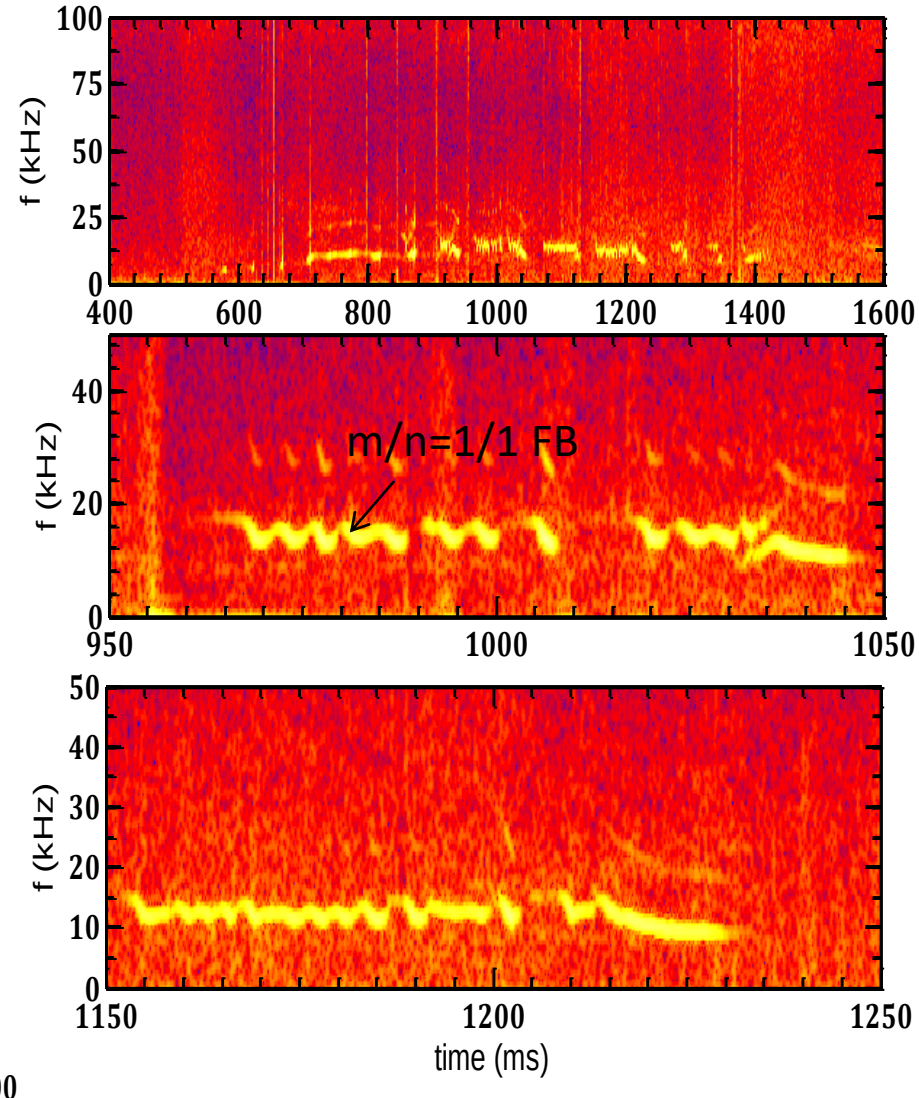

Observation of various Alfvenic modes

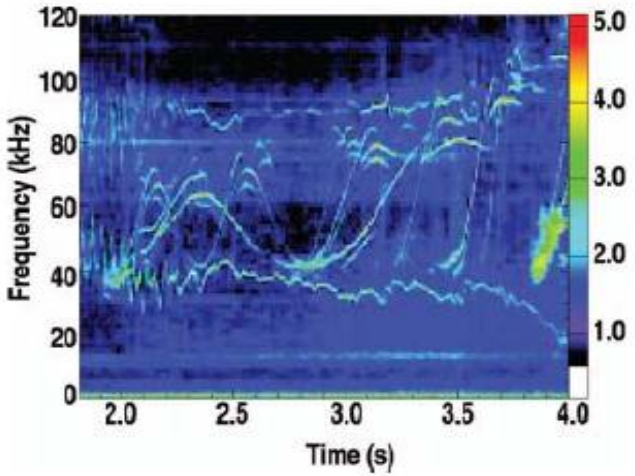

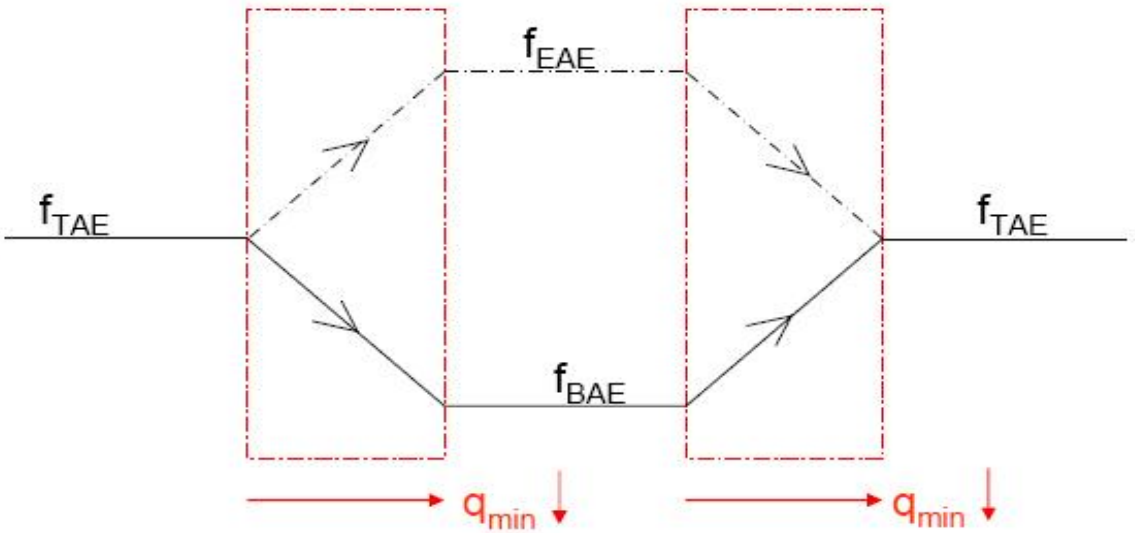

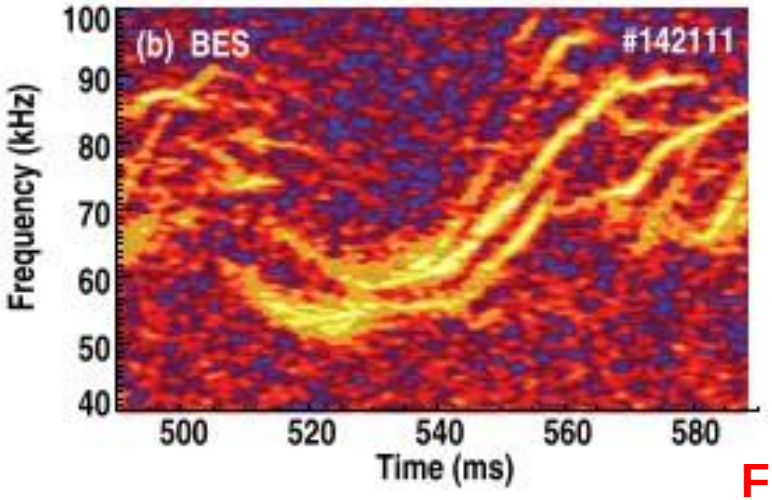

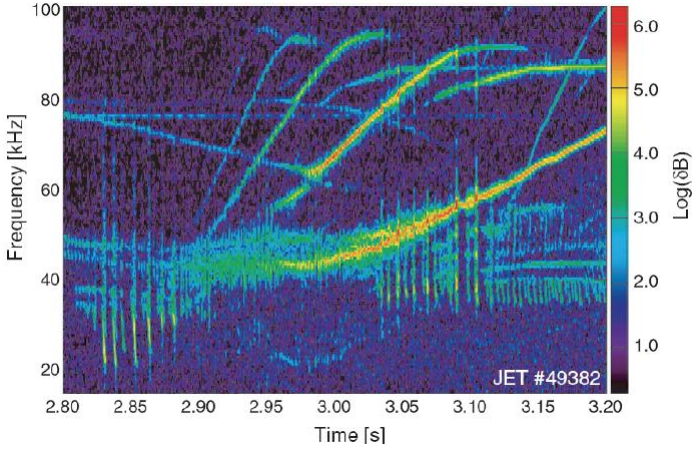

Frequency sweeping pattern: Sinusoidal

Observation of various Alfvenic modes

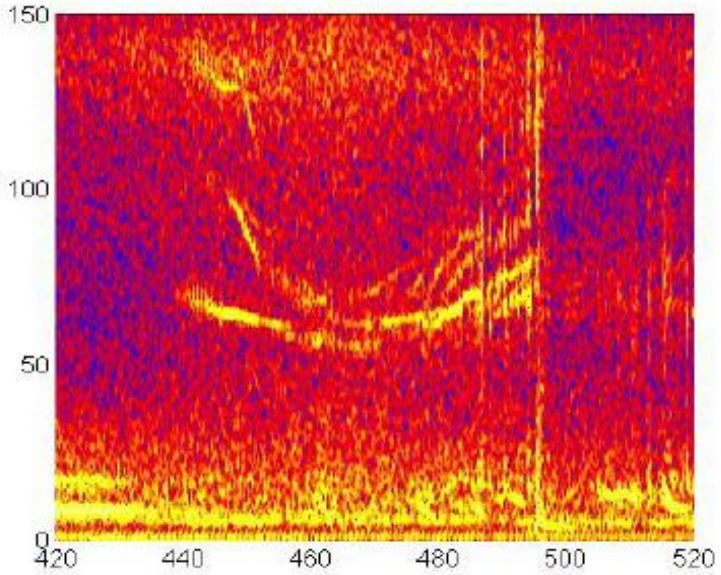

HL-2A, Chen,2012

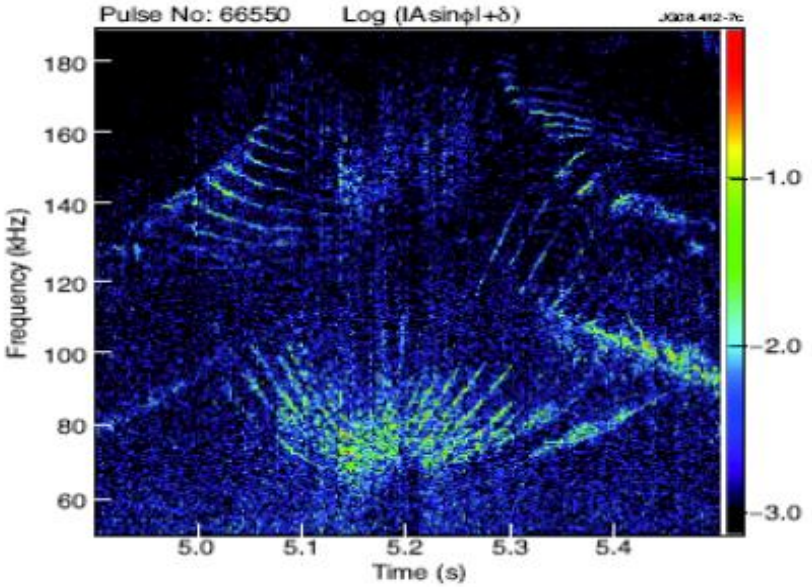

JET, Abel, PoP08

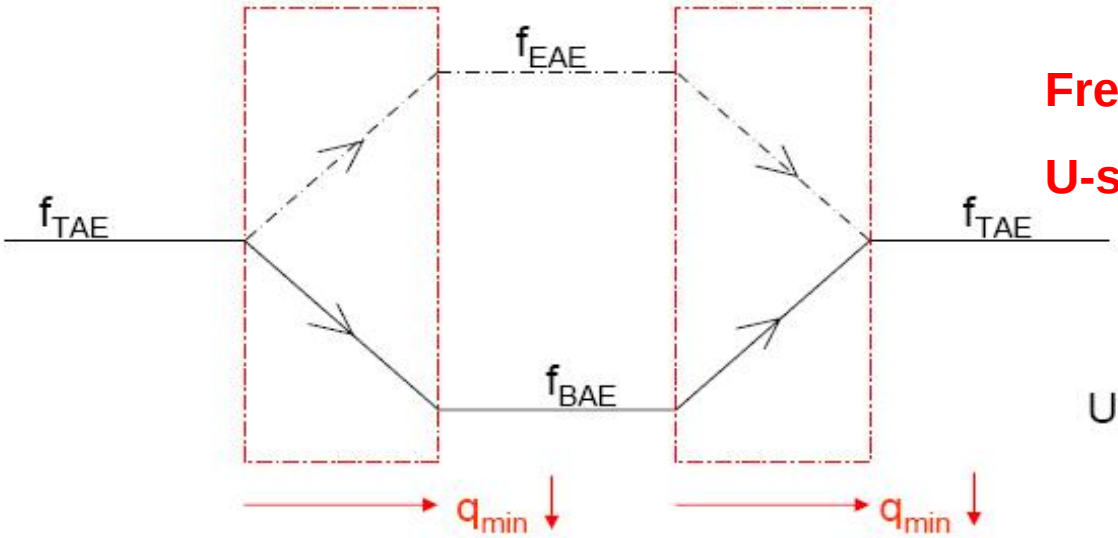

U-shape sweeping

Frequency sweeping pattern:

U-shape/ half-sinusoidal

Observation of various Alfvenic modes

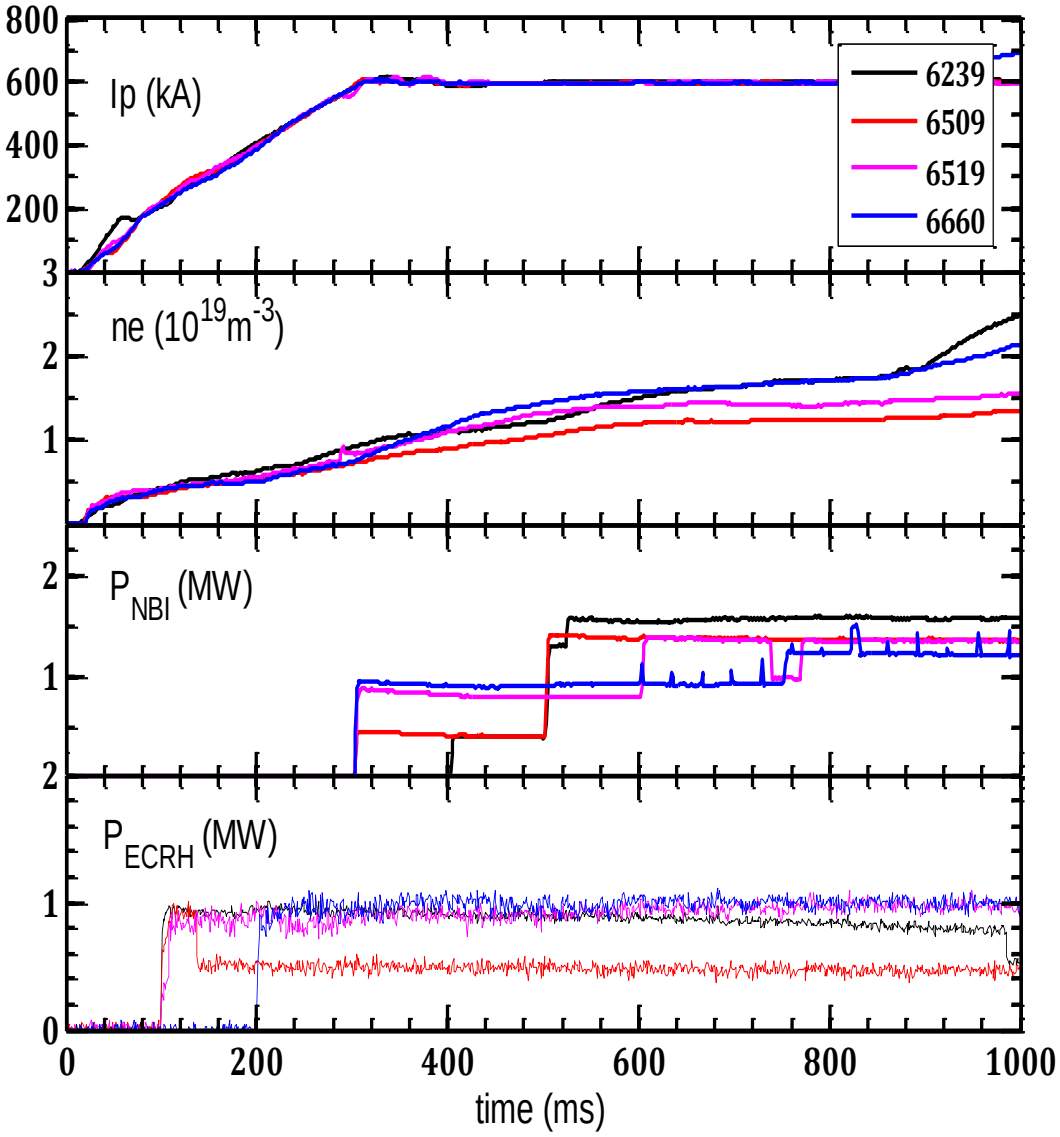

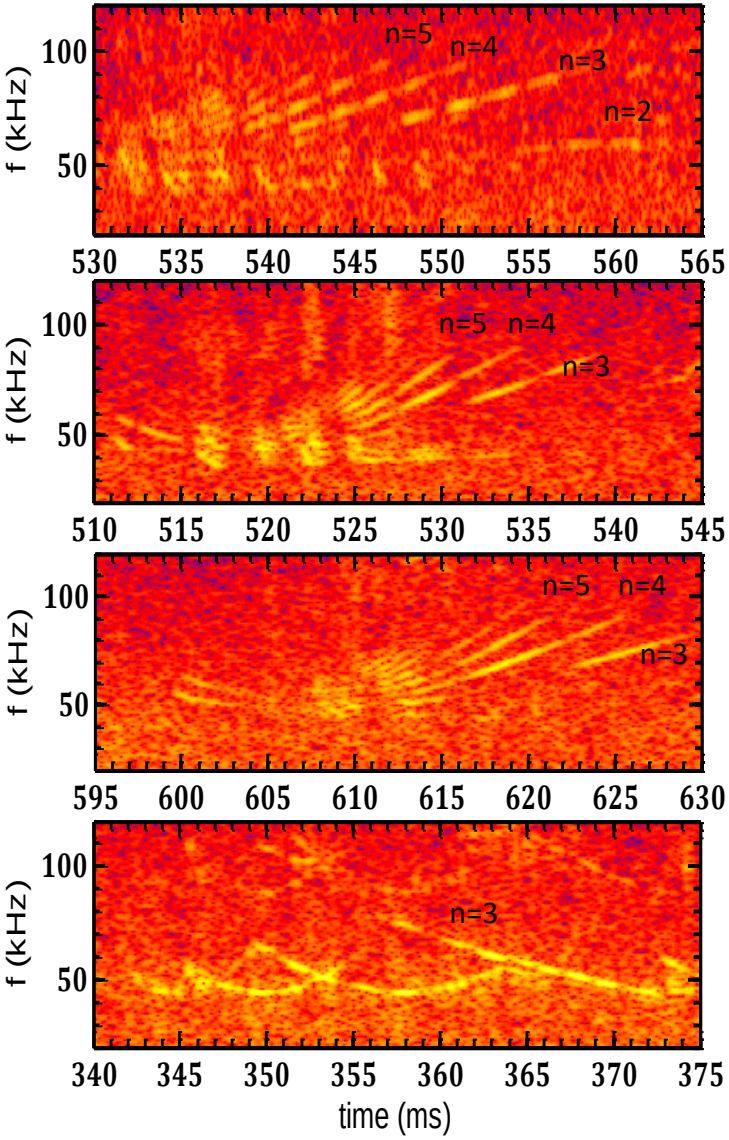

EP nonlinear physics:
Nonlinear mode-mode coupling

$$\tilde{E}_p = E_p e^{i(\vec{k}_p\cdot\vec{r}-\omega_p t)} + c.c.$$

$$\tilde{E}_q = E_q e^{i(\vec{k}_q\cdot\vec{r}-\omega_p t)} + c.c.$$

$$\tilde{E}_\pm = E_\pm e^{i(\vec{k}_\pm\cdot\vec{r}-\omega_\pm t)} + c.c.$$

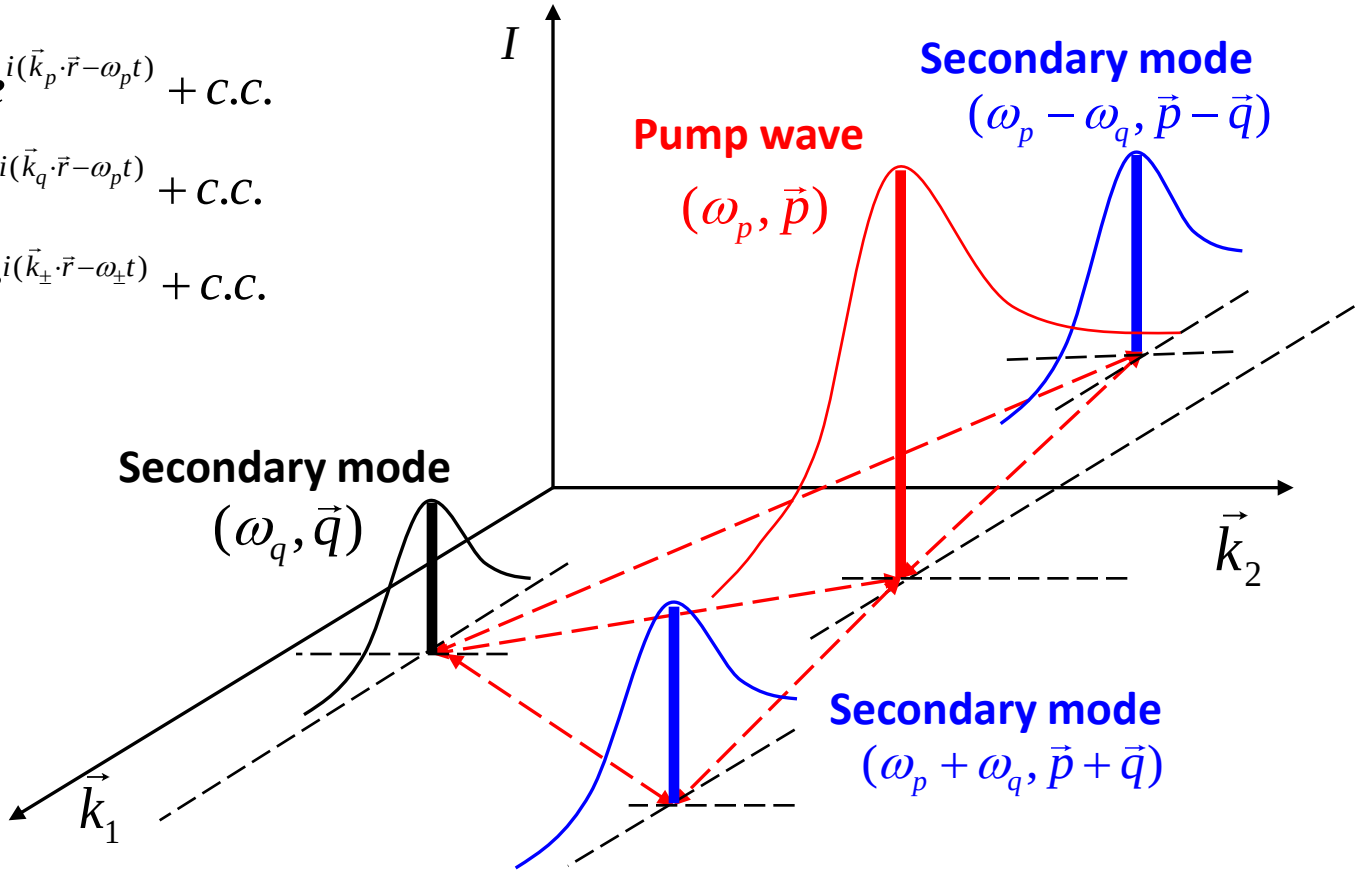

As we known, while the matching conditions are satisfied, i.e. $\omega_k = \omega_p + \omega_q$ and $\vec{k} = \vec{p} + \vec{q}$ the nonlinear interactions can occur between three waves in the plasma, and the coupled equations are bilinear and similar, and the coupling coefficients of the wave field amplitude determine the growth or damping of the waves.

EP nonlinear physics:

NL mode-mode between AE and AE/EPM

Some typical examples

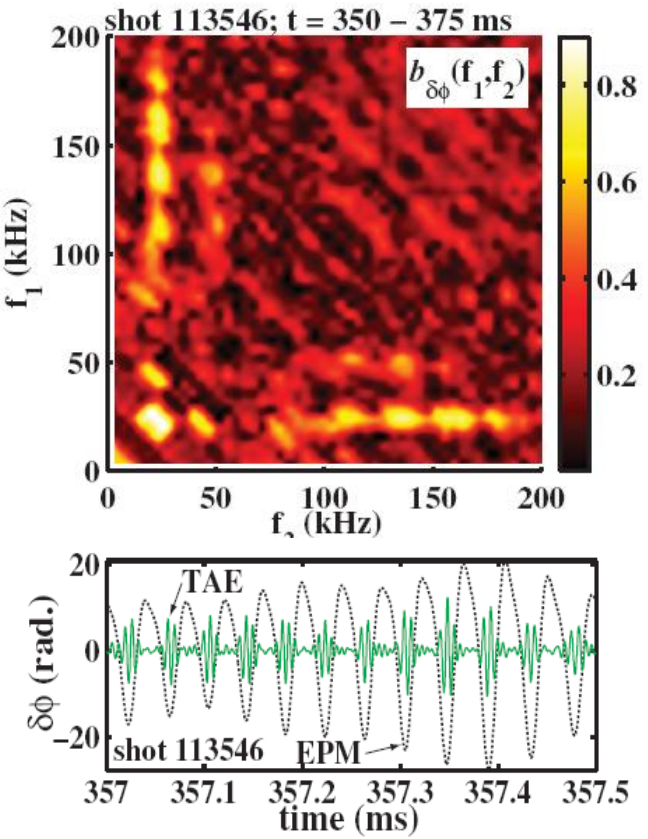

This nonlinear coupling spatially concentrates the TAE energy into a localized wave packet that is stationary in the EPM toroidal rotation frame.

N.A.Crocker, et al, PRL (2006),045002

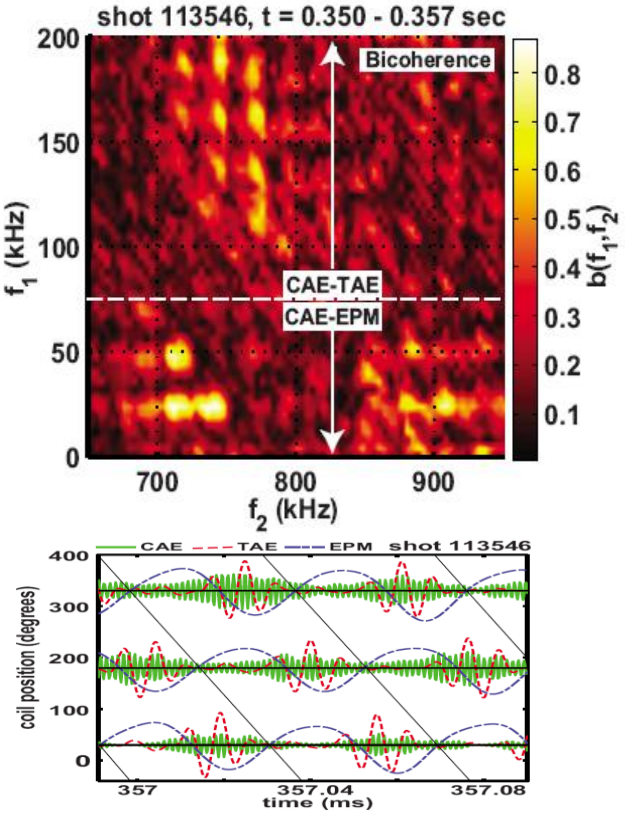

The envelope of the CAE wave packet propagates phase locked to the EPM superposition.

N.A.Crocker , et al, PoP (2009),042513

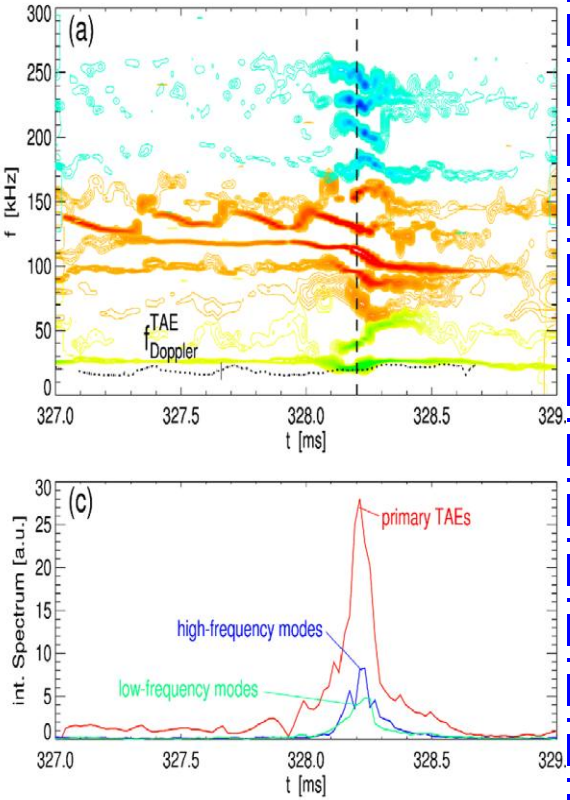

A n = 1 mode is a result of non-linear mode coupling between TAEs. The non-linear coupling leads to enhanced energetic ion transport.

M. Podesta, et al, NF (2011),063035

EP nonlinear physics:

NL mode-mode between BAEs and GAM/ZFs

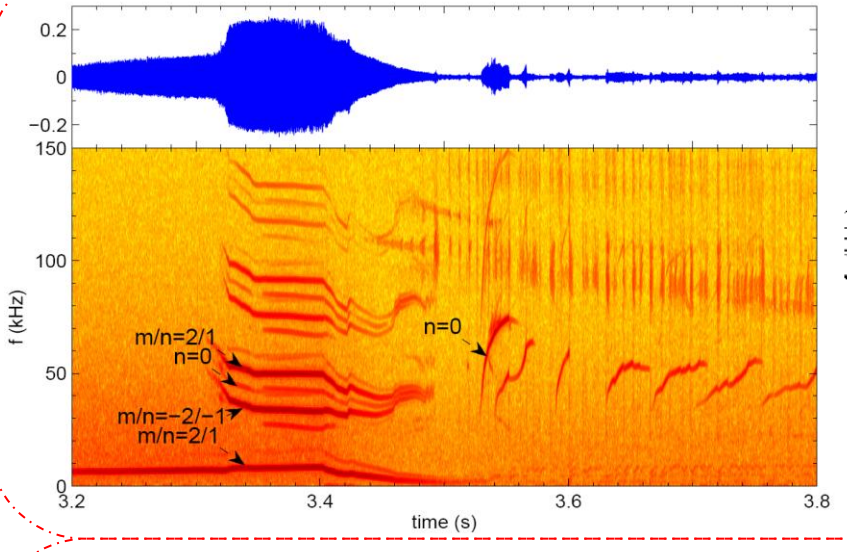

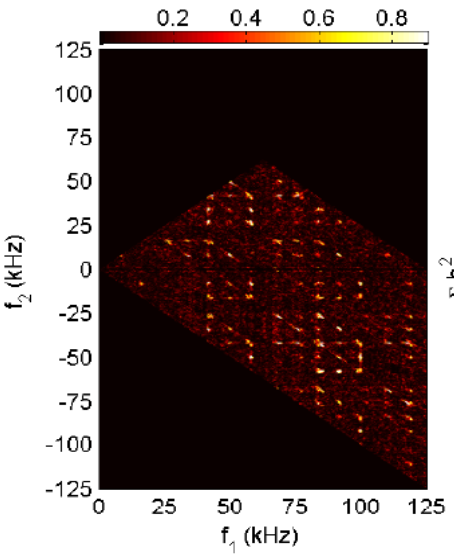

LHD

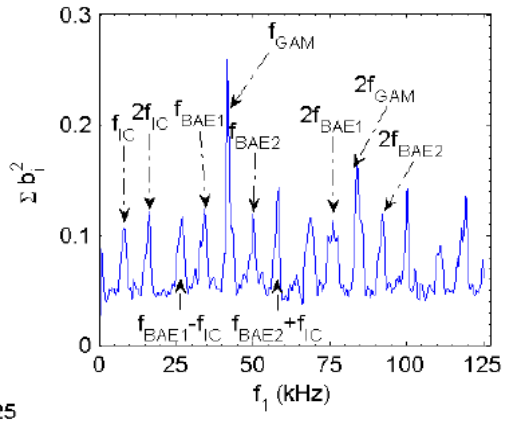

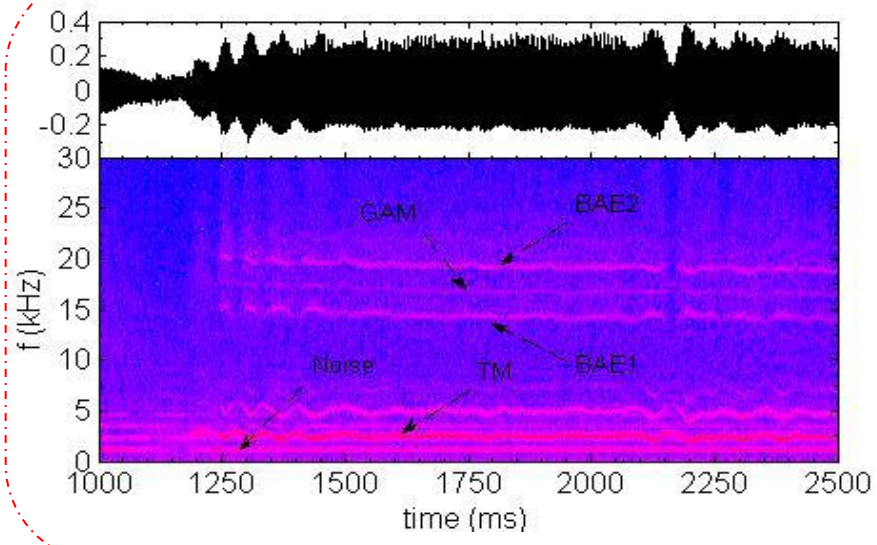

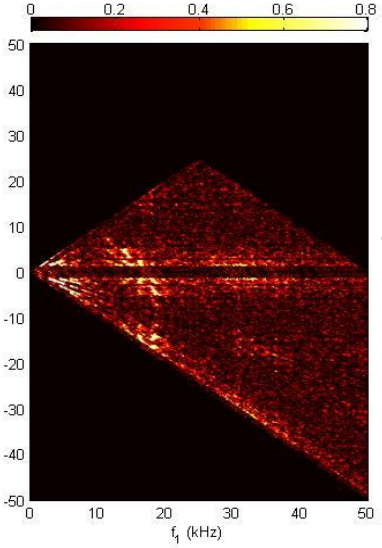

HL-2A

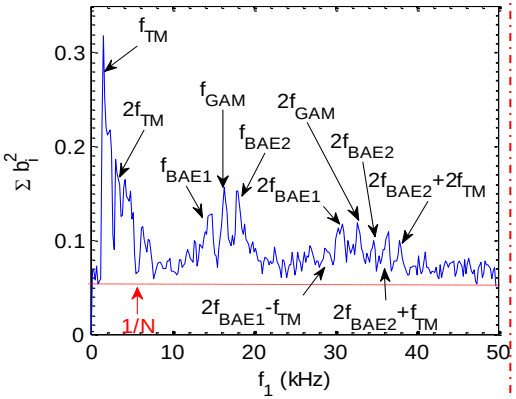

EP nonlinear physics:
Berk-Breizman（BB）model and bump-on tail problem

The evolution of the distribution is given by the kinetic equation:

$$\frac{\partial f}{\partial t}+v\frac{\partial f}{\partial x}+E\frac{\partial f}{\partial v}=\mathfrak{C}(f-f_0)$$

Krook operator: $\mathfrak{C}_K(f-f_0)=-\upsilon_a(v)(f-f_0)$ → Collision / Friction (drag)

Fokker-Plank operator: $\mathfrak{C}_{FP}(f-f_0)=\frac{\upsilon_f^2(v)}{k}\frac{\partial(f-f_0)}{\partial v}+\frac{\upsilon_d^3(v)}{k^2}\frac{\partial^2(f-f_0)}{\partial v^2}$ → Diffusion

The displacement current equation: $\frac{\partial E}{\partial t}=-\int v(f-f_0)-2\gamma_d E$

Bump on tail problem: $\frac{\partial f}{\partial t}+v\frac{\partial f}{\partial x}+E\frac{\partial f}{\partial v}=\mathfrak{C}(f-f_0)+S(v)$

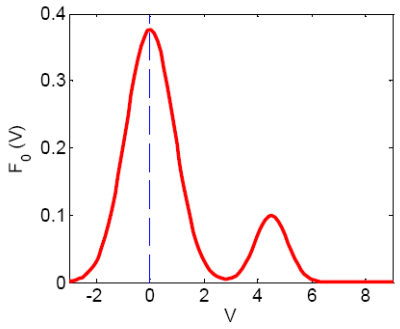

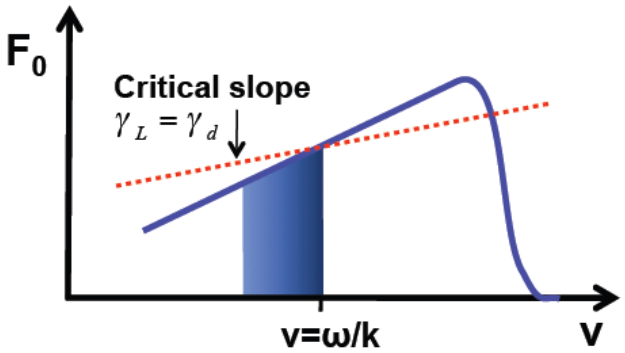

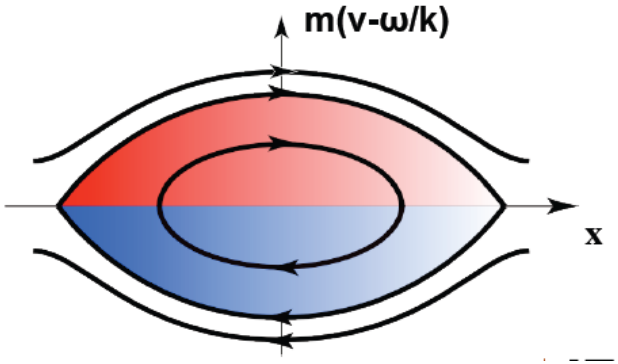

Lilley, PRL09; Lilley, Ph.D thesis; Chen, Ph.D thesis

EP nonlinear physics:

Different nonlinear regimes from BB model（pure diffusion）

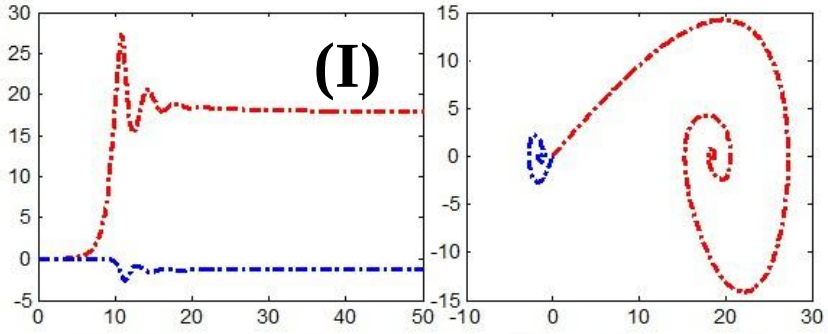

ν=4.2, β=0, α=0, $\phi=3\pi/64, \gamma_l/\gamma=1, \Delta t=0.01, A_0=0.001$

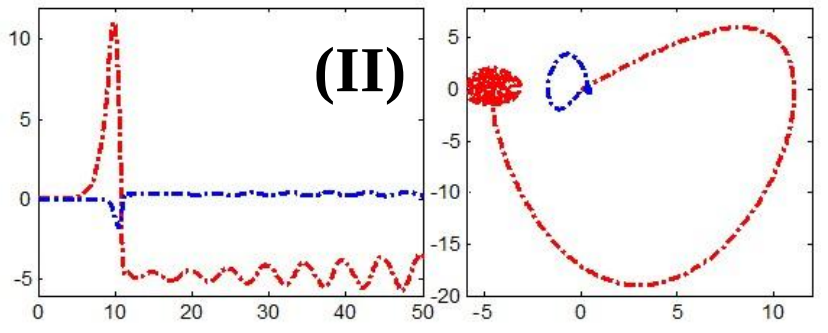

ν=2.13, β=0, α=0, $\phi=3\pi/64, \gamma_l/\gamma=1, \Delta t=0.01, A_0=0.001$

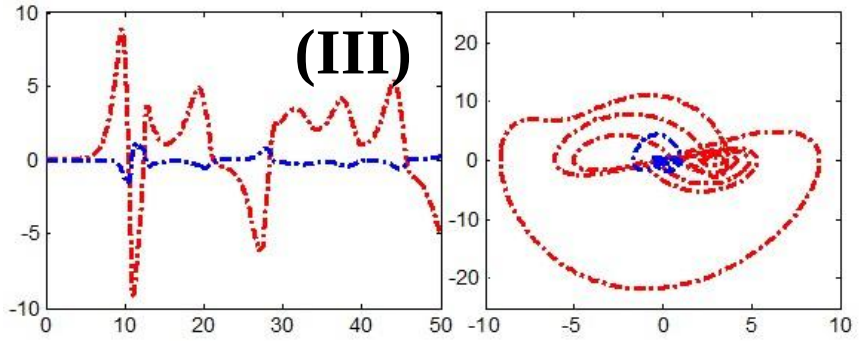

ν=1.7, β=0, α=0, $\phi=3\pi/64, \gamma_l/\gamma=1, \Delta t=0.01, A_0=0.001$

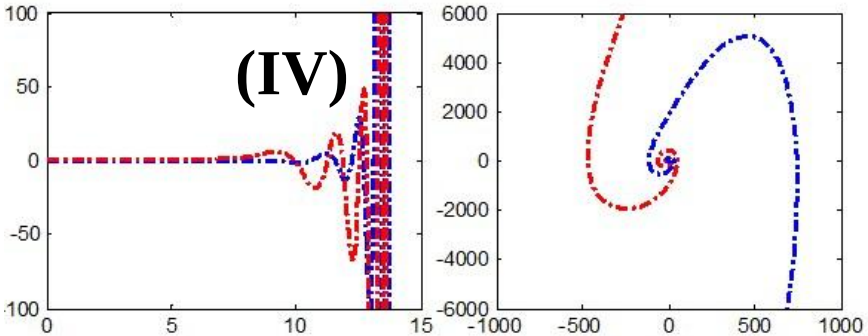

ν=1.1, β=0, α=0, $\phi=3\pi/64, \gamma_l/\gamma=1, \Delta t=0.01, A_0=0.001$

$$\frac{dA}{d\tau}=A(\tau)-\exp(i\phi)\gamma_l/\gamma\int_0^{\tau/2}dz z^2 A(\tau-z)$$
$$\times\int_0^{\tau-2z}dx\exp(-\nu^3z^2(2z/3+x)-\beta(2z+x)+i\alpha^2z(z+x))$$
$$\times A(\tau-z-x)A^*(\tau-2z-x)$$

(I) SS;(II) periodic; (III) chaotic; (IV) explosive

Berk, PRL96;Fasoli,PRL98;Heeter, PRL00;
Lilley, PRL09; Lilley, Ph.D thesis; Lesur, Ph.D thesis

Non-linear evolution of wave near threshold: $\hat{\nu}=\nu/\gamma=\nu/|\gamma_l-\gamma_d|$

ν and β decease: mode moves from steady-state into bursting and chaotic regime

EP nonlinear physics:

Different nonlinear regimes from BB model（pure collision）

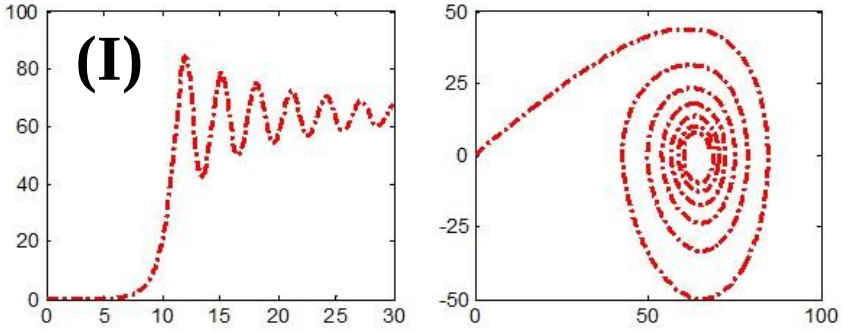

ν=0, β=4.8, α=0, ϕ=0, $\gamma_1/\gamma = 0.5, \Delta t = 0.01, A_0 = 0.001$

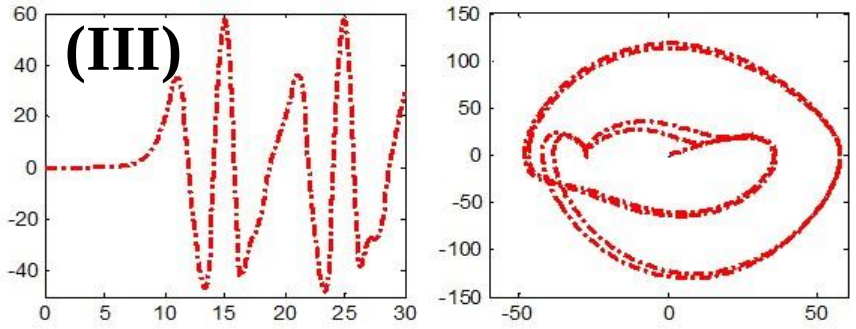

ν=0, β=2.5, α=0, ϕ=0, $\gamma_1/\gamma = 0.5, \Delta t = 0.01, A_0 = 0.001$

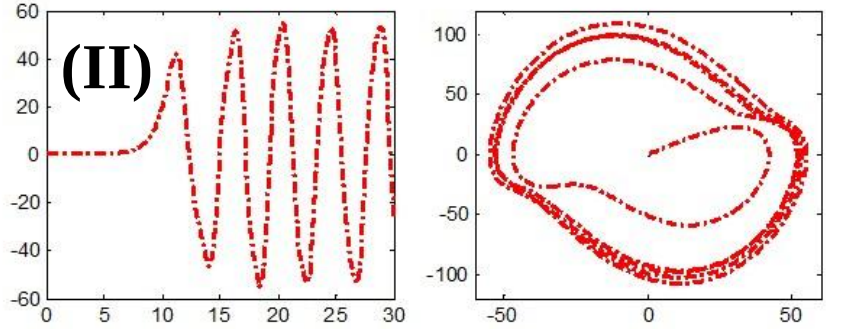

ν=0, β=2.9, α=0, ϕ=0, $\gamma_1/\gamma = 0.5, \Delta t = 0.01, A_0 = 0.001$

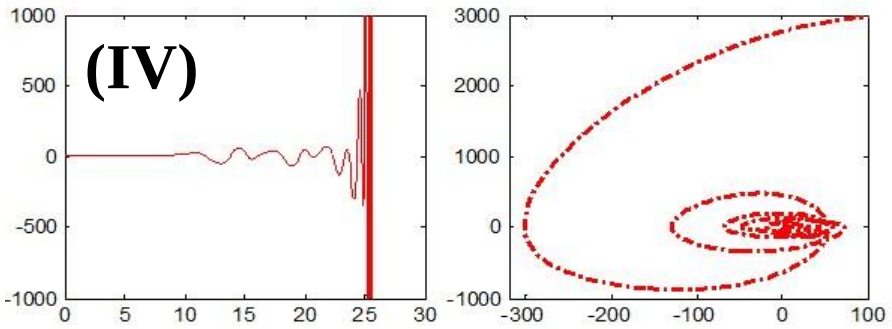

ν=0, β=2.3, α=0, ϕ=0, $\gamma_1/\gamma = 0.5, \Delta t = 0.01, A_0 = 0.001$

$$\frac{dA}{d\tau} = A(\tau) - \exp(i\phi)\gamma_1/\gamma \int_0^{\tau/2} dz z^2 A(\tau - z)$$
$$\times \int_0^{\tau-2z} dx \exp(-\nu^3 z^2(2z/3 + x) - \beta(2z + x) + i\alpha^2 z(z + x))$$
$$\times A(\tau - z - x)A^*(\tau - 2z - x)$$

(I) SS;(II) periodic; (III) chaotic; (IV) explosive

Berk, PRL96;Fasoli,PRL98;Heeter, PRL00; Lilley, PRL09; Lilley, Ph.D thesis;

Non-linear evolution of wave near threshold: $\hat{\nu} = \nu/\gamma = \nu/|\gamma_l - \gamma_d|$

ν and β decease: mode moves from steady-state into bursting and chaotic regime

EP nonlinear physics:

Evolution of holes and clumps

Fast shifting frequencies correspond to the evolution of **holes and clumps**.

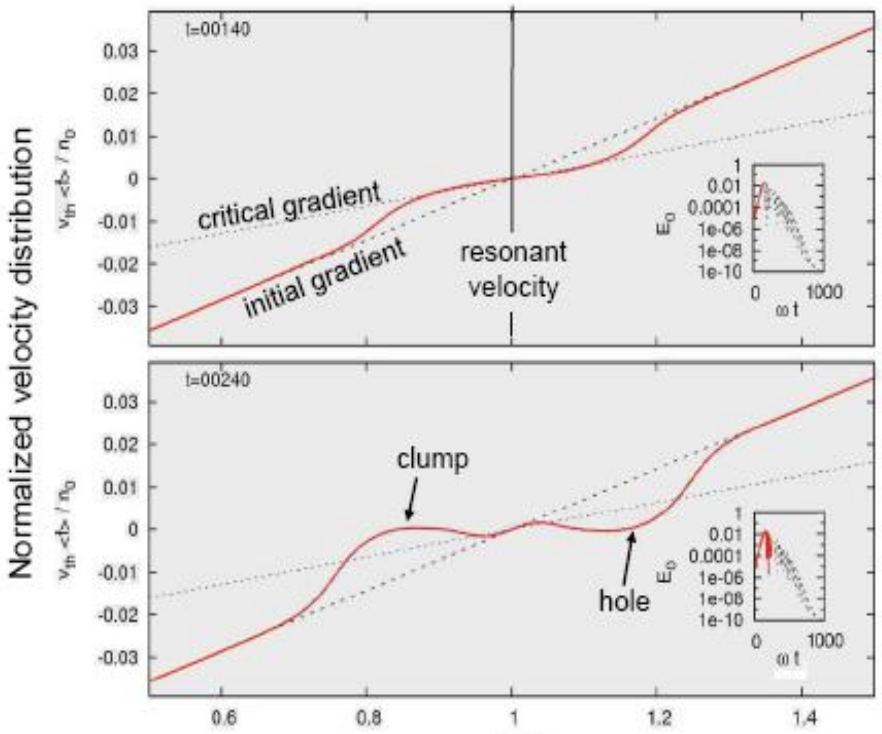

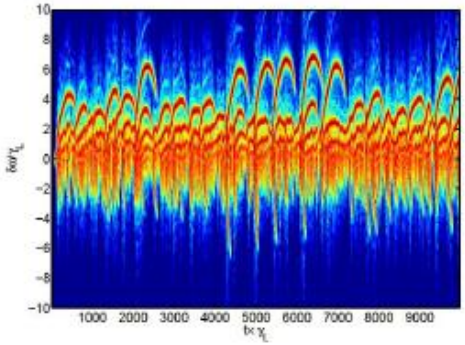

Drag + diffusion:
Hooked frequency chirp

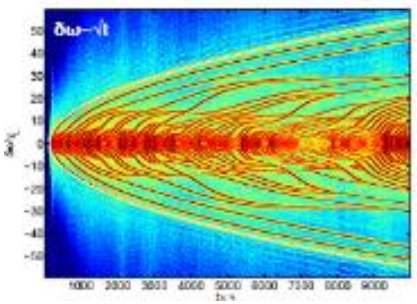

Low collisionality:

Frequency chirping

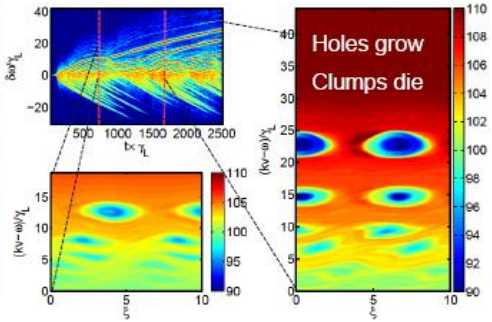

Pure drag:

No steady state

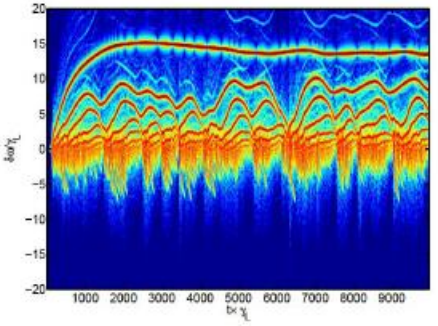

Drag + diffusion:
Steady state hole

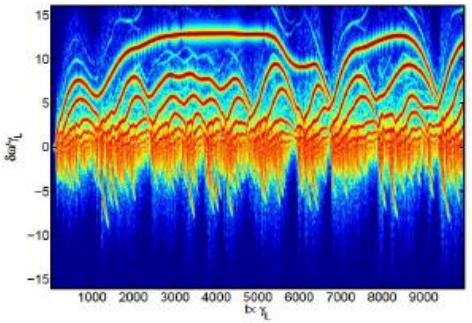

Drag + diffusion:
Undulating frequency

Lilley, PRL09; Lilley, Ph.D thesis; Lesur, Ph.D thesis

EP nonlinear physics

- For near stability threshold and small collision frequency, hole-clump will be created due to steepening of distribution function near the boundary of flattening region.
- As hole and clump moves up and down in the phase space of distribution function, the mode frequency also moves up and down. *H.L. Berk et al., PoP 6, 3102 (1999).*

- Single mode saturates due to wave-particle trapping or distribution flattening.
- Collisions tend to restore original unstable distribution.
- Near stability threshold, nonlinear evolution can be explosive when collision is sufficiently weak and result in hole-clump formation.

EP nonlinear physics

- **Mode-mode coupling can enhance damping and induce mode saturation.(**Fluid nonlinearity induces n=0 perturbations which lead to equilibrium modification, narrowing of continuum gaps and enhancement of mode damping. At high-n, mode-mode coupling leads to mode cascade to lower frequencies via ion Compton scattering. As a result, modes saturate due to larger effective damping.) D.A. Spong, et al 1994, *PoP,* **1**, 1503 F. Zonca, et al 1995, *PRL* **74**, 698, L. Chen, et al 1998, *PPCF* **40**, 1823; T.S. Hahm and L. Chen 1995, *PRL* **74**, 266
- **Multiple modes can cause resonance overlap and enhance particle loss.** H.L. Berk et al, PoP 2, 3007 (1995).

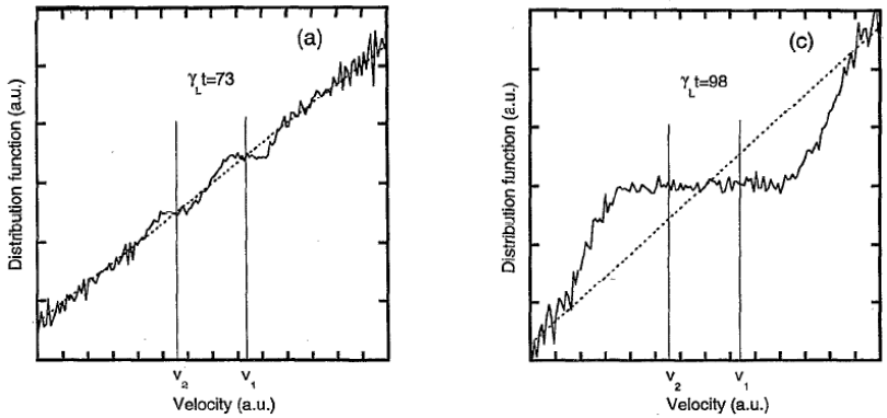

Diagnostic methods of EP phenomena

I. Mode identify，mode structures：

Mirnov probe，Soft X-ray，ECE/ECEI，CXRS，Microwave interference/reflectometry, BES，Gama ray spectrum,HIBP/IHIBP

II. Fast particle transport/loss：

Hard X-ray (CdTe/CdZnTe)， FILP, FIDA, Neutron，CTS，FP，PCI

III. Fast particle distribution：

NPA/INPA, Hard X-ray (CdTe/CdZnTe)，ECE/ECEI，FIDA,FILP

Diagnostic methods of EP phenomena

Alpha particle diagnostics: confined

- **Confined alpha particle diagnostics**

– Measurement of confined alphas is still a challenge

– Need good spatial resolution for studies of transport, ITBs, and alpha particle-driven instabilities

– Alpha velocity-space distribution measurements are important for Alfvén instability studies

– Candidate techniques:

- collective Thomson scattering
- Charge exchange recombination spectroscopy
- alpha knock-on
- charge-exchange neutralization
- gamma-ray spectroscopy

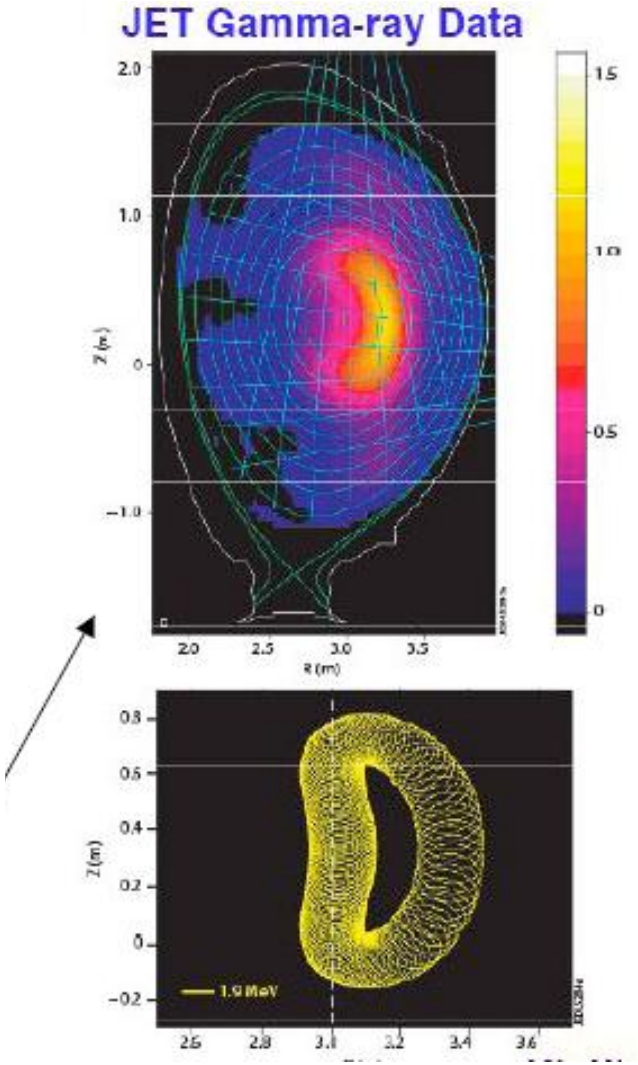

Diagnostic methods of EP phenomena

Alpha particle diagnostics: lost

- **Lost alpha particle diagnostics**
  – Measurement of lost alphas is also still a challenge

– Need to measure bombardment location, pitch angle and energy distribution, temporal behavior during MHD

– Candidate techniques:
  - Faraday cups
  - scintillator probes
  - IR camera imaging
  - gamma-ray spectroscopy

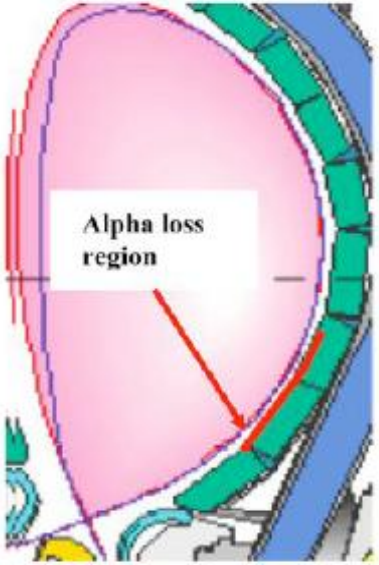

First wall region marked by the thick red line undergoes α particle bombardment due to TF ripple loss

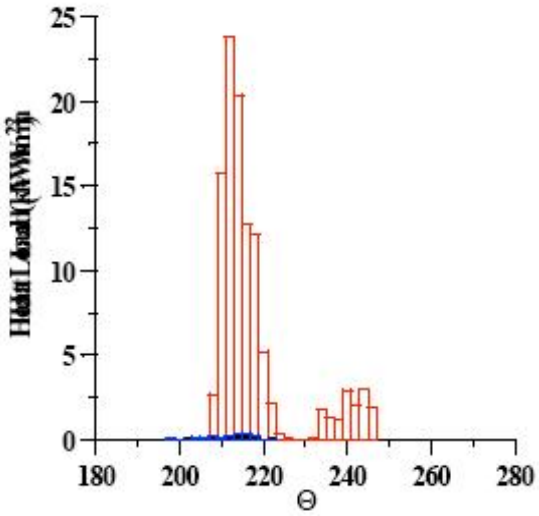

Poloidal distribution of heat load due to banana particle loss (red) and locally trapped α loss (blue)

M. Sasao et al. (PPCF 2004)

EP losses by various MHD activities: Ion FB

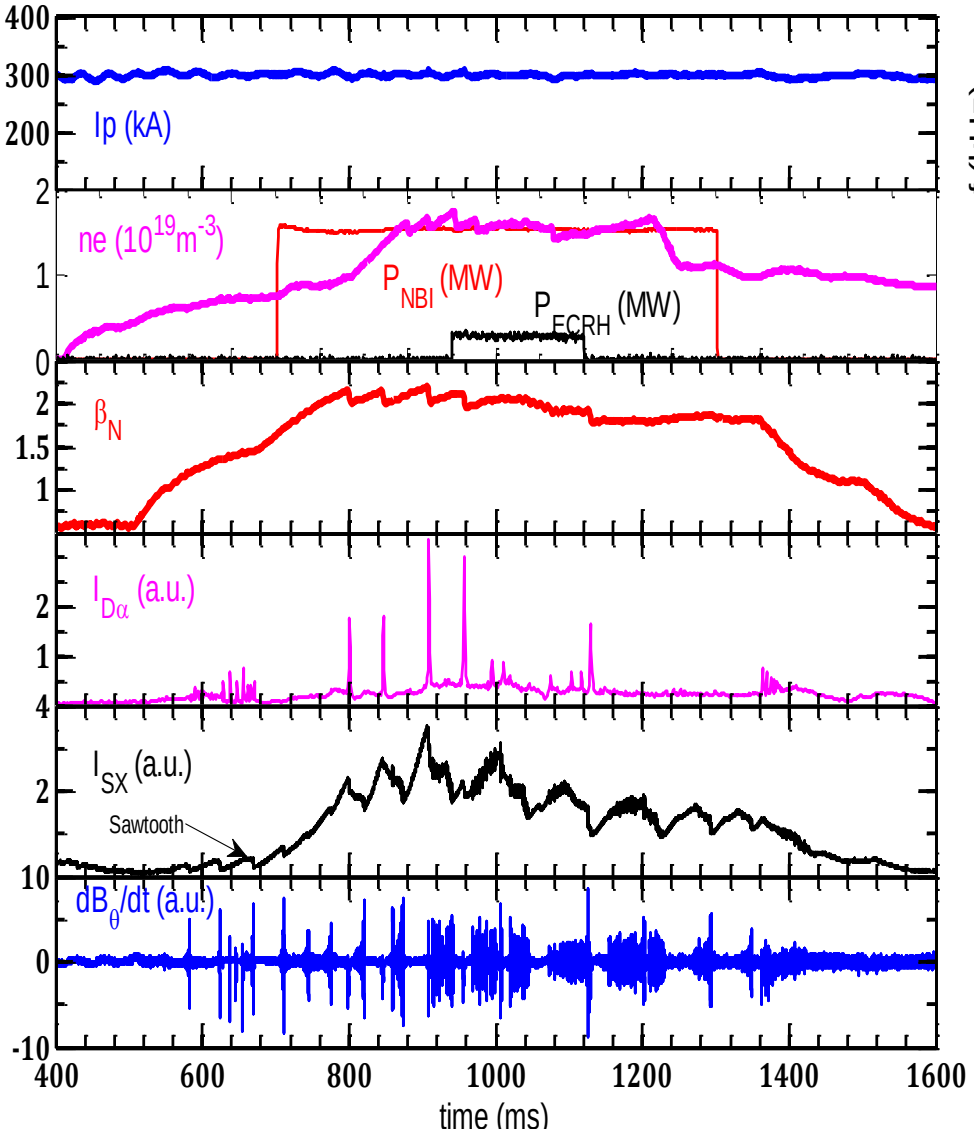

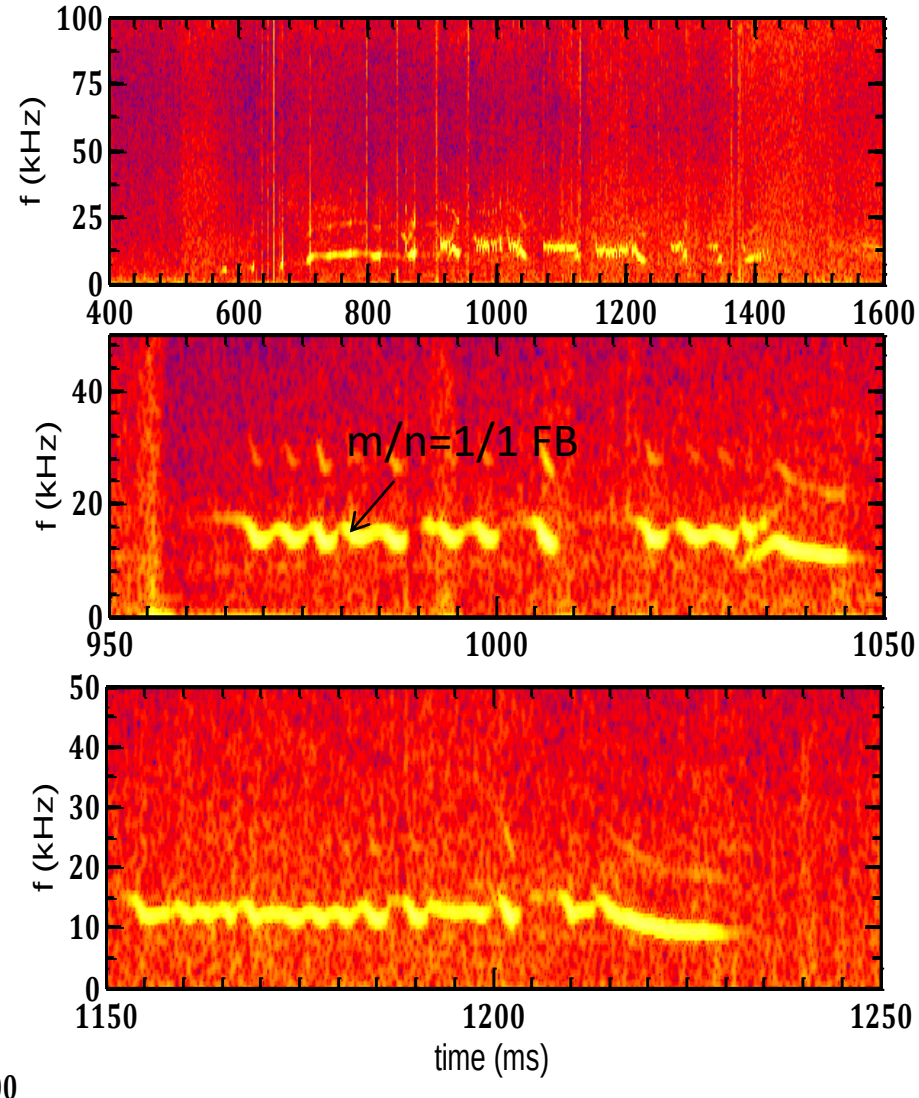

EP losses by various MHD activities:

EP loss Induced by Ion FB onHL-3

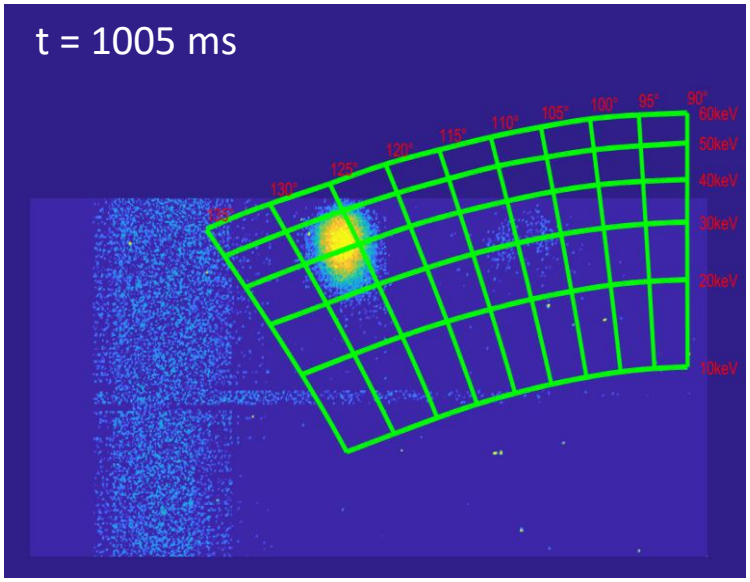

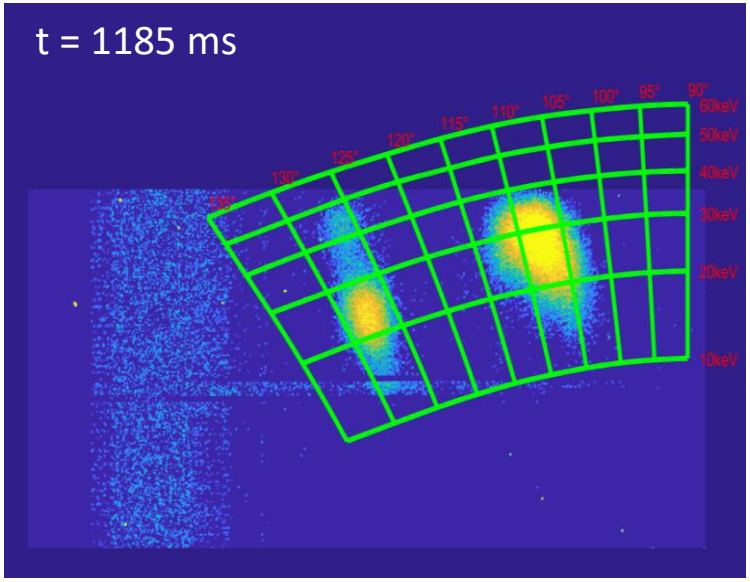

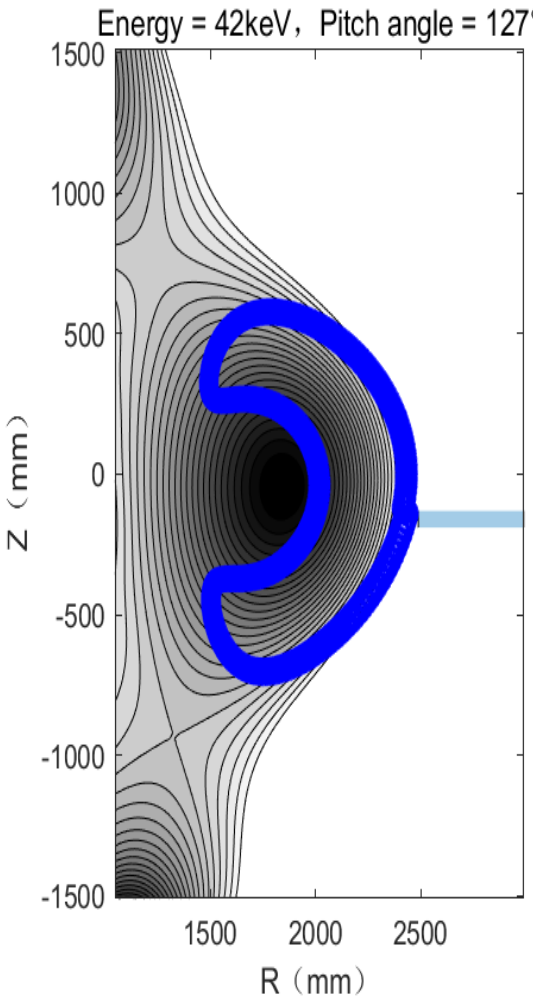

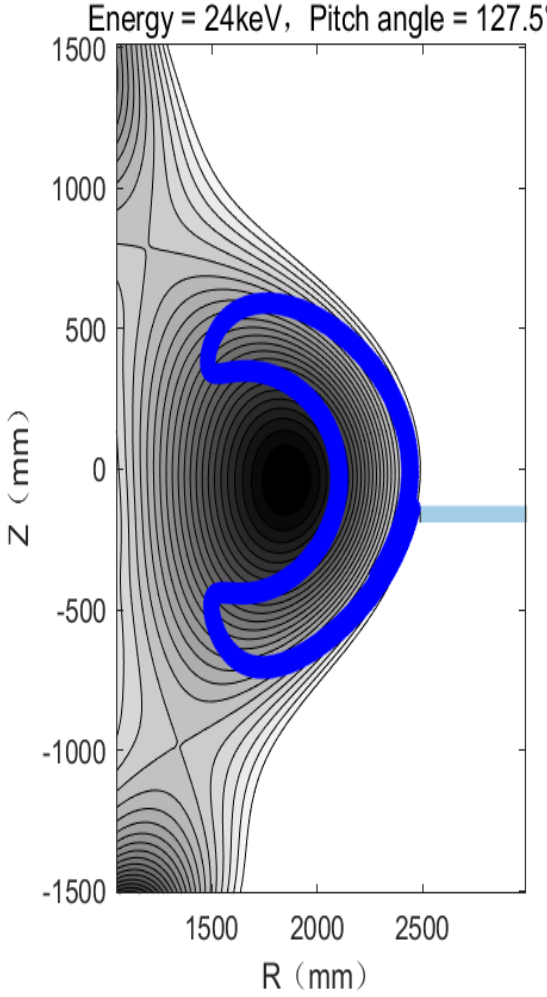

EP losses by various MHD activities:

EP loss Induced by TAE : Diffusion and Convection

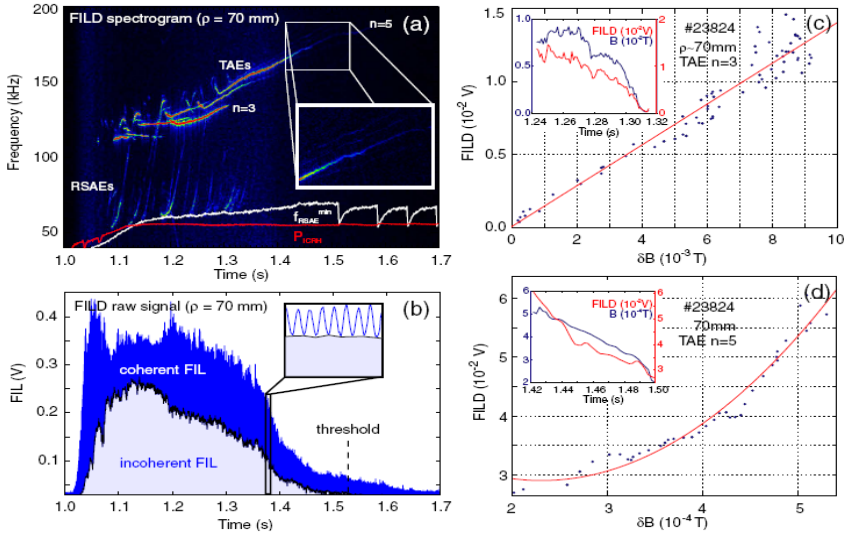

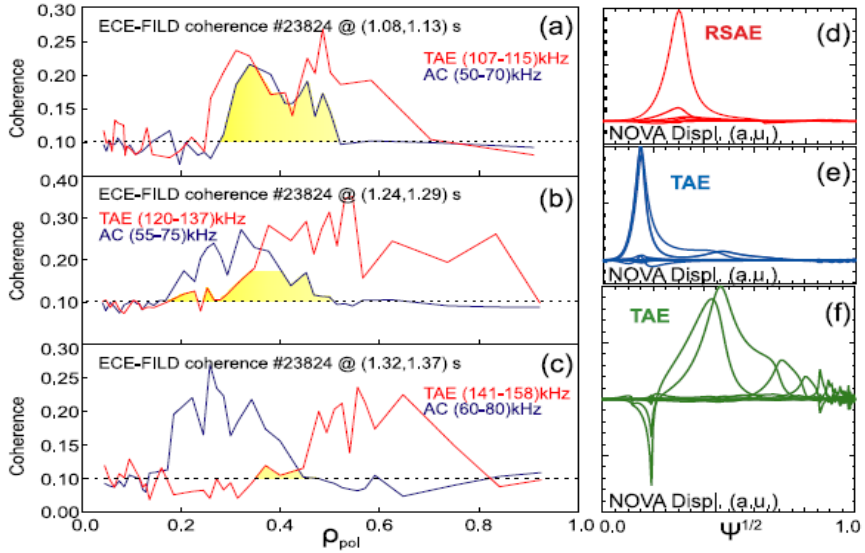

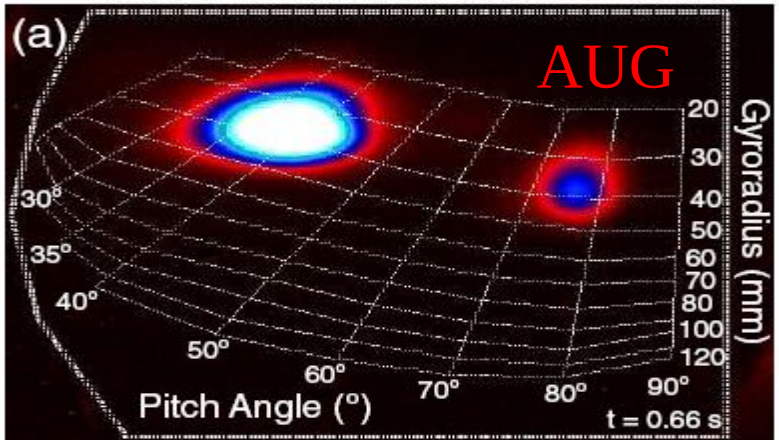

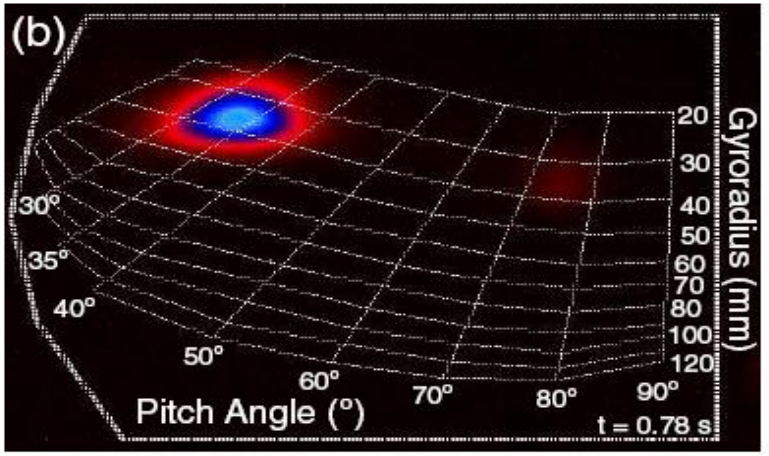

Garcia-Munoz M. et al NF 51 (2011) 103013

Garcia-Munoz M. et al 2010 PRL 104 185022

Garcia-Munoz M. et al 2008 PRL 100 055005

EP losses by various MHD activities:
EP loss Induced by TAE: TAE avalanches

- Low-*n*, quasi-stationary TAEs evolve into bursty behavior & *avalanches*
- Fast ion losses ≤30% observed (e.g. FIDA, neutrons) during avalanches
- Similar $n_{e,i}$, $T_{e,i}$, I_p, B_{tor}, P_{NB} (but different plasma shape: LSN *vs* limiter)

TAE avalanches in He and D plasmas of NSTX

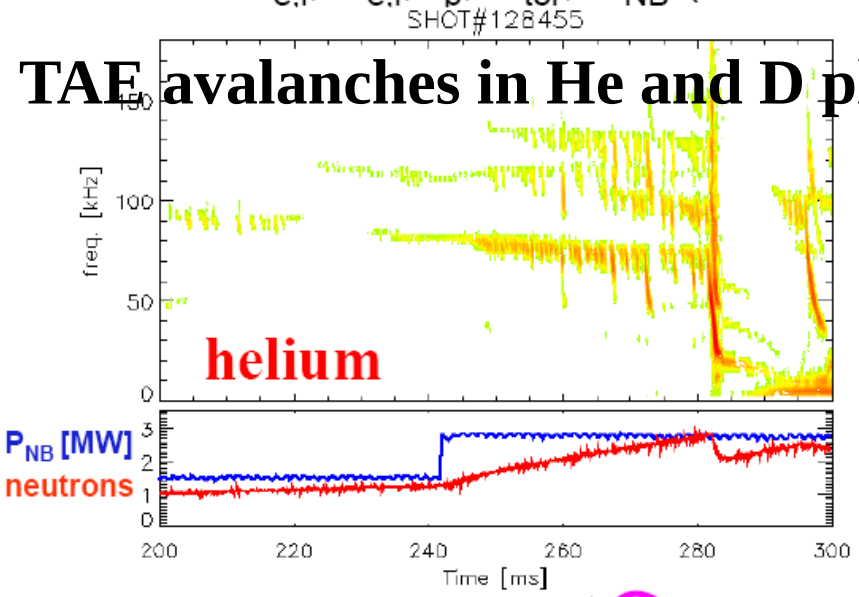

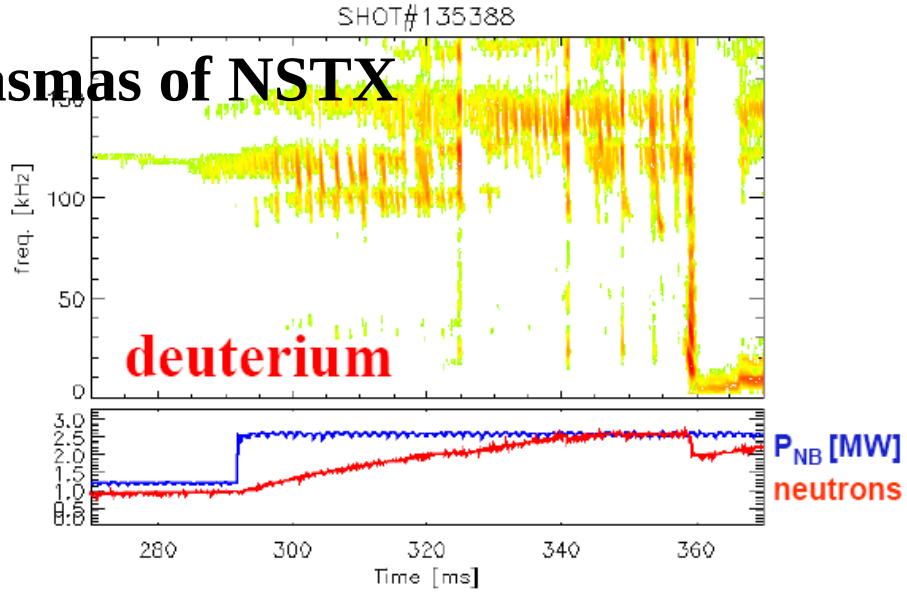

Podesta, 51st APS-DPP Meeting 2009

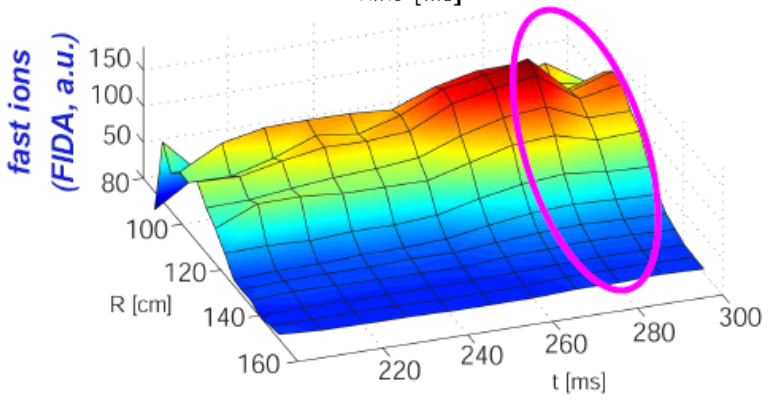

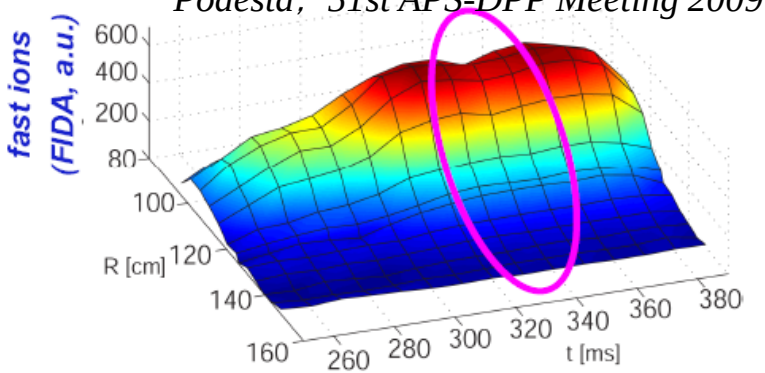

EP losses by various MHD activities:
EP loss Induced by fishbone and EGAM

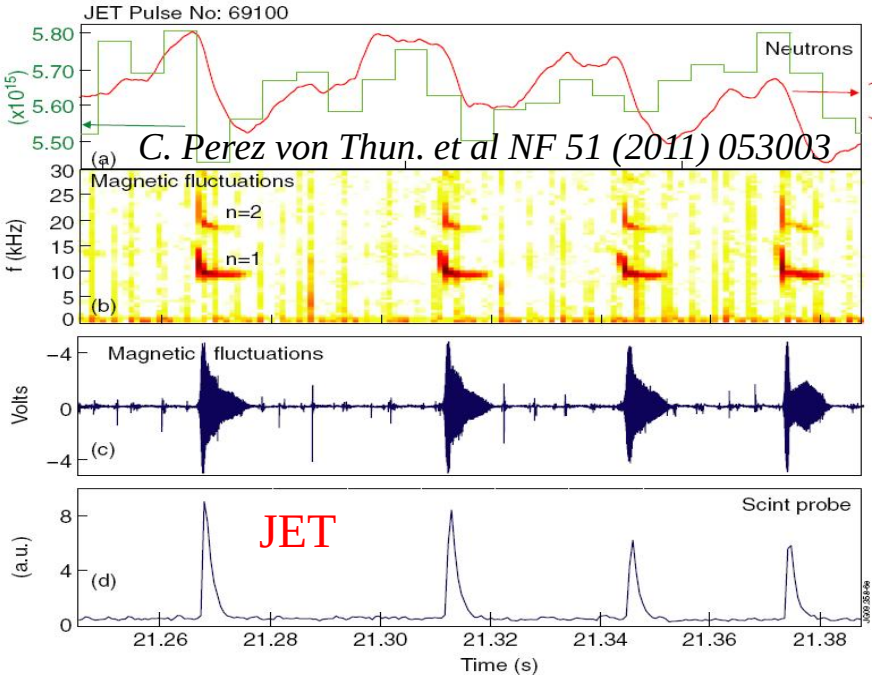

C. Perez von Thun. et al NF 51 (2011) 053003

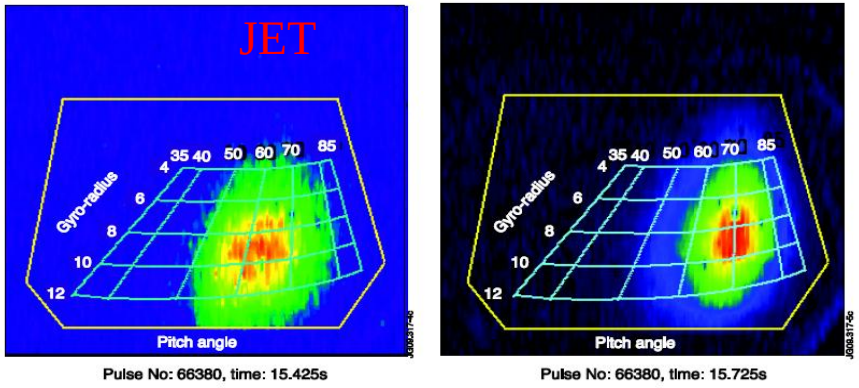

Nabais F. et al NF 50 (2010) 115006

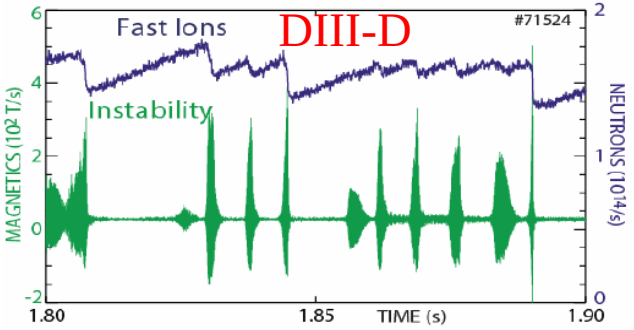

Duong H H *et al* **1993** *NF* **33** 749

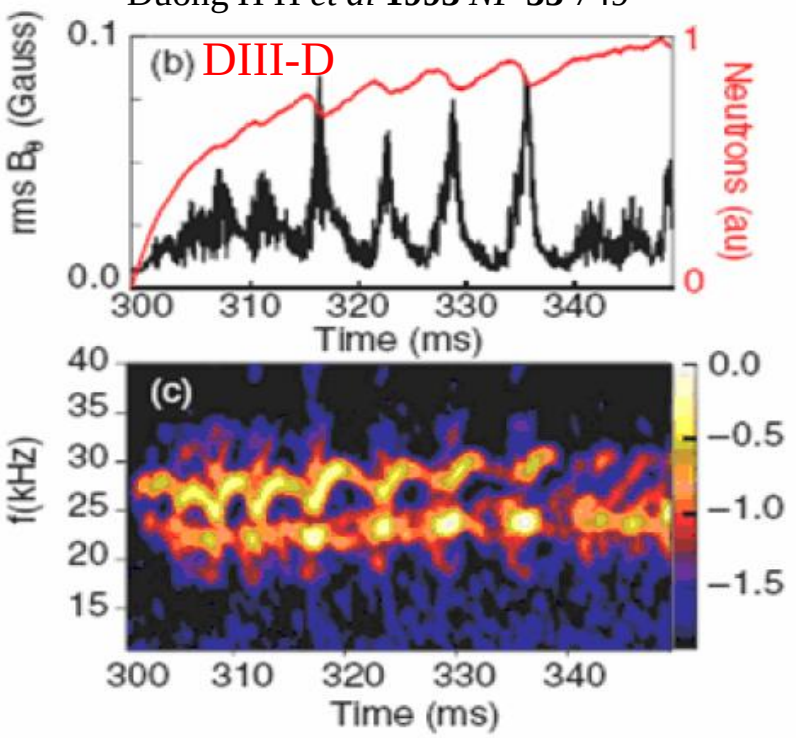

Nazikian R. et al 2008 PRL 101 085002

EP losses by various MHD activities:
EP loss Induced by TAE+FB/LLM on HL-3

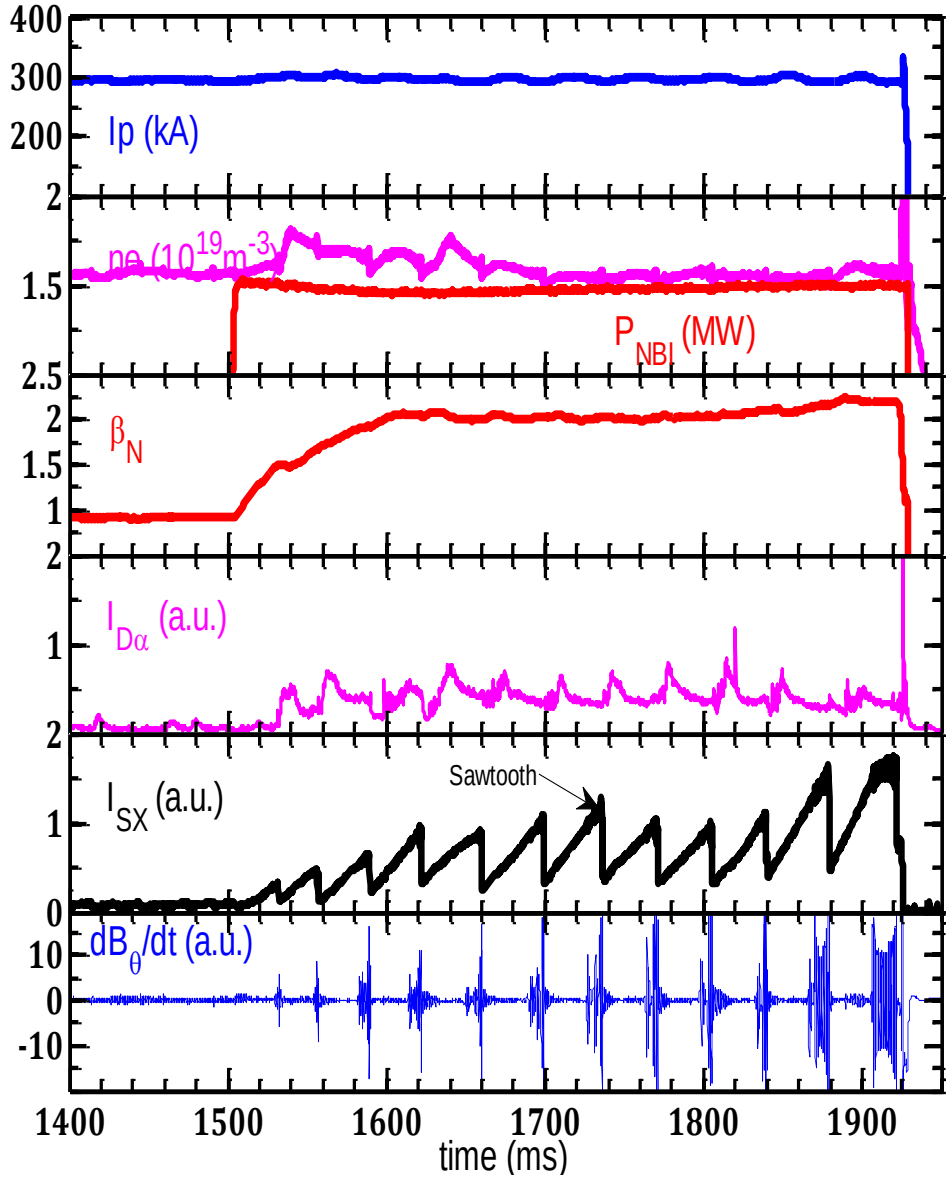

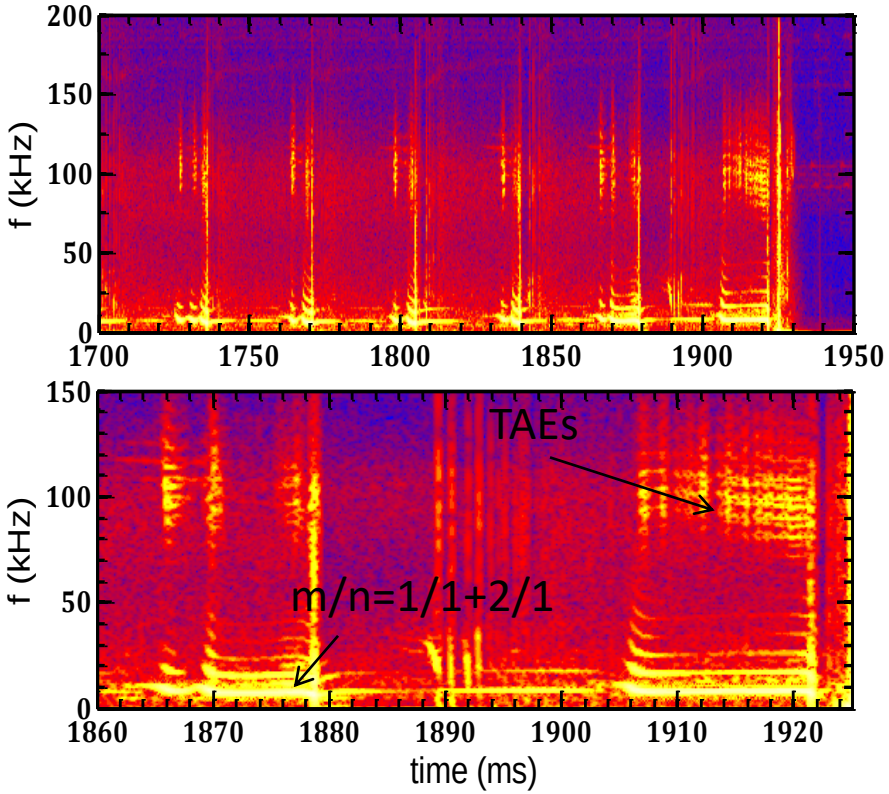

EP losses by various MHD activities:
EP loss Induced by TAE+FB/LLM on HL-3

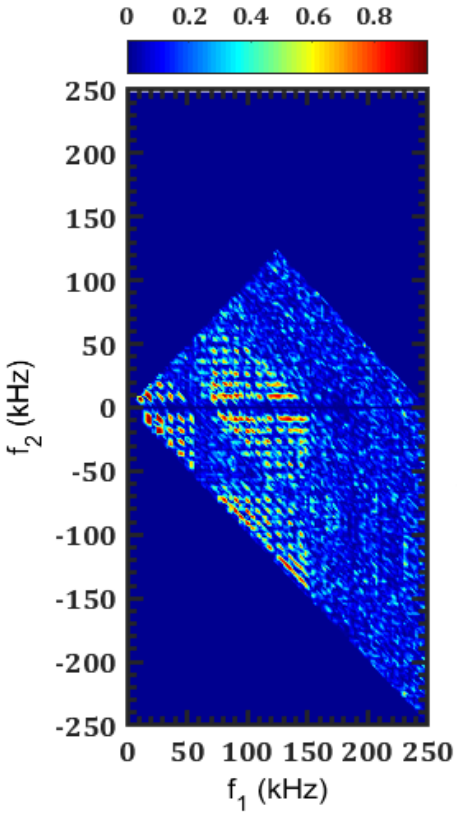

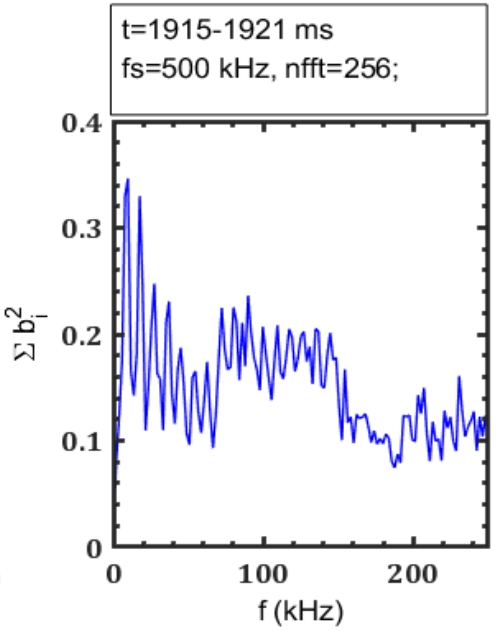

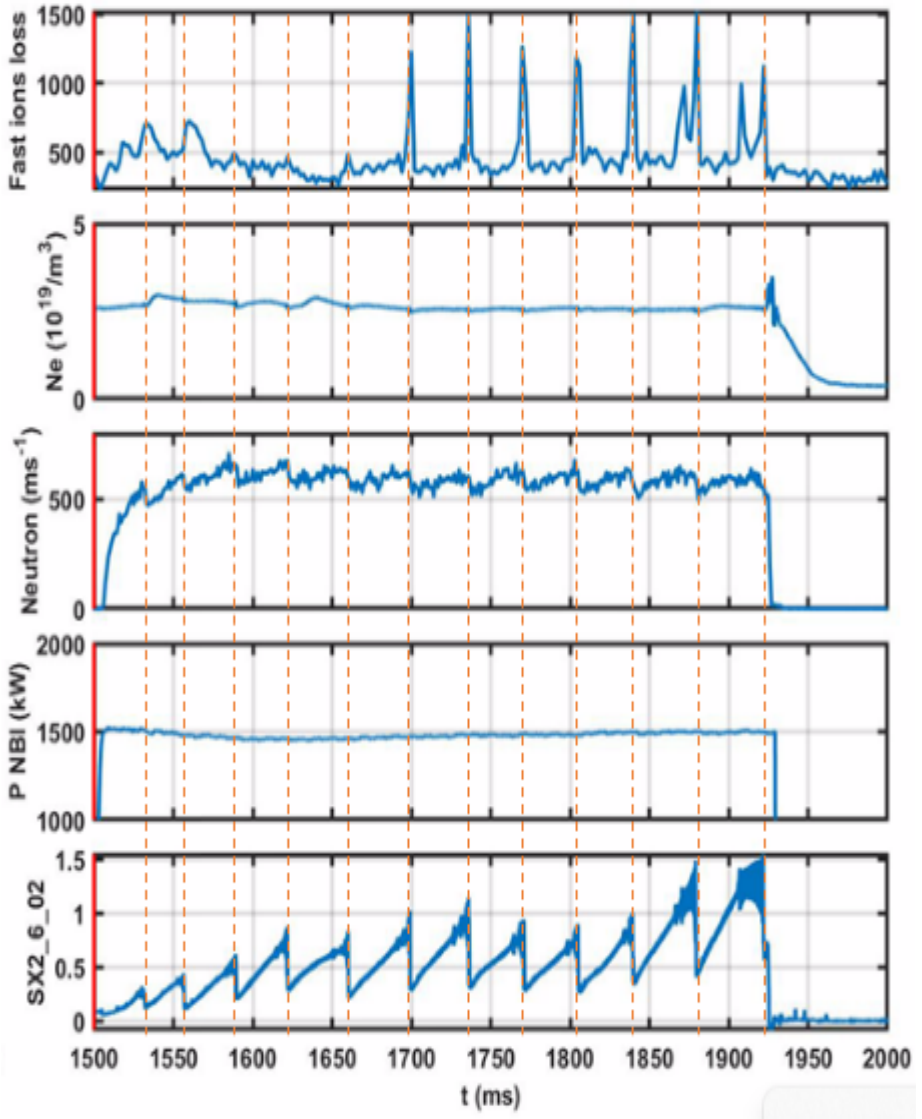

EP losses by various MHD activities:
EP loss Induced by TAE+FB/LLM on HL-3

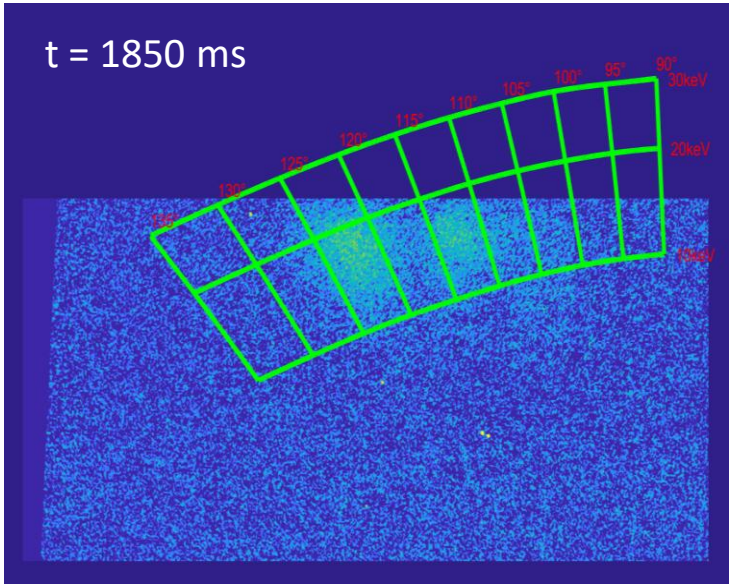

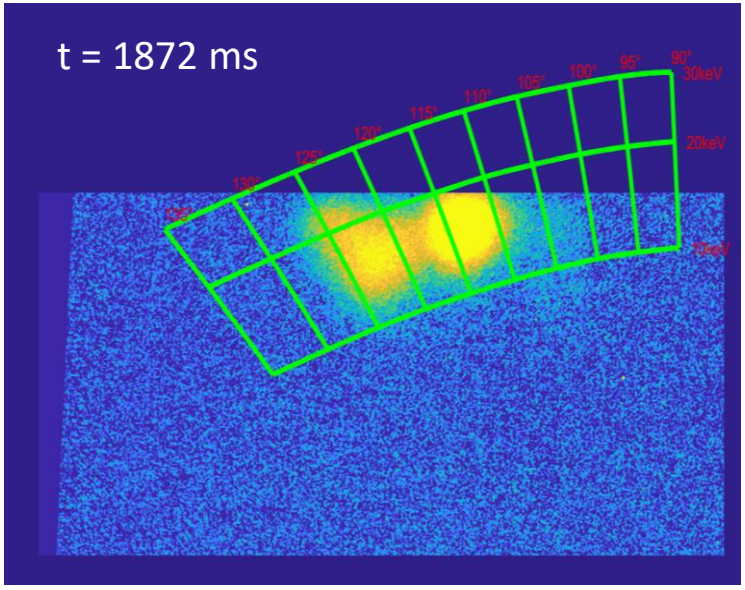

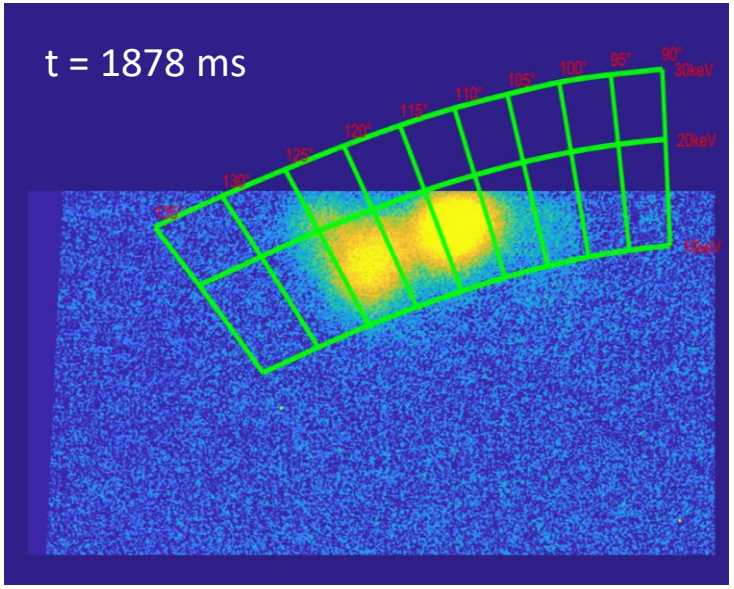

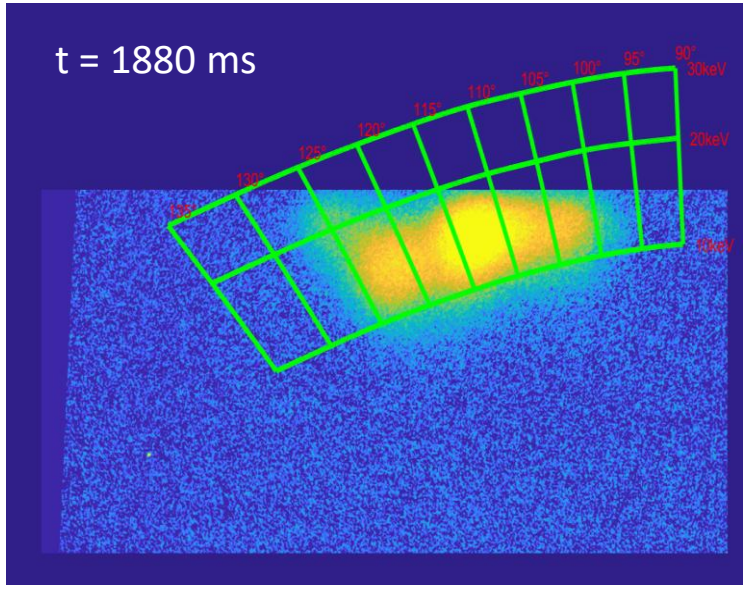

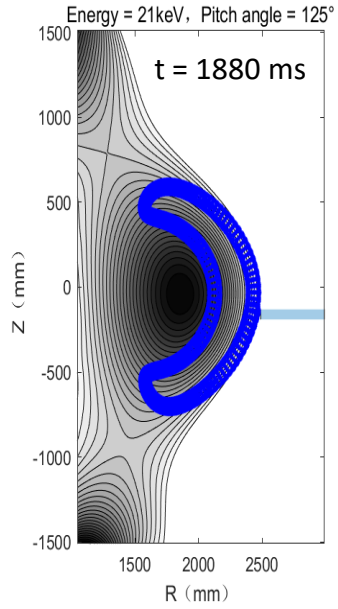

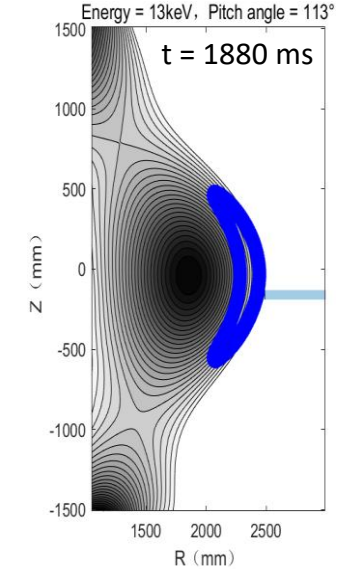

EP losses by various MHD activities:
EP loss Induced by EPMs

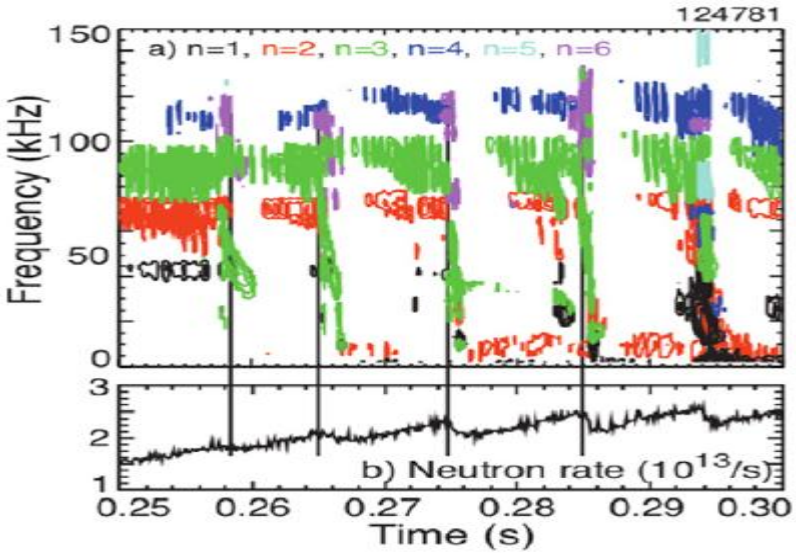

- Mode frequencies at ends of chirps are consistent with rotation frequency near core.
- Frequency chirps start in TAE gap.
- Toroidal mode number progresses upwards from n=1 to n=5 through a series of multiple bursts for each n.

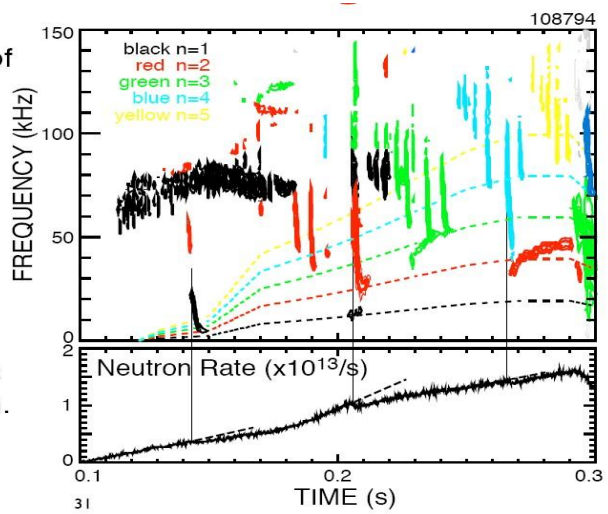

TAE avalanches - of interest beyond NSTX because they represent a form of non-linear losses which might be important in bigger, higher field machines (ITER, DEMO)

EPMs - a fishbone like mode. Losses on NSTX tend to be larger than for avalanches but scaling beyond NSTX is uncertain.

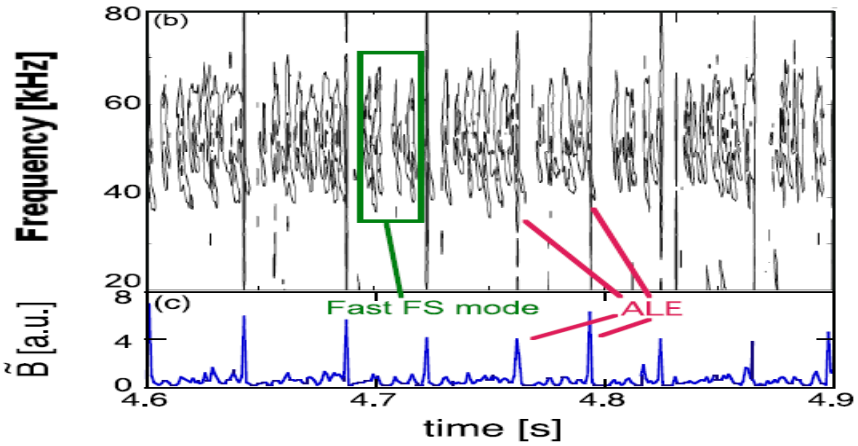

From
The 14th Workshop on Active Control of MHD Stability, Nov. 10 - 12, 2009, PPPL
E. D. Fredrickson et al

Abrupt large-amplitude event（ALE）on JT-60U

M. Ishikawa, et al, NF (2005),1474

EP losses by various MHD activities:
Abrupt massive migrations of EP

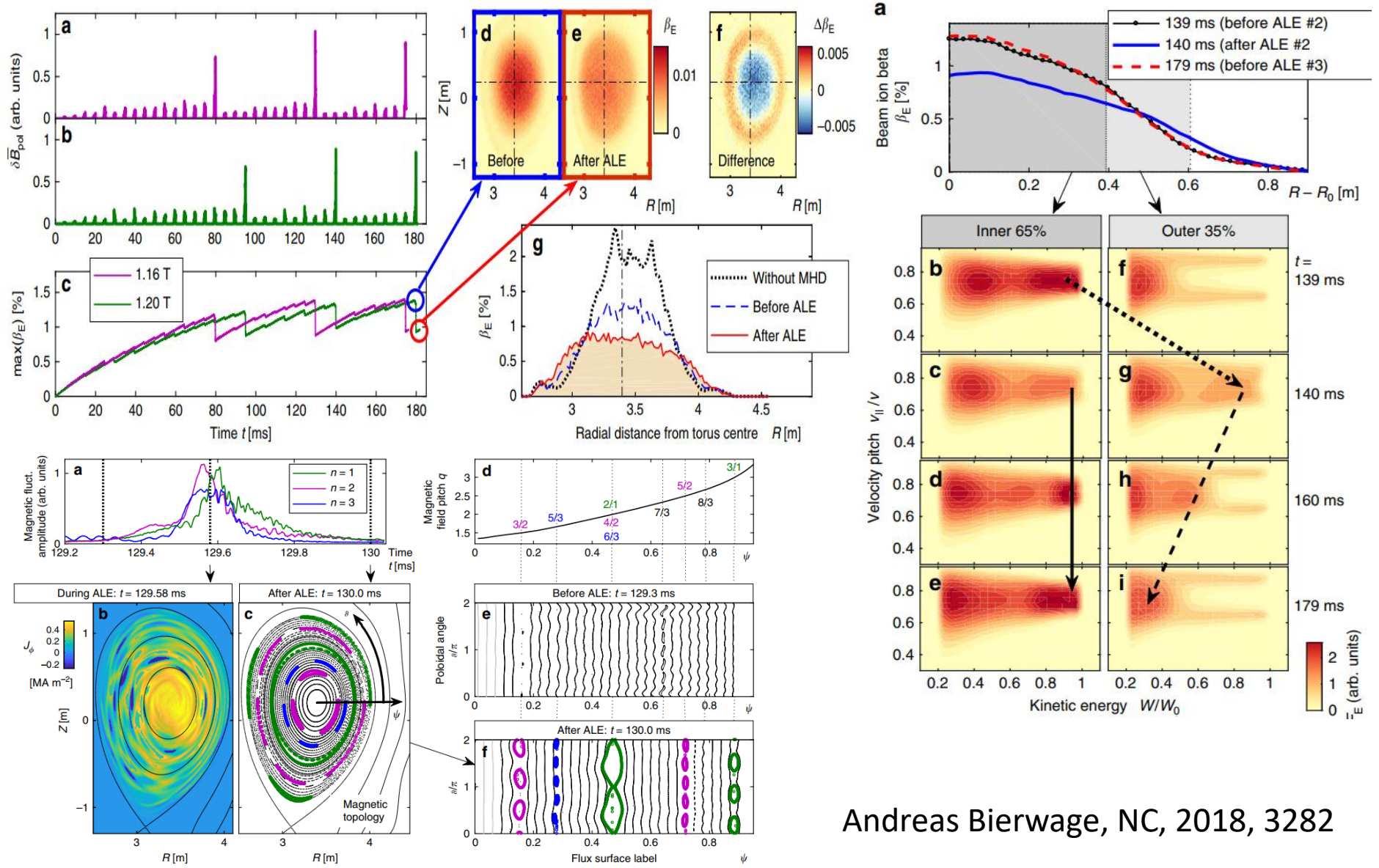

Andreas Bierwage, NC, 2018, 3282

EP losses by various MHD activities:
EP loss Induced by ELMs

Frequent, small ELMs are often accompanied by large fluxes of fast-ion losses during and pre-ELM crash.

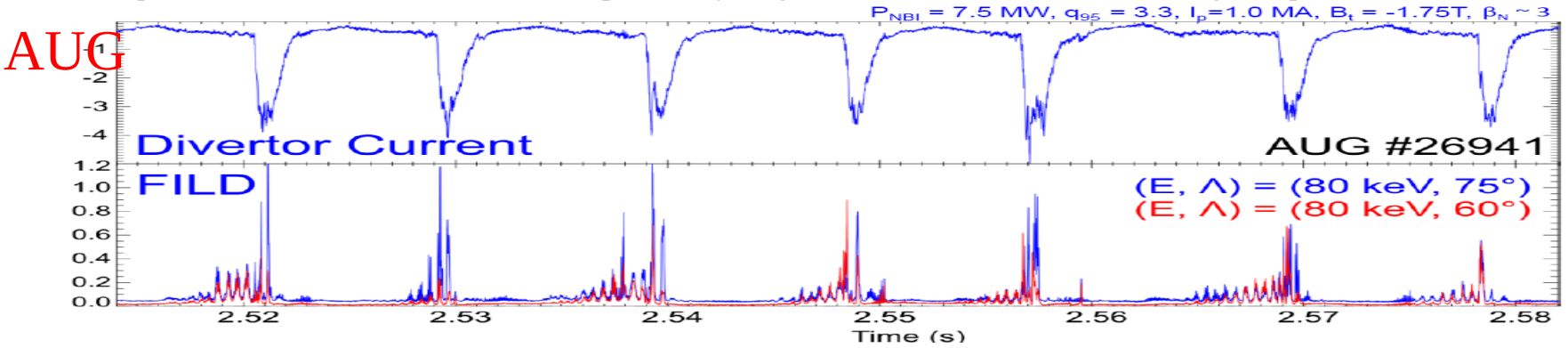

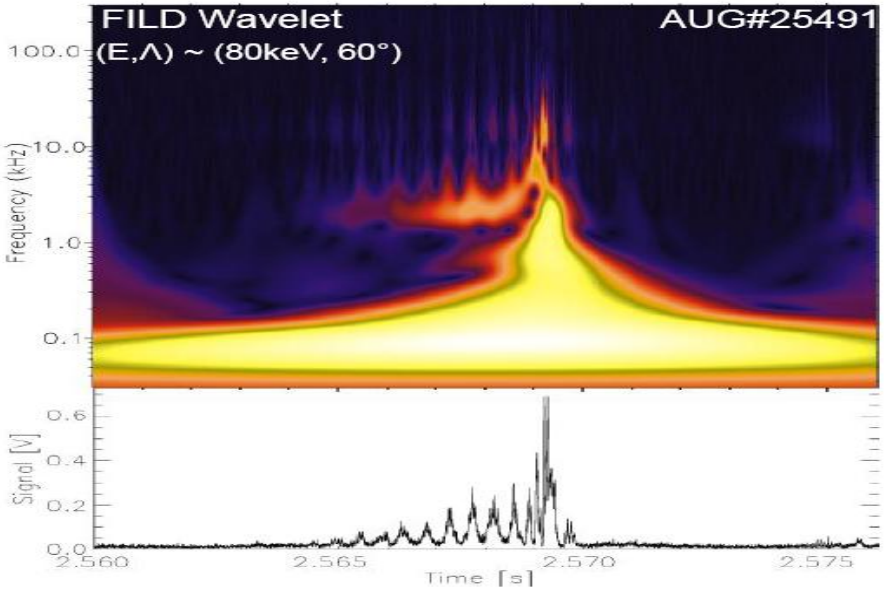

Fast-Ion Losses Increasing Towards ELM Crash

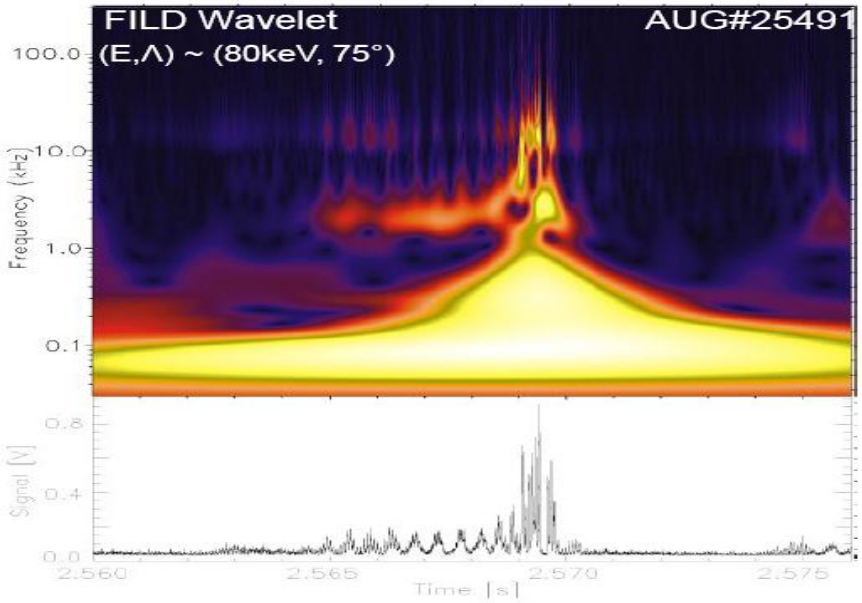

Deeply trapped particles are more strongly affected.

M. Garcia-Munoz，12th IAEA TM on EPs Austin, Texas USA（2011）, O-11

EP losses by various MHD activities:
Fusion product losses by fishbone

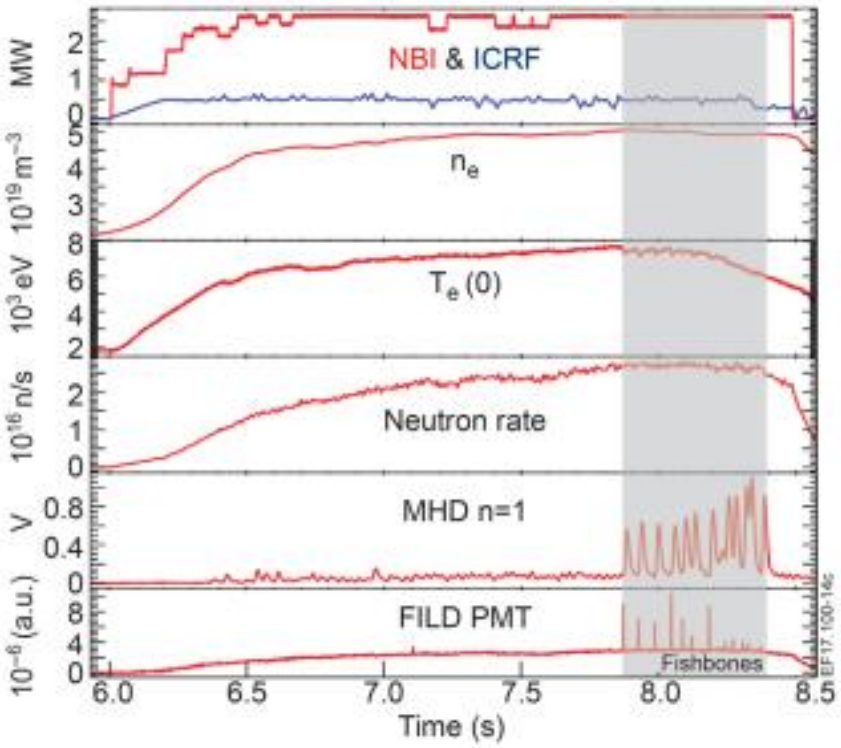

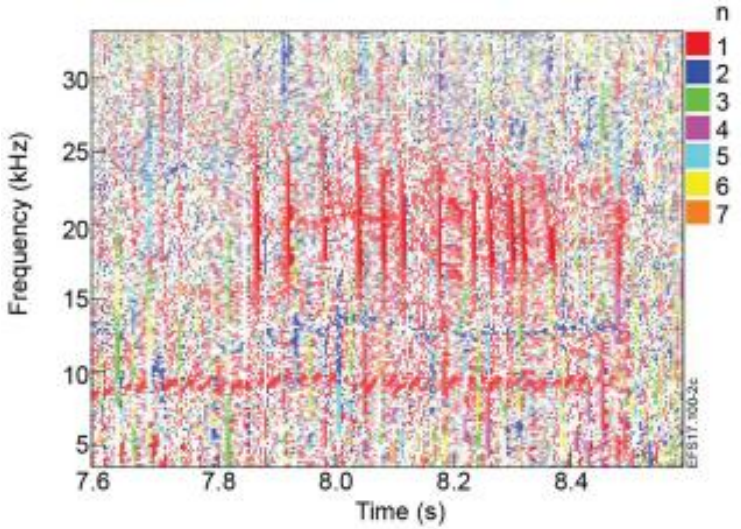

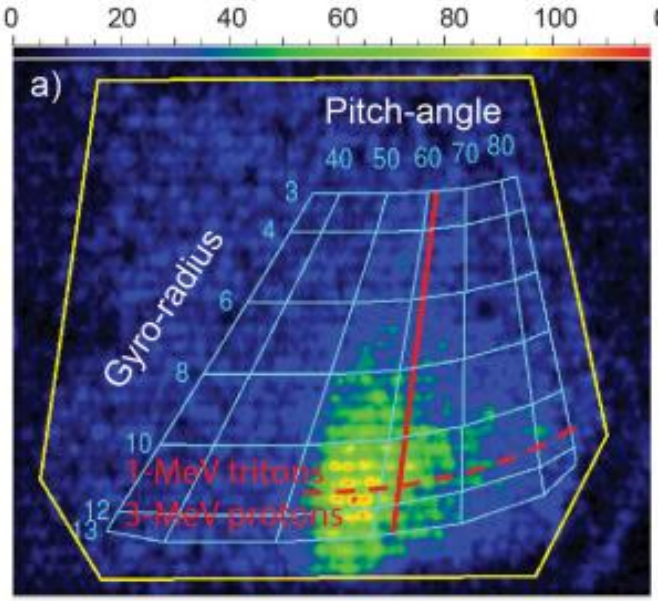

D+D=*p*(3MeV)+*t*(1MeV);
D+D=*n*(2.5MeV)+^{3}*He*(0.82MeV);

Kiptily, *et al*, NF2018, 014003.

Summary

- **Energetic particles:**

– TF ripple induced EP loss
– Destabilization of various Alfven-type instabilities (lead to anomalous transport)
– Redistribution and loss (reduces alpha particle heating efficiency; causes heat loading and damage to plasma-facing components)

- **Integrated with overall plasma behavior:**

– Macro-stability (e.g., fishbone & monster sawtooth; ballooning mode; disruption and runaway electron)
– Transport (e.g., profile modification; rotation generation)
– Heating and current drive (e.g., dominant nonlinear self-heating)
– Edge physics (e.g., resistive wall mode stabilization)
– Burn dynamics (e.g., thermal burn stability, fuel dilution by helium ash)

Some related contents to plasma transport, please see next lecture : Effects of energetic-particles and related instabilities on the plasma transport

高能量粒子实验物理

Part-II: Effects of energetic-particles and related instabilities on the plasma transport

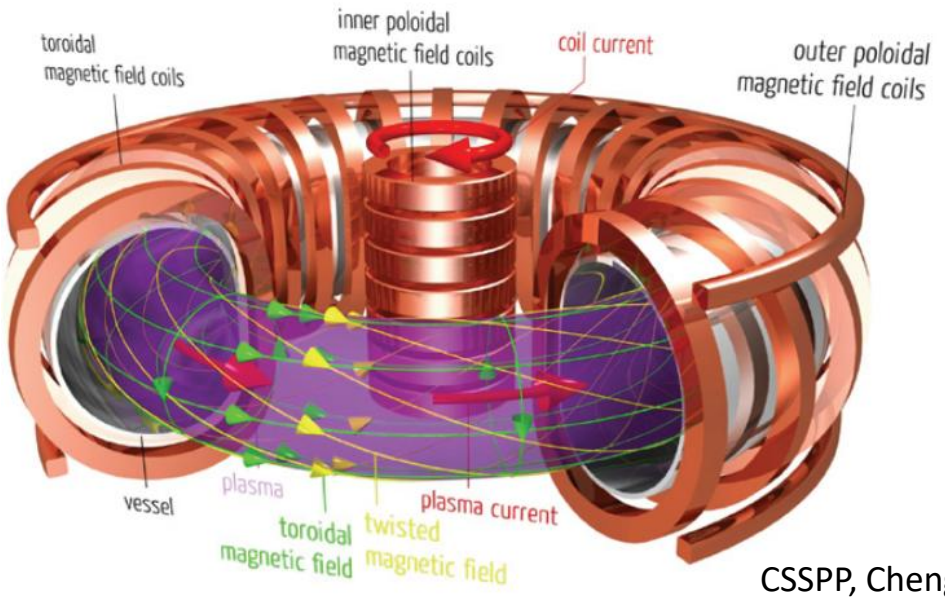

Wei Chen 陳偉

Southwestern Institute of Physics

CSSPP, Chengdu, July 18, 2024

EP/EP instability effects on plasma transport

- To our knowledge, many experimental results indicate EPs and related instabilities have important effects on the plasma transport, including H-mode and transport barrier physics.

- These phenomena mentioned here are extremely complex which not only cover wave-particle interaction but also wave-wave coupling, meanwhile it also refers to various spatial-temporal scales, so it has a big challenge for the multi-scale physics and simulation.

- Therefore, they are not conclusive. Here only throw out a minnow to catch a whale. The related validation is needed, especially mechanisms. Many parameters (local&global) are needed to measure, such as EP redistribution/transport, E_r, flow shear and turbulence measurements.

Outline

- Multi-scale interactions associated with EP/ EP instabilities
- Improvement of confinement induced by small AE burst
- EP instabilities related to transport channel
- EP instabilities related to ZFs/GAM
- EP instabilities decay into ZFs/GAM and other modes
- Transport barriers and nonlocal triggered by EP instabilities
- ELM triggered by EP instabilities
- Pedestal collapse triggered by nonlinear dynamics of AEs
- MHD spectroscopy
- Summary

Multi-scale interactions

Increasing Spatial Scale

(I)

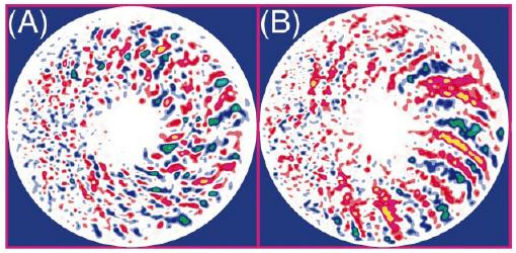

❖*Z. Lin, Science, 1998*

I. Micro-scale (L~ ρ_i)

Drift-wave turbulence
(High-n mode, n>>1)
- ❖**ITG**
- ❖**TEM**
- ❖**…**

No strict bounds !

(II)

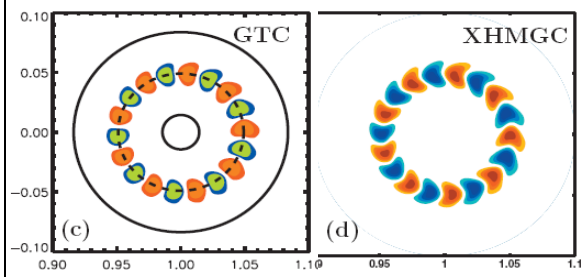

❖*H. Zhang, PoP, 2010*

II. Meso-scale (L~ρ_{EP})

Alfven eigenmode & ZFs
(Low & Moderate-n mode)
- ❖**TAE/RSAE**
- ❖**BAE**
- ❖**ZF/GAM**
- ❖**…**

(III)

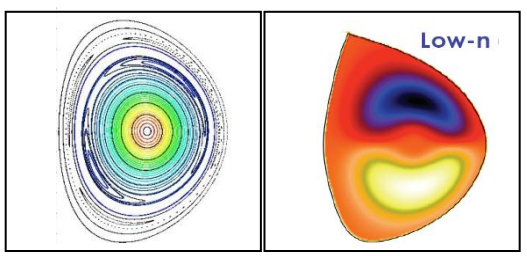

❖*NIMROD Progress Report,2001*
❖*G. Fu, M3D-K code, 2008*

III. Macro-scale (L~ a)

MHD mode & EGAM
(Low-n mode, n=0&1)
- ❖**Sawtooth**
- ❖**Tearing mode**
- ❖**Kink mode**
- ❖**EGAM**
- ❖**…**

Multi-scale interactions:
SAW instability excited by thermal ions

A “Sea of Core Localized Alfven Eigenmodes” Observed in DIII-D Quiescent Double Barrier (QDB) Plasmas

Nazikian et al PRL 105006 (2006)

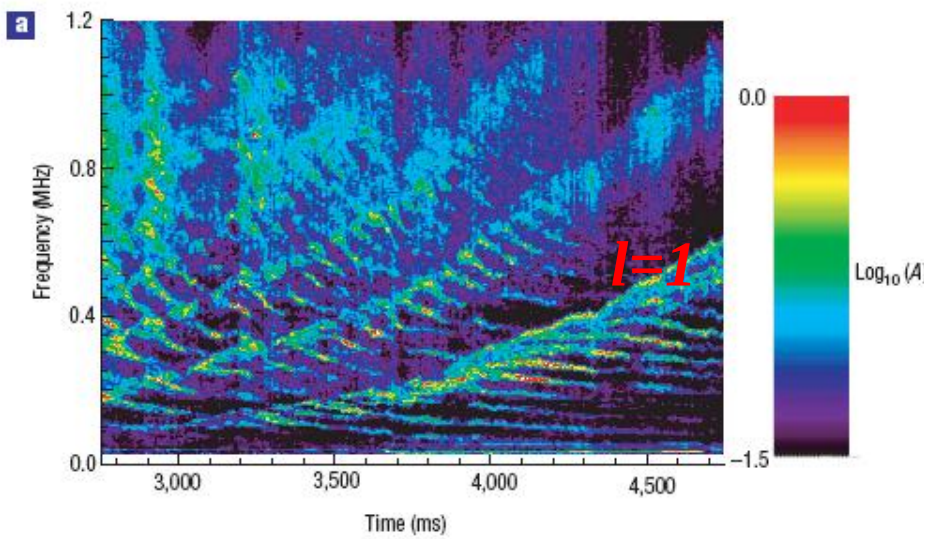

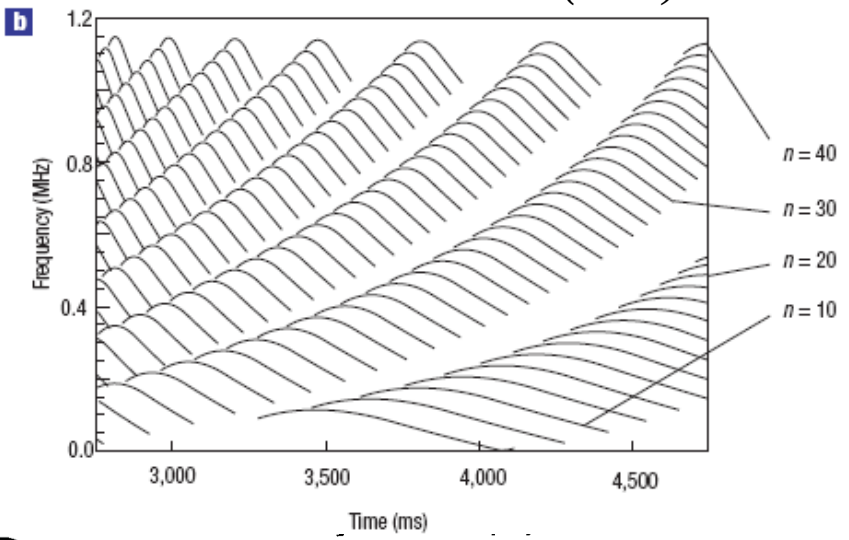

Thermonuclear ringtones !

Cowley, Nature physics 299 (2006)

n=40 ⇒ $k_\theta \rho_{it} \sim O(1)$ ⇒ **SAW instability by thermal ions !**

Band of modes *m=n+l, l=1,2,3, …*

$f_{n+1}-f_n \sim = f_{rot}$, $v_{//} \sim = 0.3 v_A$

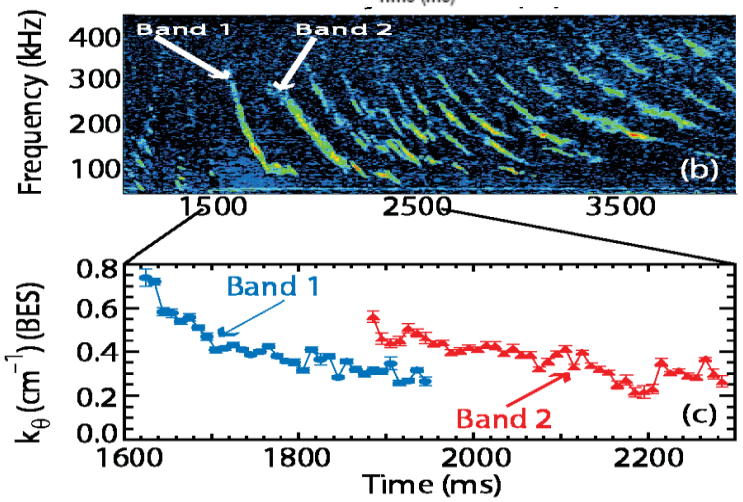

Multi-scale interactions:
Nonlinear coupling between BAEs/EGAM/LF MHD

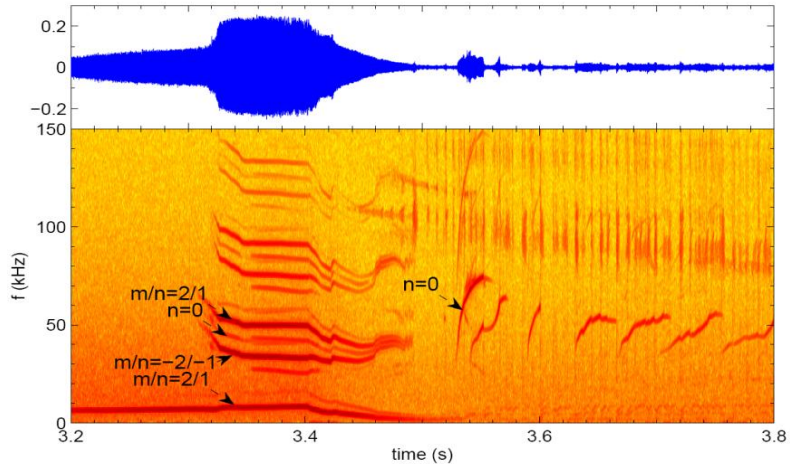

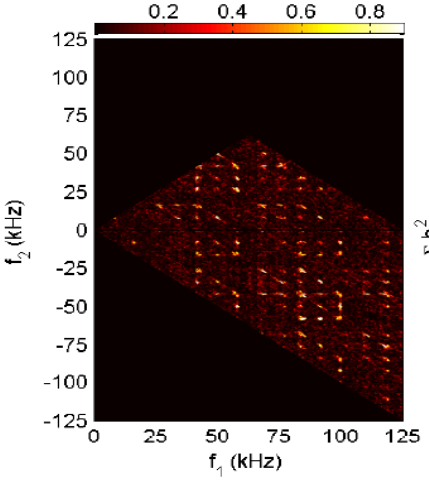

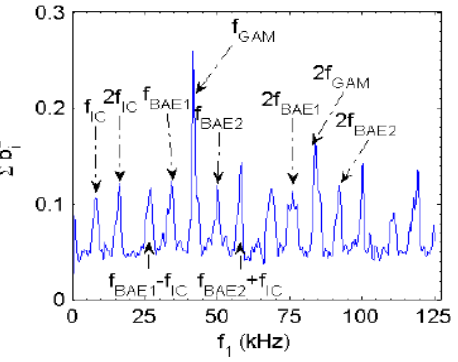

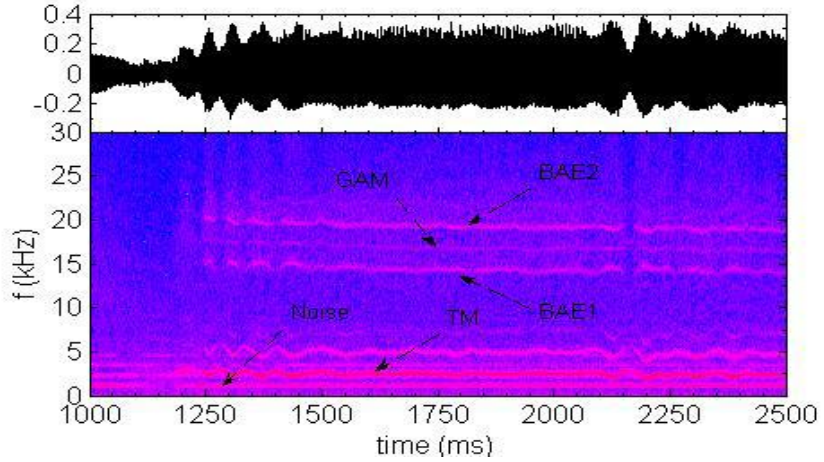

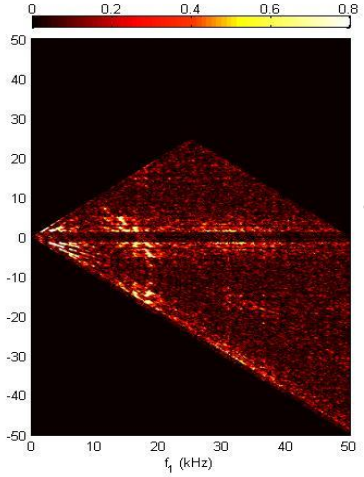

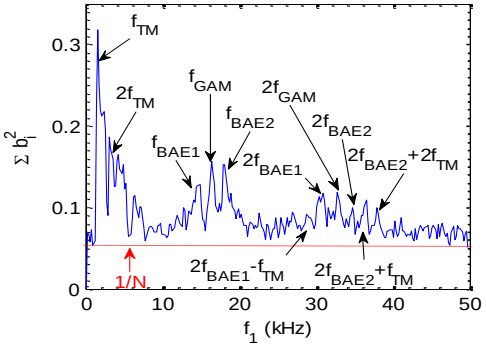

Multi-scale interaction: produce different scale structures, determine their excitation/saturation/damping, transfer wave energy among different scale structures, affect the plasma confinement/transport.

Multi-scale interactions:

Nonlinear modulation between AITG/KBM and kink mode, turbulence

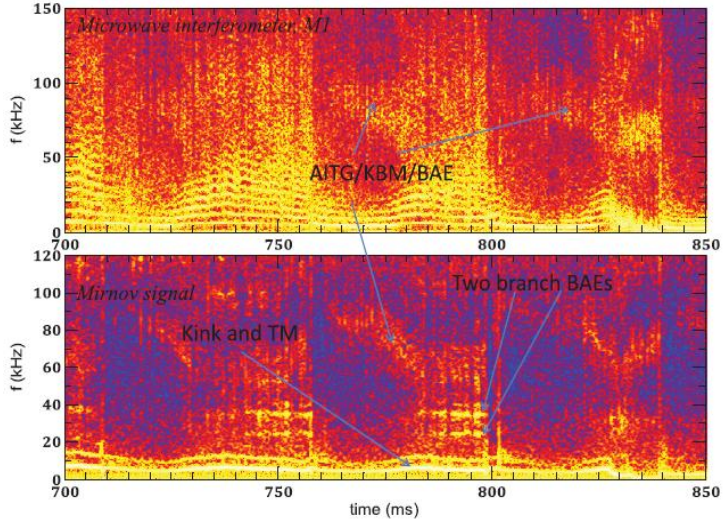

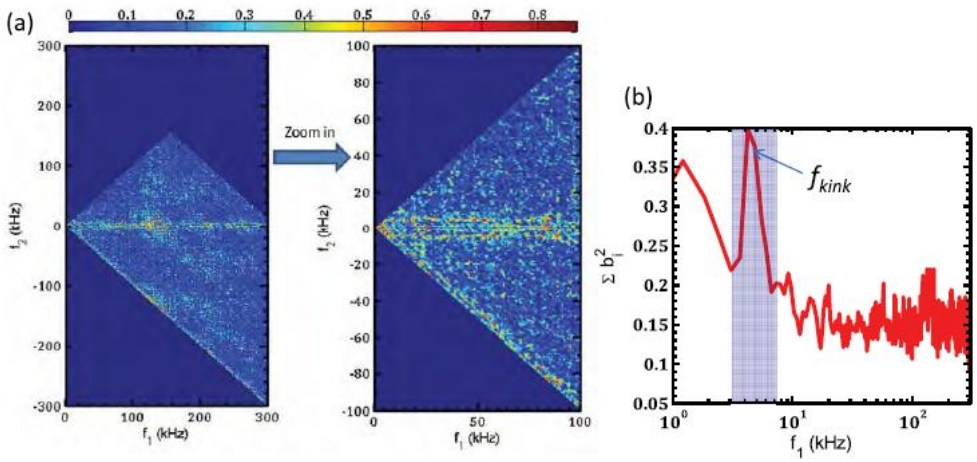

Auto- (*a*) and squared-bicoherence (*b*) of the envelope of the microwave interferometer in the range f = 300-40 kHz

- Multi-scale interactions have been observed recently in the HL-2A core NBI plasmas, including the synchronous coupling between 1/1 kink mode and 2/1 tearing mode, nonlinear couplings of TAE/BAE and 2/1 TM near q = 2 surface, AITG/KBM/BAE and 1/1 kink mode near q = 1 surface, and between 1/1 kink mode and high-frequency turbulence.

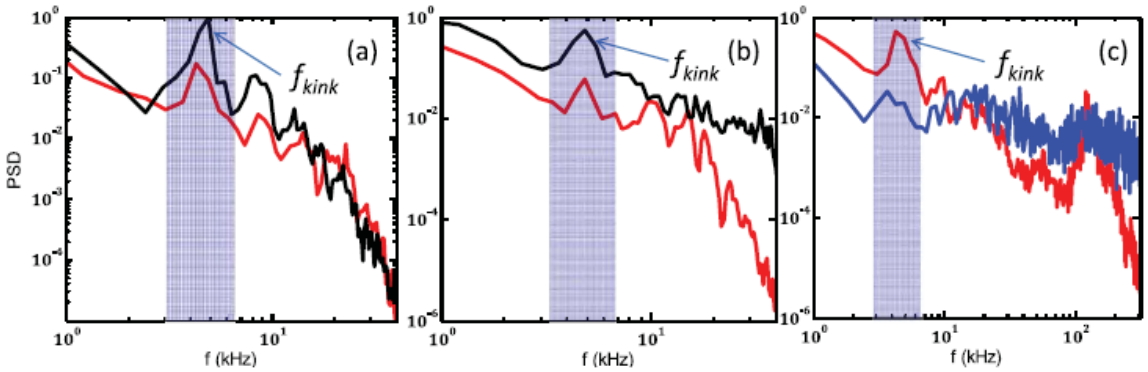

Power spectrum densities (PSDs) of the envelopes of microwave interferometer (red), core ECEI (blue) and Mirnov (black) signals. Filter range: (*a*) 40–90 kHz, (*b*) 90–240 kHz and (*c*) 40–240 kHz.

Chen, et al, NF (lett.) ***57*** *(2017) 11400311*

Improvement of confinement triggered by small TAE bursts

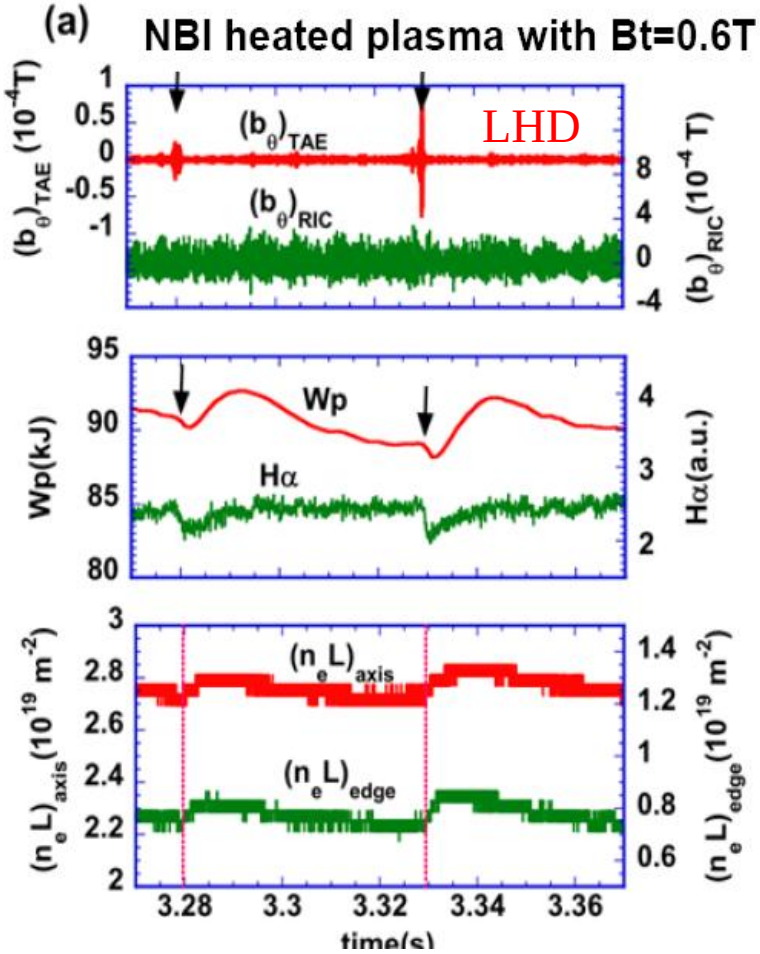

Just after the TAE burst,

❖jump up stored energy and the line averaged electron density

❖sharp drop and slow recovery of Hα-emission.

Transient improvement of confinement triggered by TAE bursts.

Change in E_r caused by the loss and/or redistribution of co-passing EPs.

K Toi, et al., PPCF 53, 024008 (2011).

AEs maybe induce fusion power enhancement in future reactors when the modes become large amplitudes.

Sugiyama, et al, PPCF2018, in press.

EPs/EPIs related to transport channel

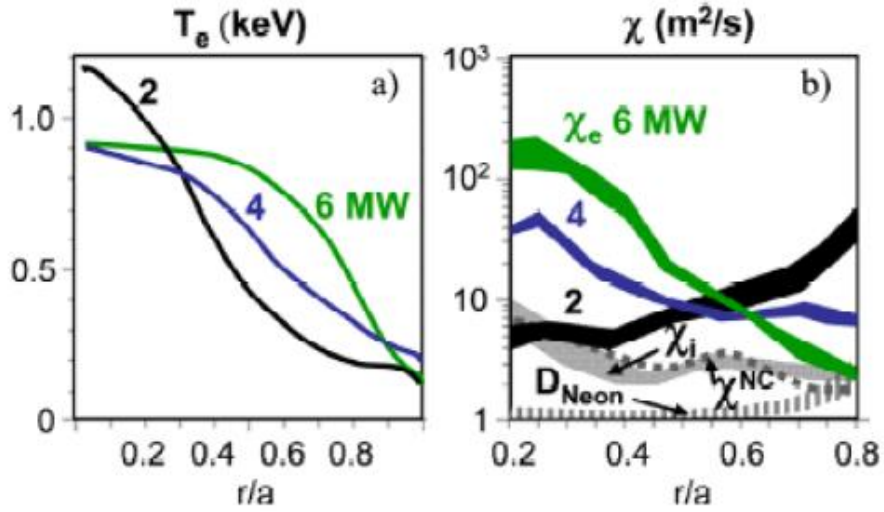

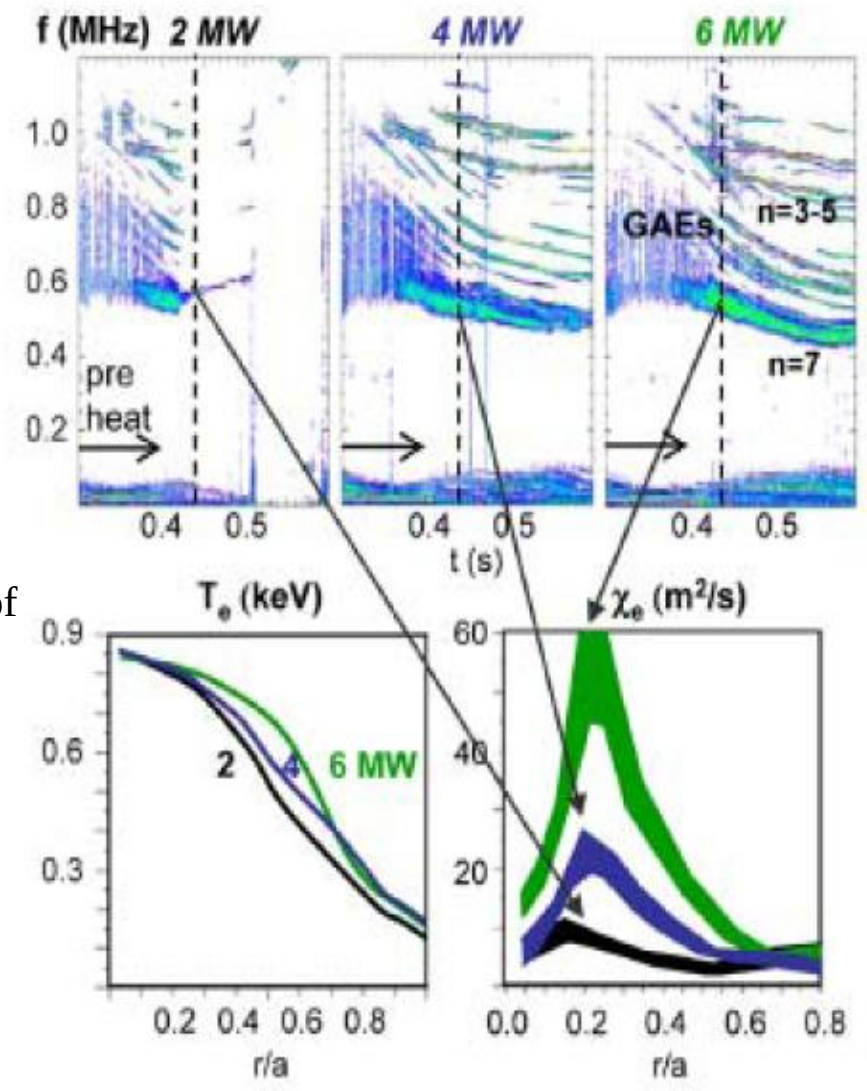

EPs instabilities can affect plasma heating and rotation by channeling the energy and momentum of the energetic ions to the region where the destabilized waves are damped. Because of the energy channeling, the plasma core may not be heated by the energetic ions even when these ions have a very peaked radial distribution. The momentum channeling can lead to plasma rotation and frequency chirping due to the Doppler shift varying in time.

D. Stutman et al., PRL 102, 115002 (2009).

Kolesnichenko Y I, et.al. 2010 PRL 104 075001

Kolesnichenko Y I et al 2010 NF 50,084011

EPs/EPIs related to ZFs/GAM

Oscillatory Zonal Flows Driven by Interaction between Energetic Ions and Fishbone-like Instability in CHS

S Ohshima, *PPCF* ***49*** *(2007) 1945*

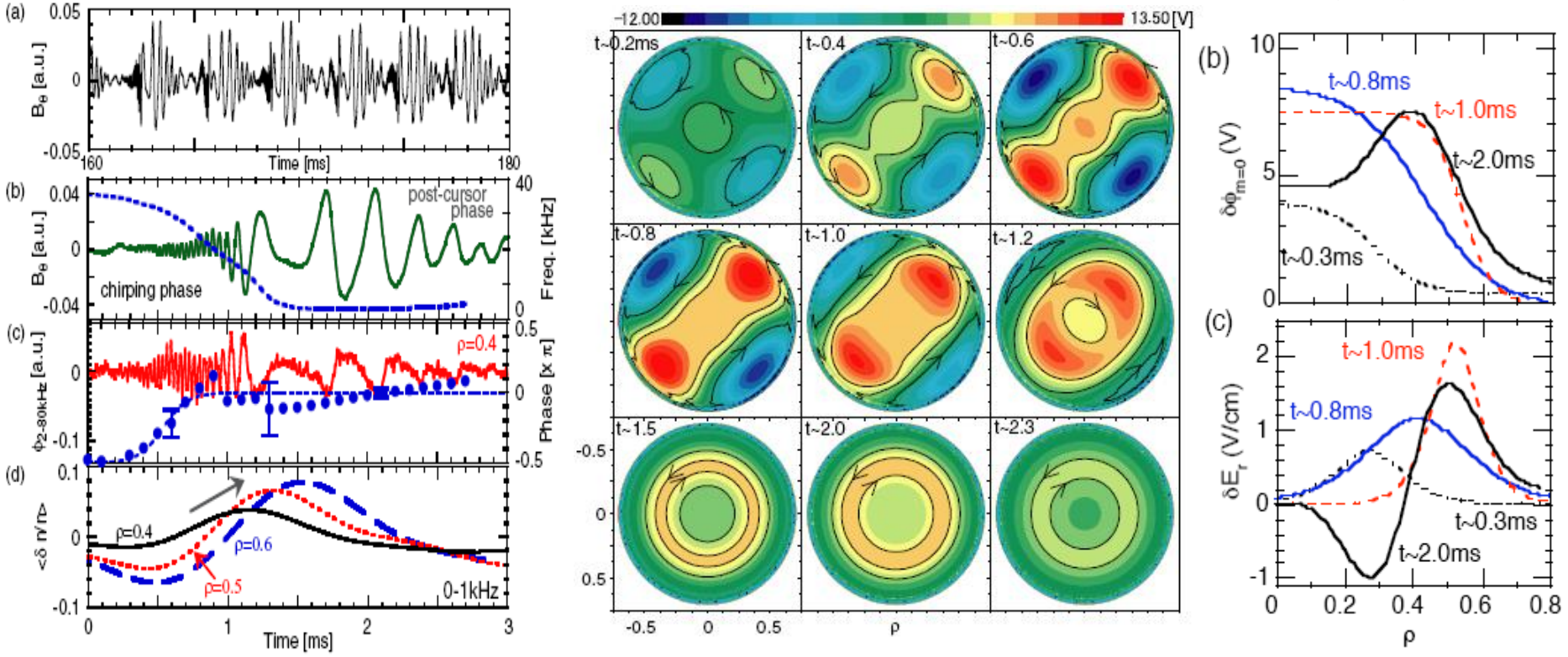

The results have given the finest observation of the internal structure of plasma quantities, such as electric field, density and magnetic field distortion, which nonlinearly develop during the MHD phenomenon. In particular, the finding of a new kind of oscillating zonal flow driven by interaction between energetic particles and MHD modes should be emphasized for burning state plasmas.

EPs/EPIs related to ZFs/GAM

EGAM can modulate amplitude of high frequency of density fluctuations.

LHD

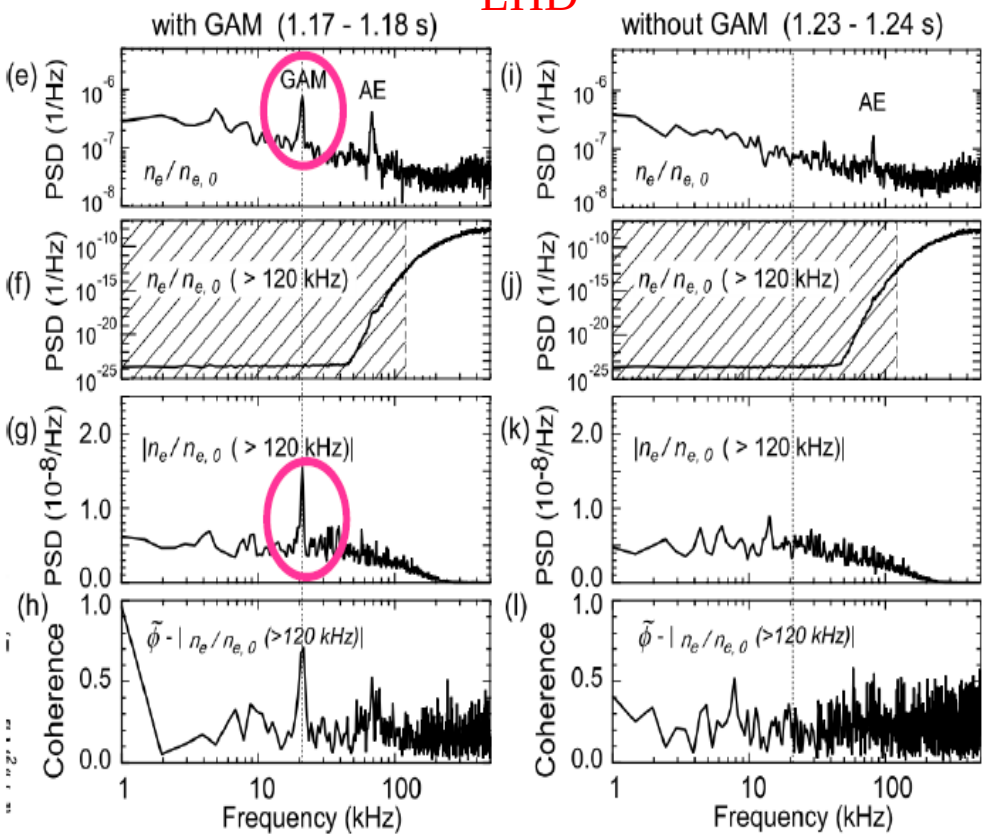

Significant coherence between **electrostatic potential fluctuation** and **envelope of the high-freq. density fluctuation** is observed at f_{GAM}.

High-freq. fluctuation is modulated by the **ExB flow** associated with the GAM.

This modulation is consistent with the observation of **E_r fluctuation**.

T. Ido, et al., NF 51, 073046 (2011).

EPs/EPIs related to ZFs/GAM

BAE+IC ➡ EGAM/GAM

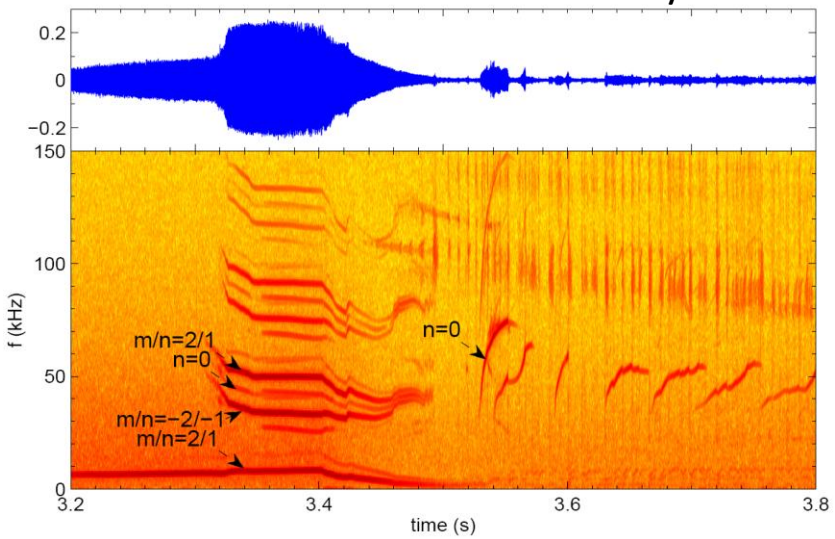

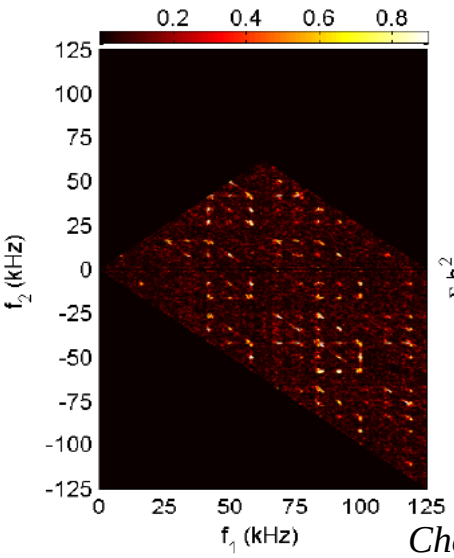

LHD

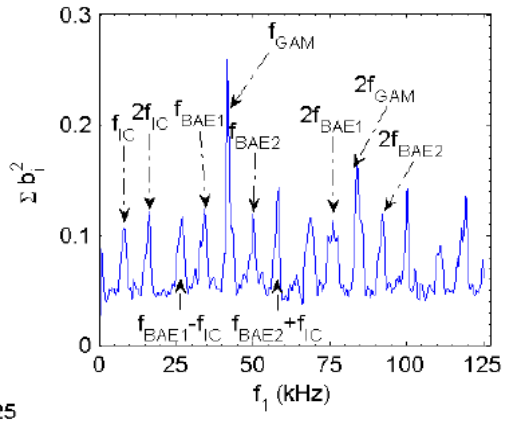

Chen W , ITC2011, O-1.

BAE+TM ➡ EGAM/GAM

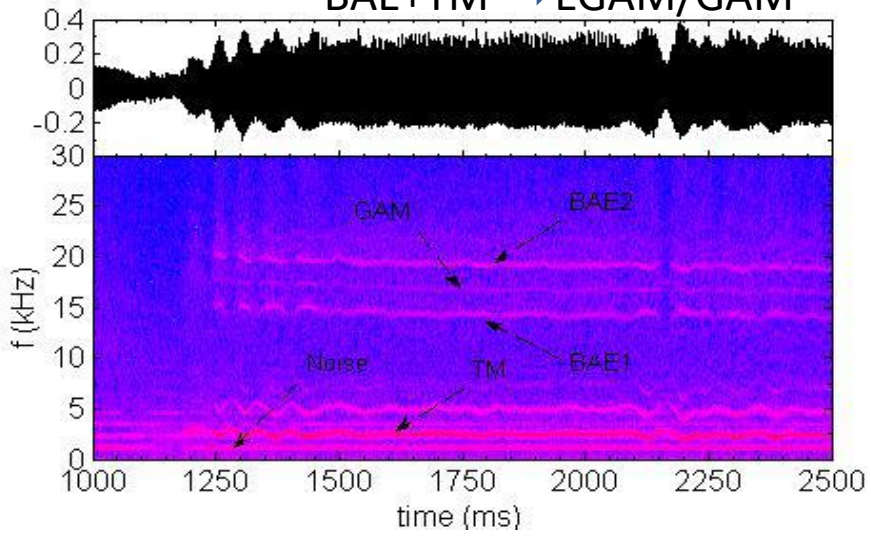

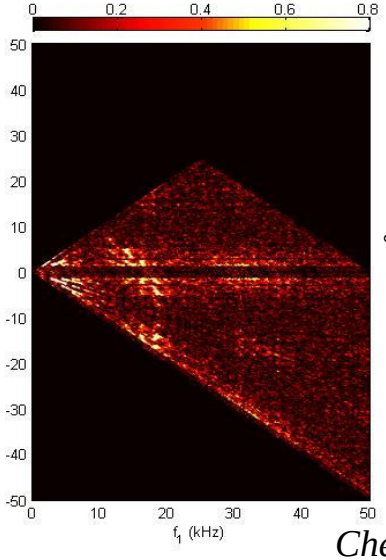

HL-2A

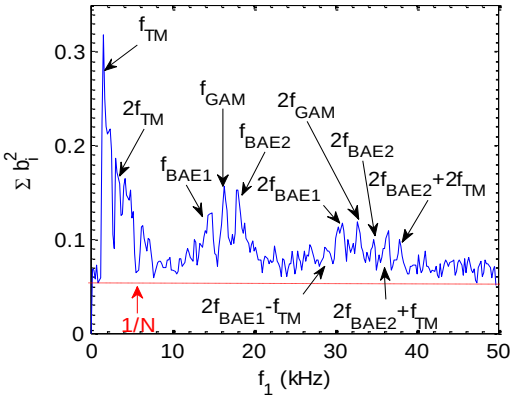

Chen W, IAEA2012, EX/5-3.

EPs/EPIs related to ZFs/GAM

Zonal flow and GAM generated by nonlinearity of EP instabilities.

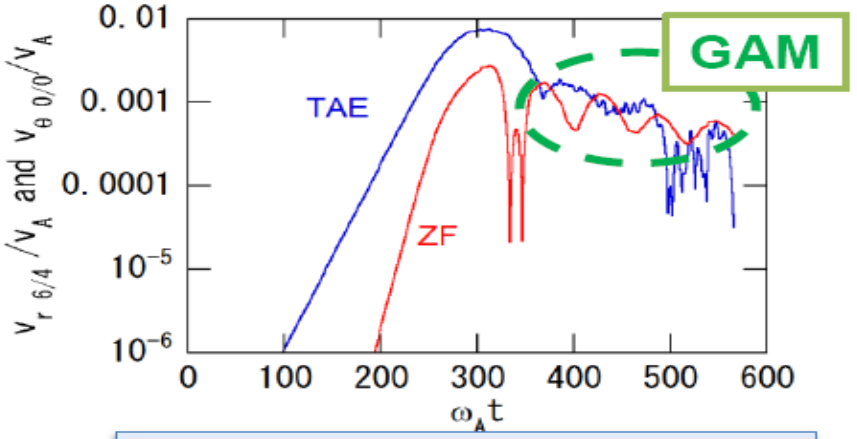

Evolution of TAE and ZF

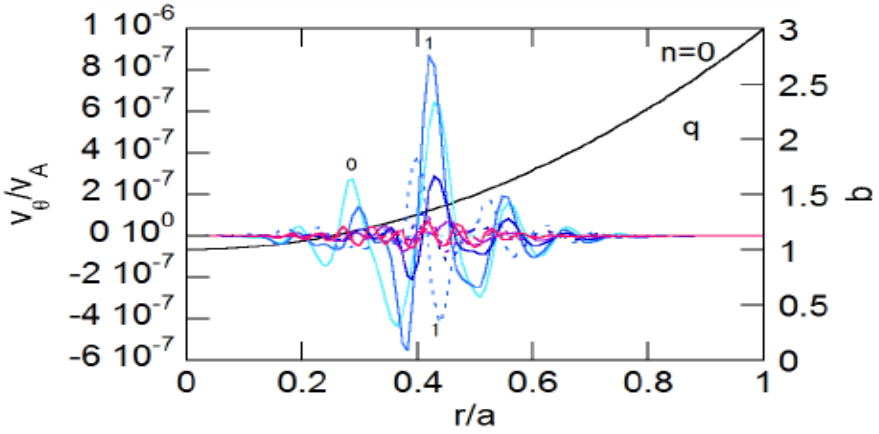

Spatial profile of ZF

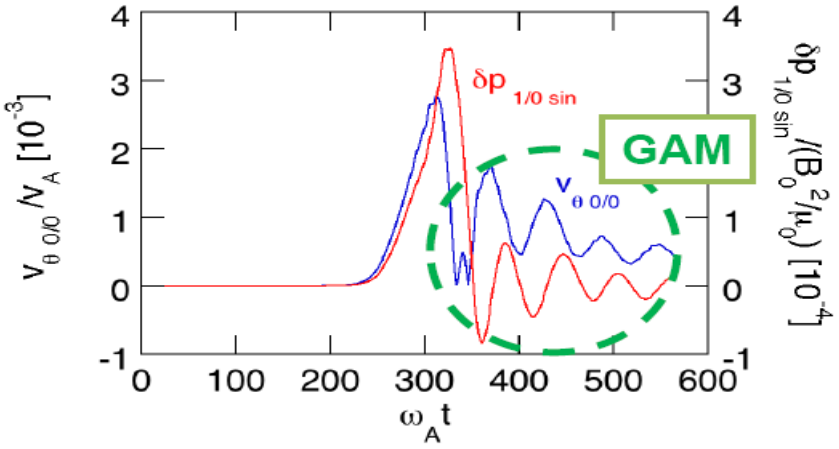

n = 0 modes, **ZF**, are primarily generated by the coupling of two n = 4 harmonics of the TAE mode.

n=0 mode oscillates after TAE saturation →**GAM**

Y. Todo, et al., NF 50, 084016 (2010).

EP instabilities decay into ZFs/GAM and other modes

Nonlinear Excitations of Zonal Structures by Toroidal Alfvén Eigenmodes

Liu Chen*
Institute for Fusion Theory and Simulation, Zhejiang University, Hangzhou 310027, People's Republic of China and Department of Physics and Astronomy, University of California, Irvine, California 92697-4575, USA

Fulvio Zonca
Associazione Euratom-ENEA sulla Fusione, Via E. Fermi 45–C.P. 65–00044 Frascati, Italy and Institute for Fusion Theory and Simulation, Zhejiang University, Hangzhou 310027, People's Republic of China

PRL 109, 145002, 2012

It is shown that zonal flow or structure spontaneous excitation is more easily induced by finite amplitude TAEs including the proper trapped-ion responses, causing the zonal structure to be dominated by the zonal current instead of the usual zonal flow.

Nonlinear Decay and Plasma Heating by a Toroidal Alfvén Eigenmode

Z. Qiu,[1,*] L. Chen,[1,2] F. Zonca,[3,1] and W. Chen[4]
[1]*Institute for Fusion Theory and Simulation and Department of Physics, Zhejiang University, Hangzhou, People's Republic of China*
[2]*Department of Physics and Astronomy, University of California, Irvine California 92697-4575, USA*
[3]*ENEA, Fusion and Nuclear Safety Department, C.R. Frascati, Via E. Fermi 45, 00044 Frascati (Roma), Italy*
[4]*Southwestern Institute of Physics, P.O. Box 432 Chengdu 610041, People's Republic of China*

PRL 120, 135001, 2018

A TAE can parametrically decay into a GAM and KTAE in a toroidal plasma. This decay process, in addition to contributing to the nonlinear saturation of EP or α-particle driven TAE instability, could also contribute to the heating as well as regulating the transports of thermal plasmas.

Transport barriers triggered by EP instabilities:

Fast ITBs triggered by fishbone

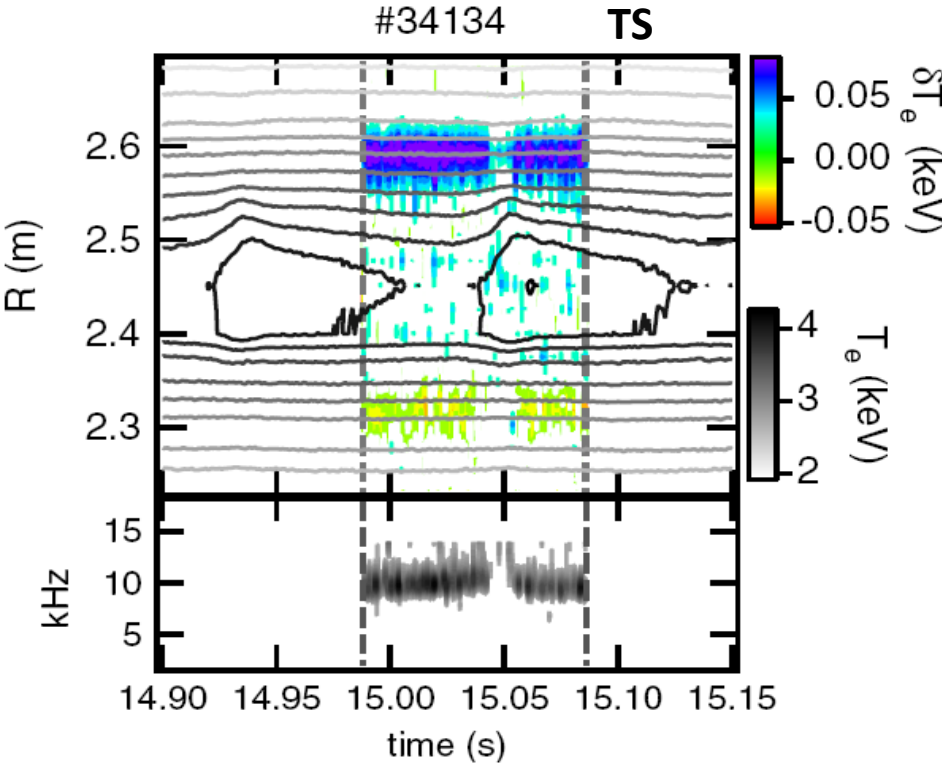

Contour plot of electron temperature superimposed to the radial structure of the MHD mode (top), and frequency of the mode (bottom).

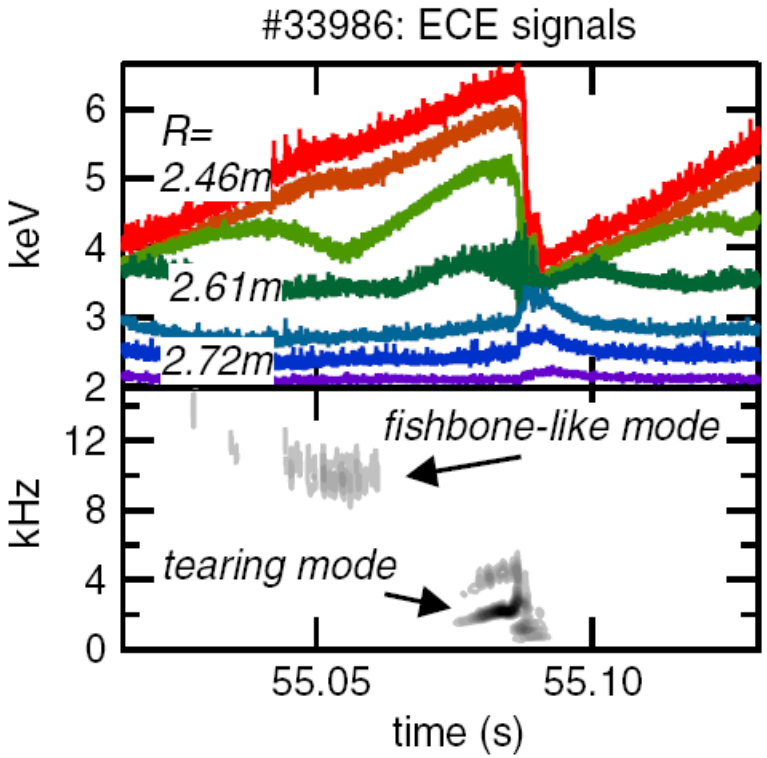

MHD activity during the GO-regime: time trace of electron temperature at various positions (top) and spectrogram of ECE signal at R = 2.6m. *Magnet, et al NF2006, 797*

The presence of MHD modes manifests the importance of low order rational values of the safety factor for oscillating regimes, and for the triggering of transport barriers in negative magnetic shear plasmas.

Transport barriers triggered by EP instabilities:

Fast ITBs triggered by fishbone

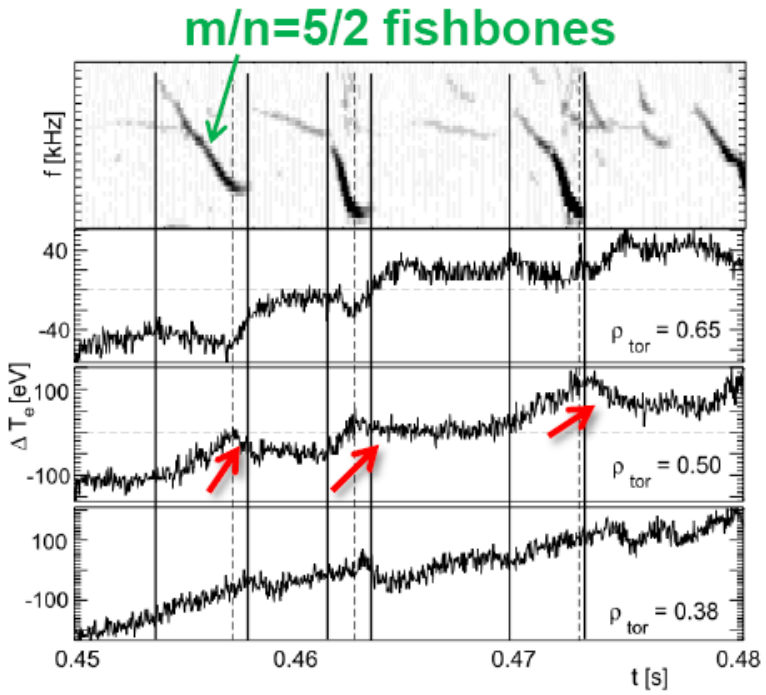

During the period of frequency whistling down, the temperature rapidly rises in the region close to the outer surface of (rho~0.5).

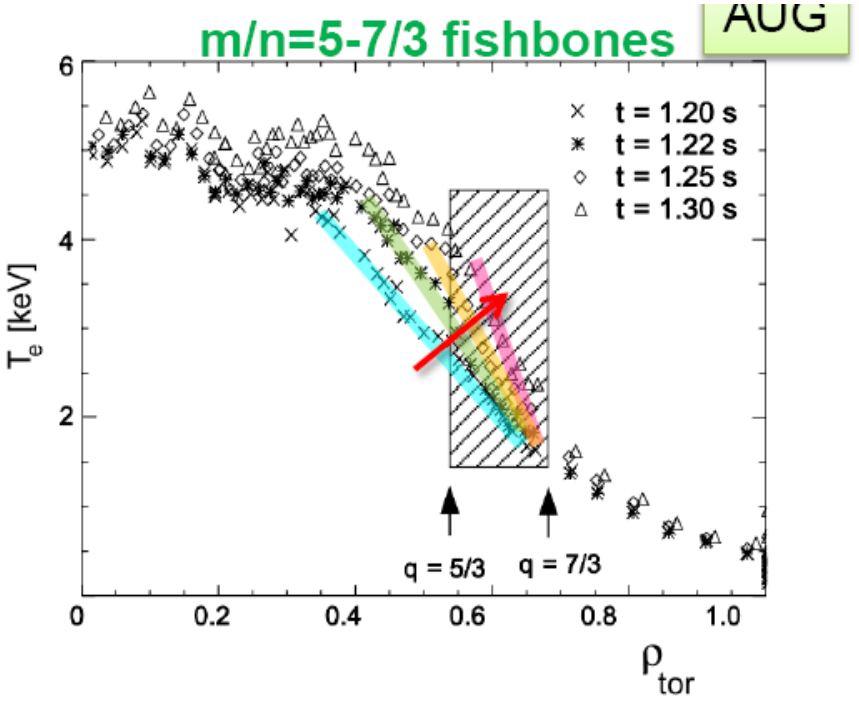

Immediately after the onset of fishbones, temperature gradient was increased at the radial location of the corresponding rational surfaces of the fishbones.

EP instability leads to **EP redistribution.**
→ J_r^{EP} → E_r → **ExB shear flow**
→ **Turbulence Suppression** → **ITB formation**

S. Gunter, et al., N 41, 1283 (2001)

Transport barriers triggered by EP instabilities:

Fast ITBs triggered by fishbone

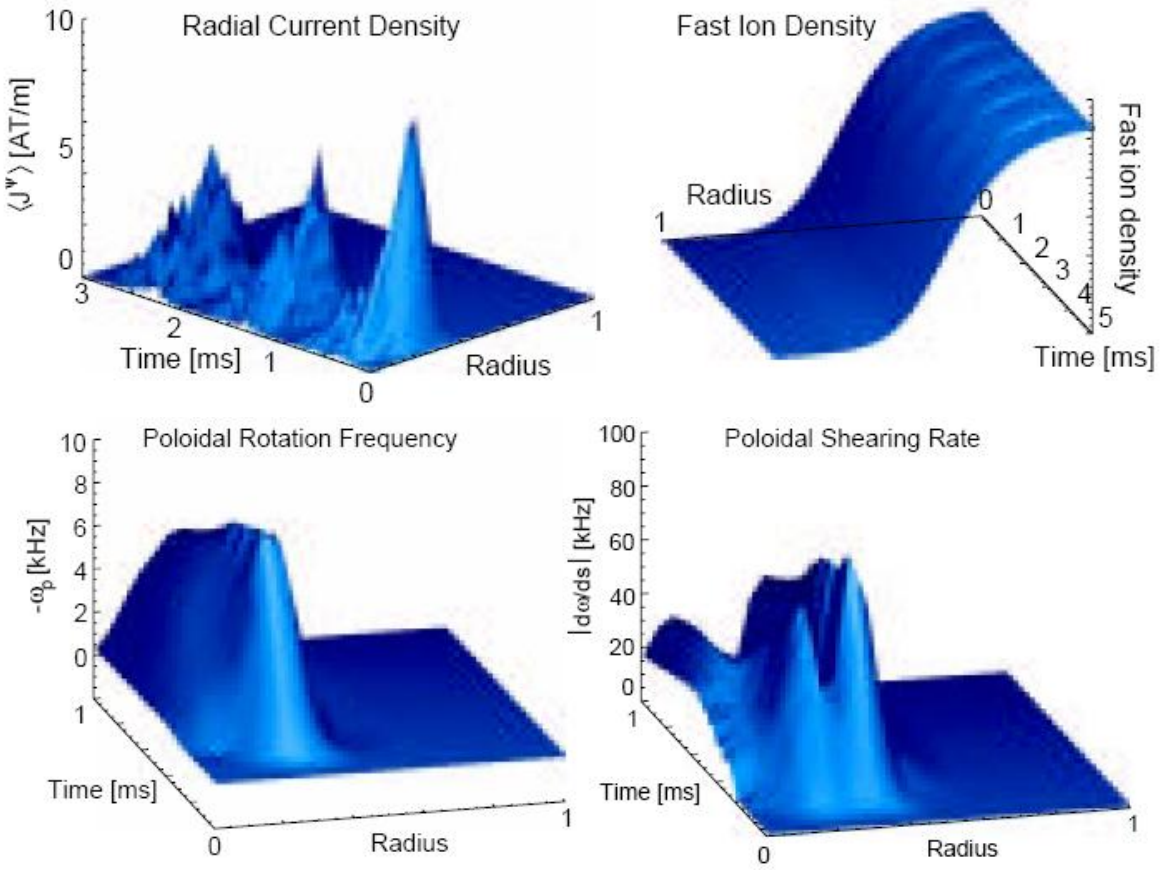

Time dependent radial fast ion current density and the corresponding variation of fast ion radial distribution function arising from fishbone bursts every 1 ms.

Calculation of the poloidal rotation arising from the HAGIS simulation of a fishbone burst and the corresponding poloidal shearing rate.

*Pinches S.D. et al 2001 ECA **25A** 57*

The mechanism by which this happens may be summarized as follows: The fast ions resonantly interact with the kink distortion of the magnetic field and are radially expelled leading to a radial current, or equivalently, an electric field. This produces a sheared E × B flow which if sufficiently large to overcome the growth rate of the turbulent eddies ($\omega_{E\times B} > \gamma_{max}$) can lead to their destruction and to a region of reduced radial transport.

Transport barriers triggered by EP instabilities:

ITB triggering at low-order rational q_{min}

ITB formation by low order rational surface

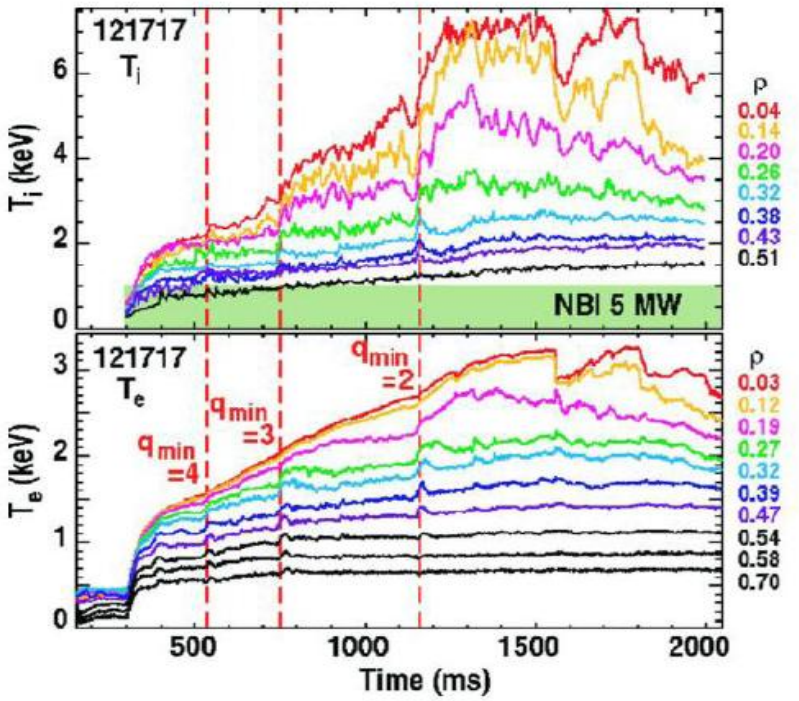

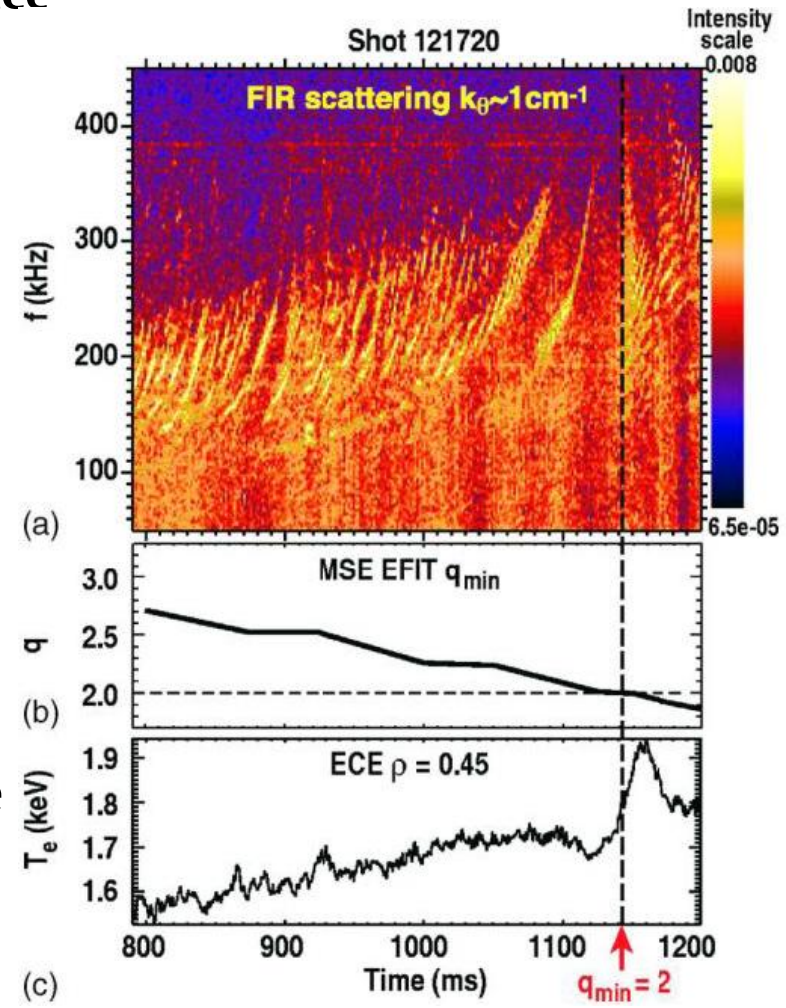

- Ion and electron transport change in the vicinity of integer q_{min}.
- "Grand cascade" of RSAEs at integer values of q_{min} .

M. E. Austin, et al, PoP 13, 082502 (2006).

Transport barriers triggered by EP instabilities:

ITB triggering at low-order rational q_{min}

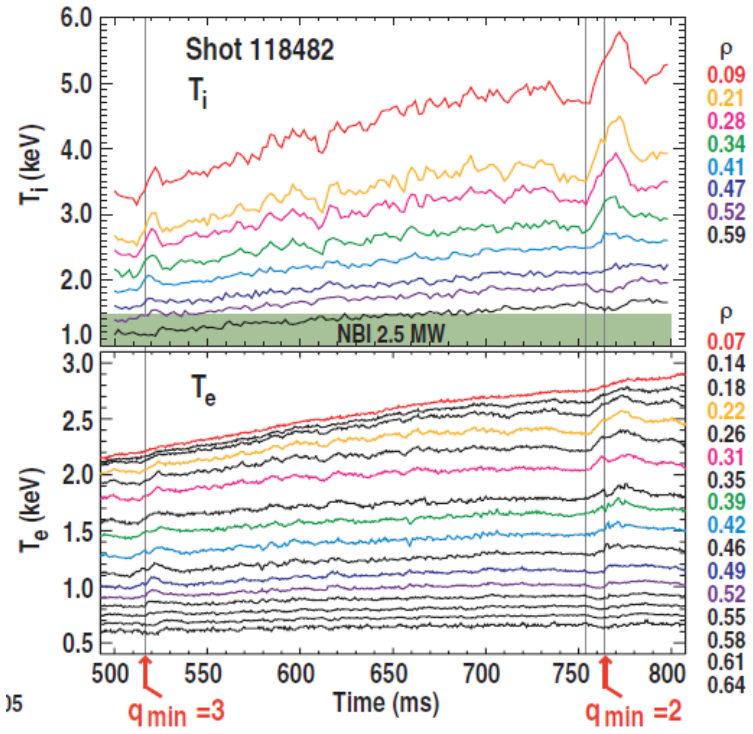

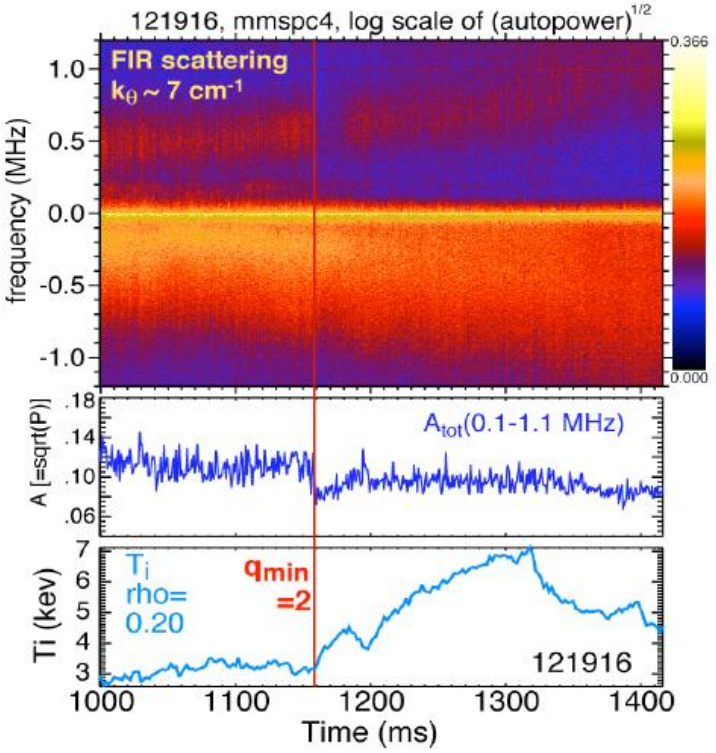

- Typical L-mode NCS discharge with step-wise changes in transport near integer $q_{min.}$
- Sustained core barrier formation when q_{min} is near integer requires correct input power.

- Both transient and long term changes are seen in intermediate k data.
- Drop in low k fluctuations (k <3cm^{-1}) also seen on BES.
- The persistent reduction is consistent with steady state core barrier.

Transport barriers triggered by EP instabilities:

ITB triggering at low-order rational q_{min}

As seen through the radial–temporal evolution of the flux-surface averaged E × B shear $\gamma_{E\times B} = r\partial r(Er/rB)$, localized dipolar layers of maximum shear emerge that define "valleys" of radially concentrated mean flows and hindered turbulent transport (bottom) interspersed between regions of turbulent avalanching.

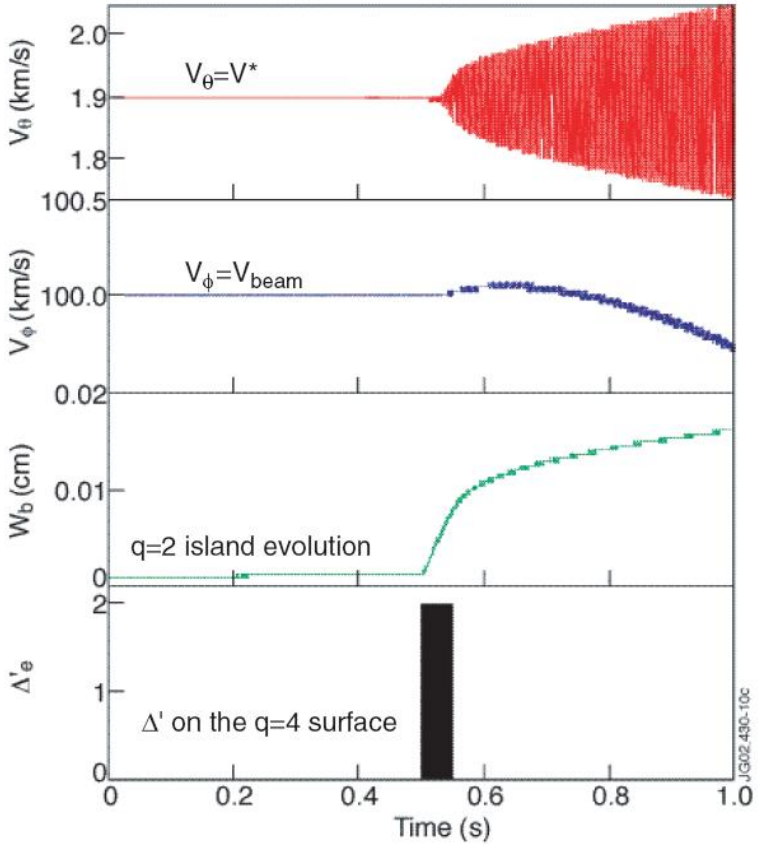

Simulation of the poloidal and toroidal flow at the $q = 2$ surface when an edge perturbation grows at the $q = 4$ surface at the edge. As coupling occurs (at $t = 0.5$s), the $q = 2$ island grows, and the poloidal velocity starts to be strongly affected. The oscillations of V_θ indicate that the two modes are not fully locked, but braking of the plasma flow does occur.

Once an ITB is triggered, an $E \times B$ shear flow develops and its location follows the integral q surface.

Joffrin, et al NF2003, 1167

Transport barriers triggered by EP instabilities:

ITB triggering at low-order rational q_{min}

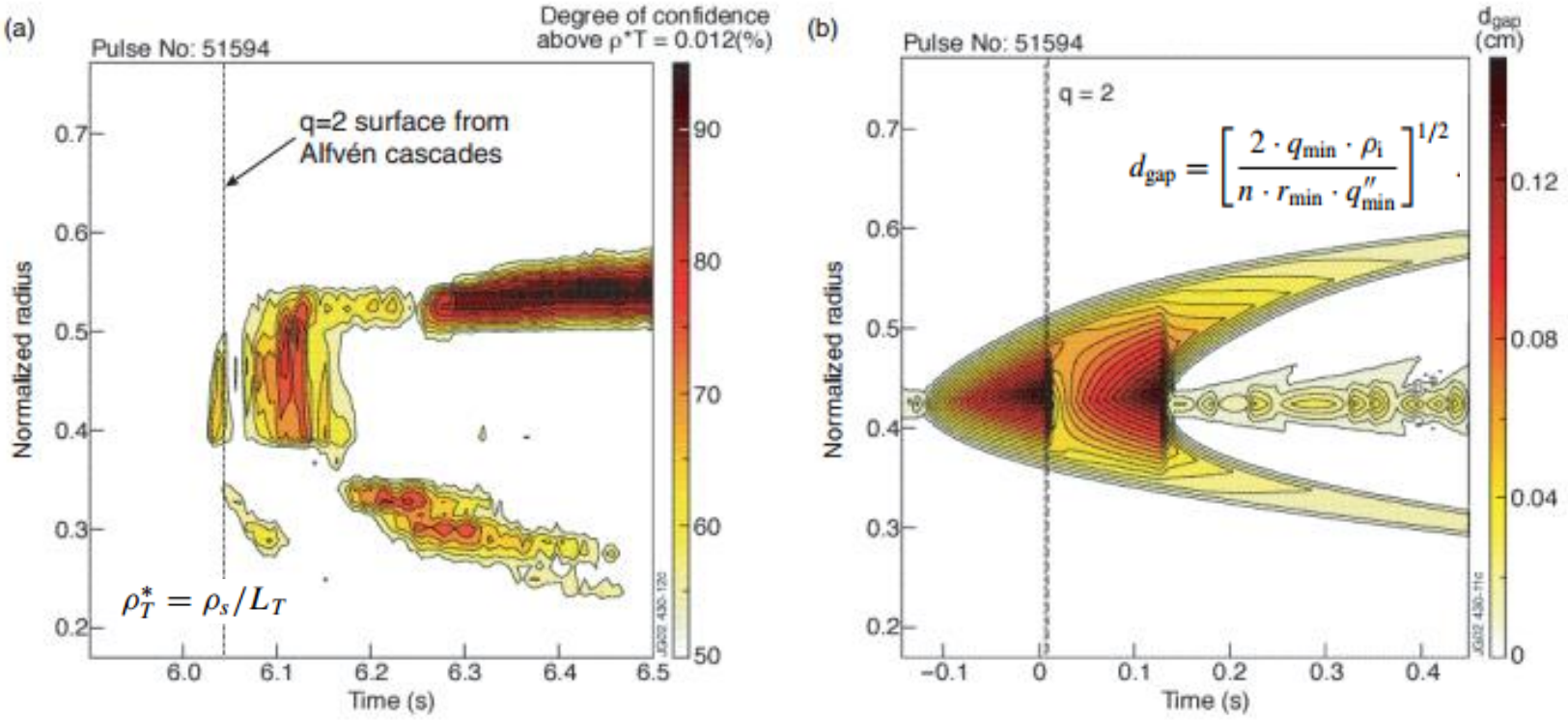

- Two ITBs can be created at two different radial positions once q_{min} passes the q = 2 surface. The time when q_{min} passes the integral q = 2 surface is determined by Alfven cascade analysis and is also indicated.
- Simulation of the gap (d_{gap}) between rational surfaces when the q profile evolves through the q = 2 integral surface.

Joffrin, et al NF2003, 1167

Transport barriers triggered by EP instabilities:

ETB triggered by EGAM

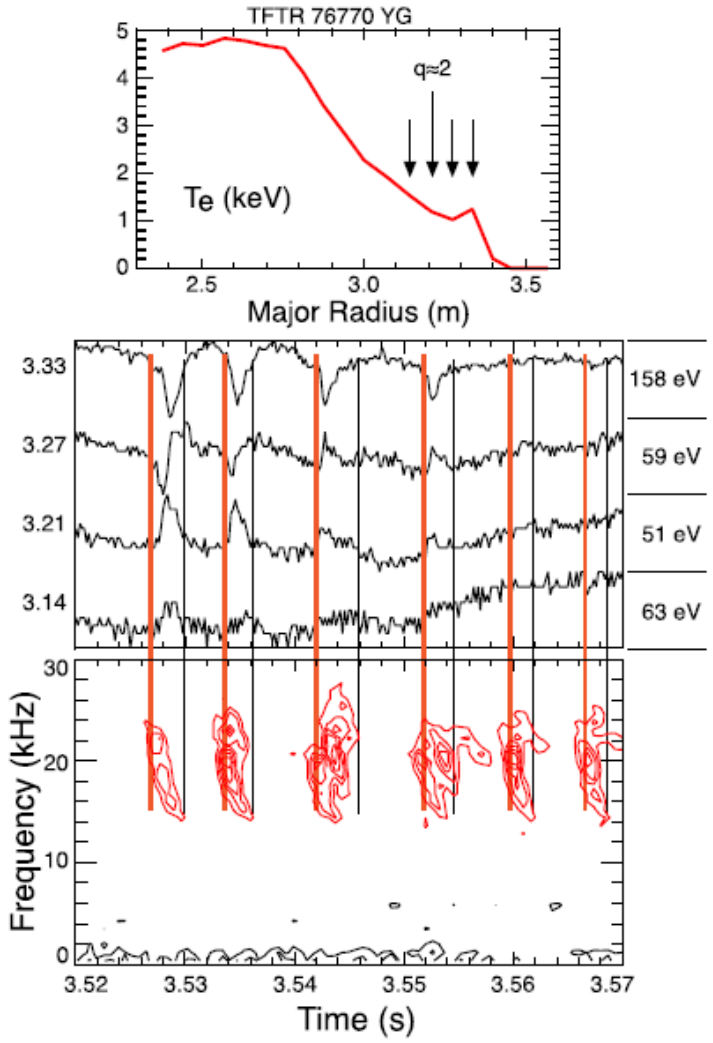

(a) Electron temperature profile measured with Grating Polychromator (GPC), arrows show locations of channels plotted in, (b) four GPC channels showing effect of GAM bursts on edge electron temperature, (c) spectrogram showing frequency evolution of GAM bursts.

Axi-symmetric beam-driven mode (ABM) /GAM did affect the electron thermal transport, causing perturbations in the edge temperature, which might be interpreted as the formation of a transient transport barrier.

*Fredrickson, et al PoP **22**, 032501 (2015)*

Fast ion-induced anomalous transport barrier

F-ATB is characterized by a full suppression of the turbulent transport—caused by strongly sheared, axisymmetric E × B flows. *A. Di Siena, et al PRL **127**, 025002 (2021)*

The trigger mechanism is shown to be a mainly electrostatic resonant interaction between EPs, generated via ion-cyclotron-resonance heating, and plasma microturbulence.

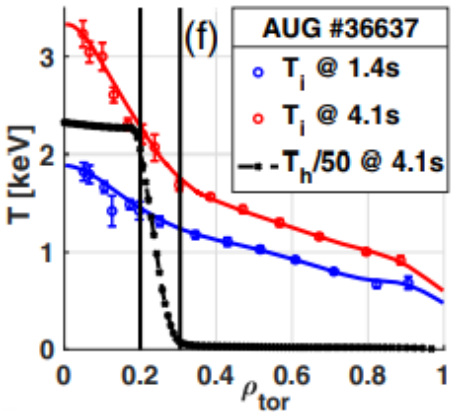

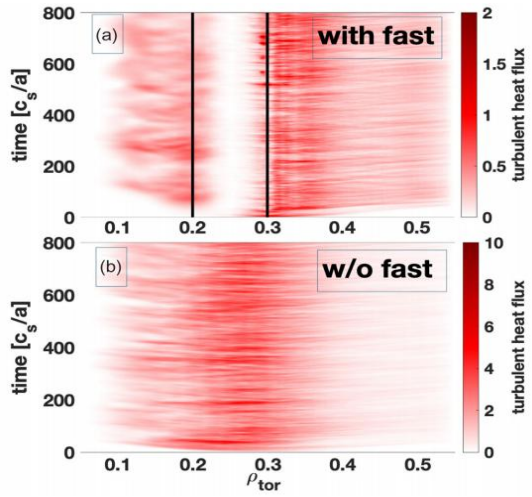

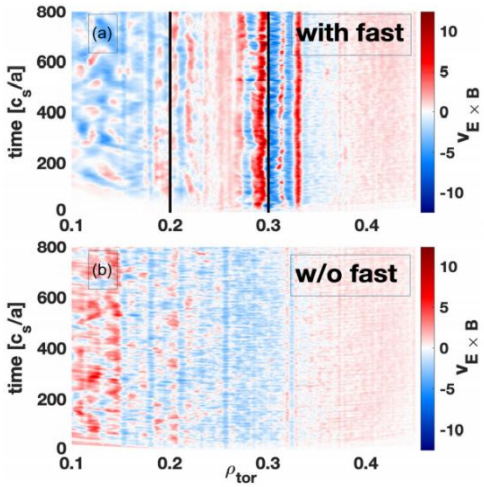

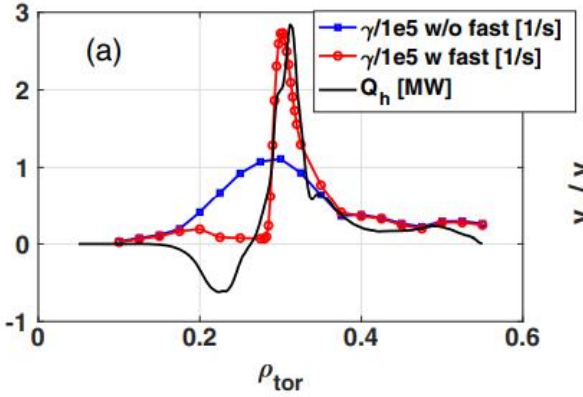

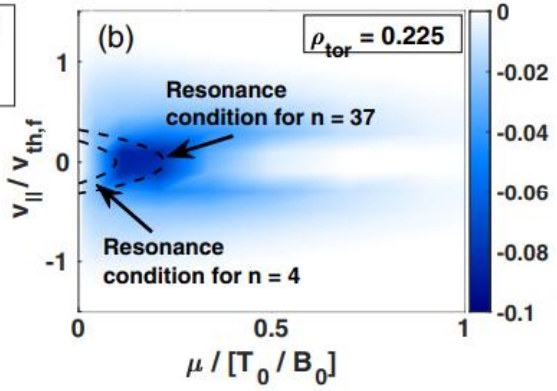

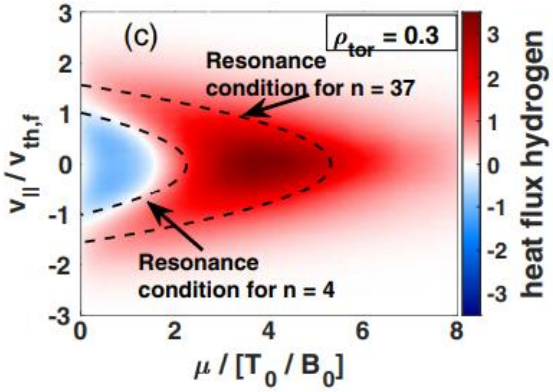

Nonlocal triggered by EP instabilities

Phenomenal description and magnetic perturbation

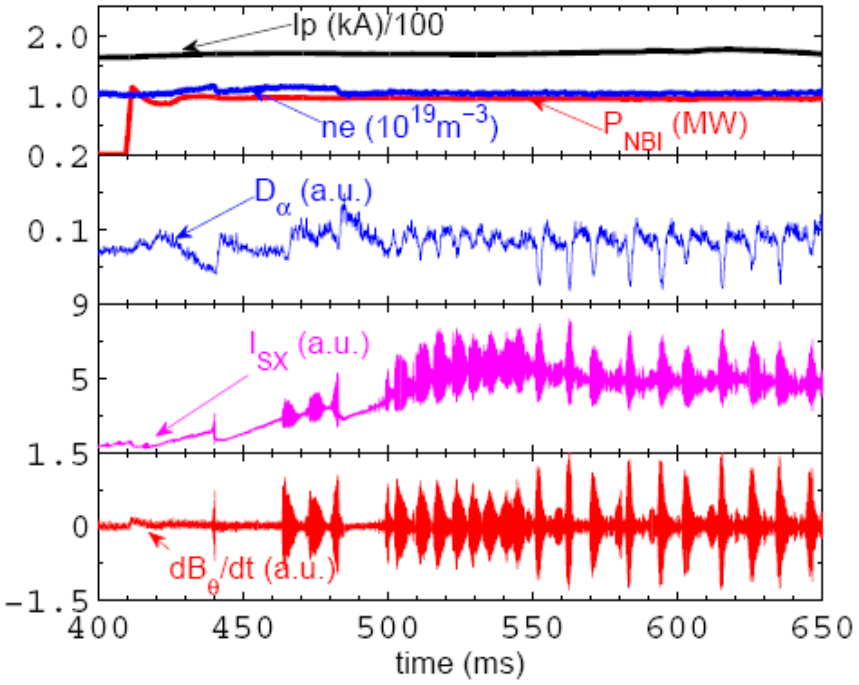

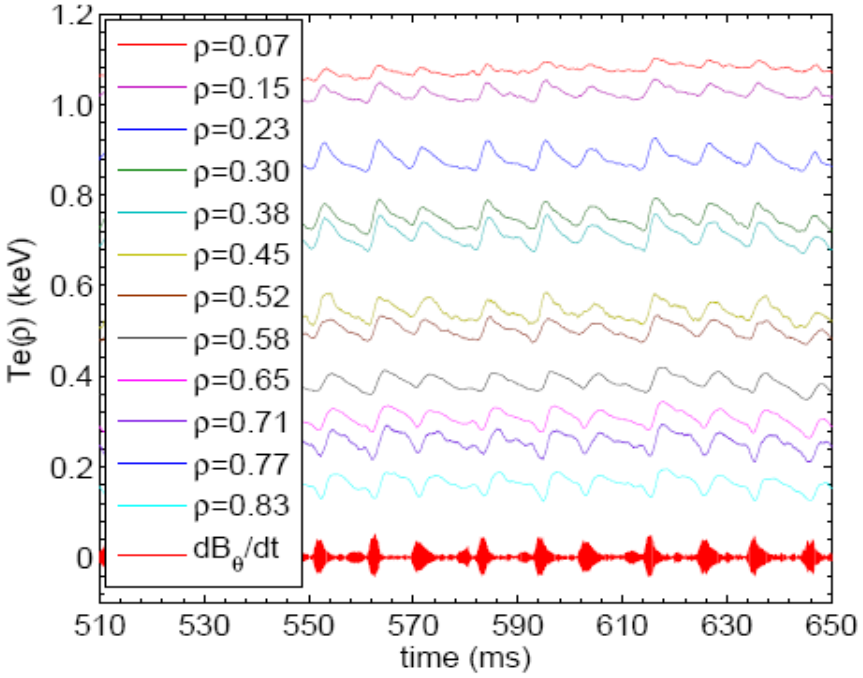

With the FB bursting it is found that the core (localization of FB, \rho < 0.30) heating leads to a simultaneous decrease (but not slow increase) in temperature at the plasma edge. The reversal radius of temperatures is \rho=0.55, which is near q=3/2 rational surface. The effect reveals fast anomalous transport of core heat pulses to plasma edge, not compatible with diffusive time scales. It is a new-type nonlocal response which is a counterpart to that induced by the edge heating/cooling pulse.

Nonlocal triggered by EP instabilities

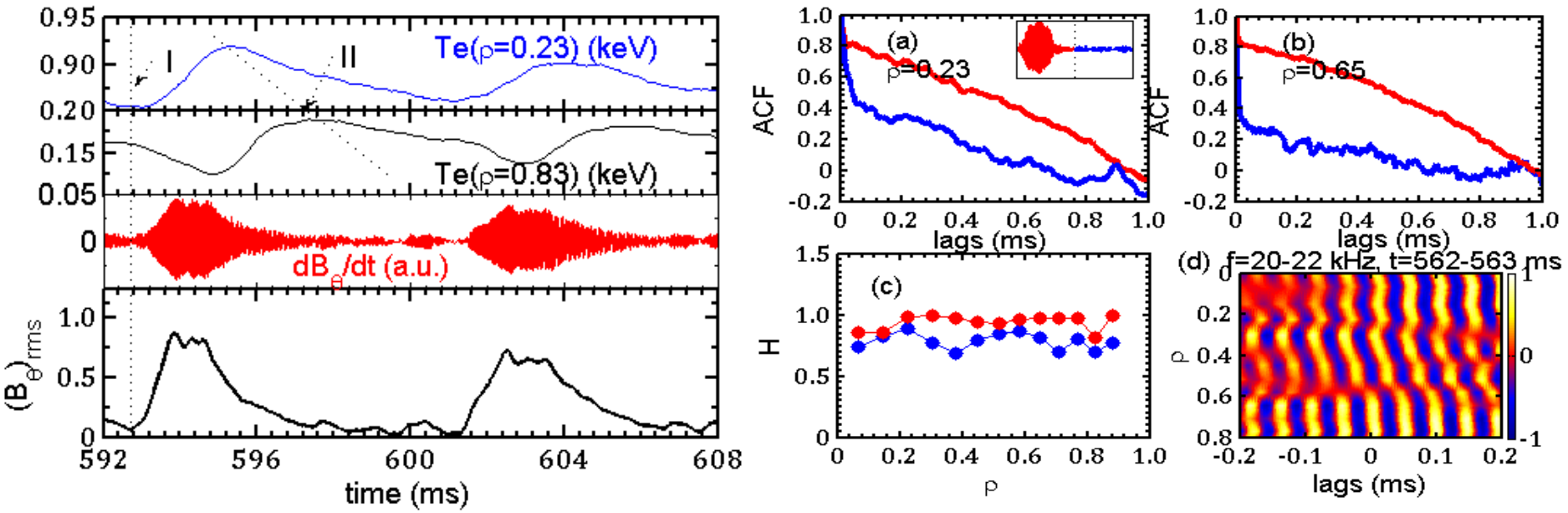

A new-type nonlocal transport, which is triggered by the fishbone, is observed on HL-2A.

- The rapid core heating leads to a simultaneous decrease in temperature in the edge.
- I: fast time response, ~50us; II: slow time response, ~3ms.

Auto-correlation function (ACF) coefficients (a-b) of ECE signals at two radial positions and spatial profiles (c) of Hurst exponents (H, obtained by R/S method) from ECE signals. ACFs and Hurst exponent both enhances during the fishbone and nonlocal transport. And so the new-type nonlocal transport is potentially linked to self-organized critical (SOC) dynamics.

W. Chen, et al. NF (lett.) 56, 044001 (2016).

ELM triggered by EP instabilities

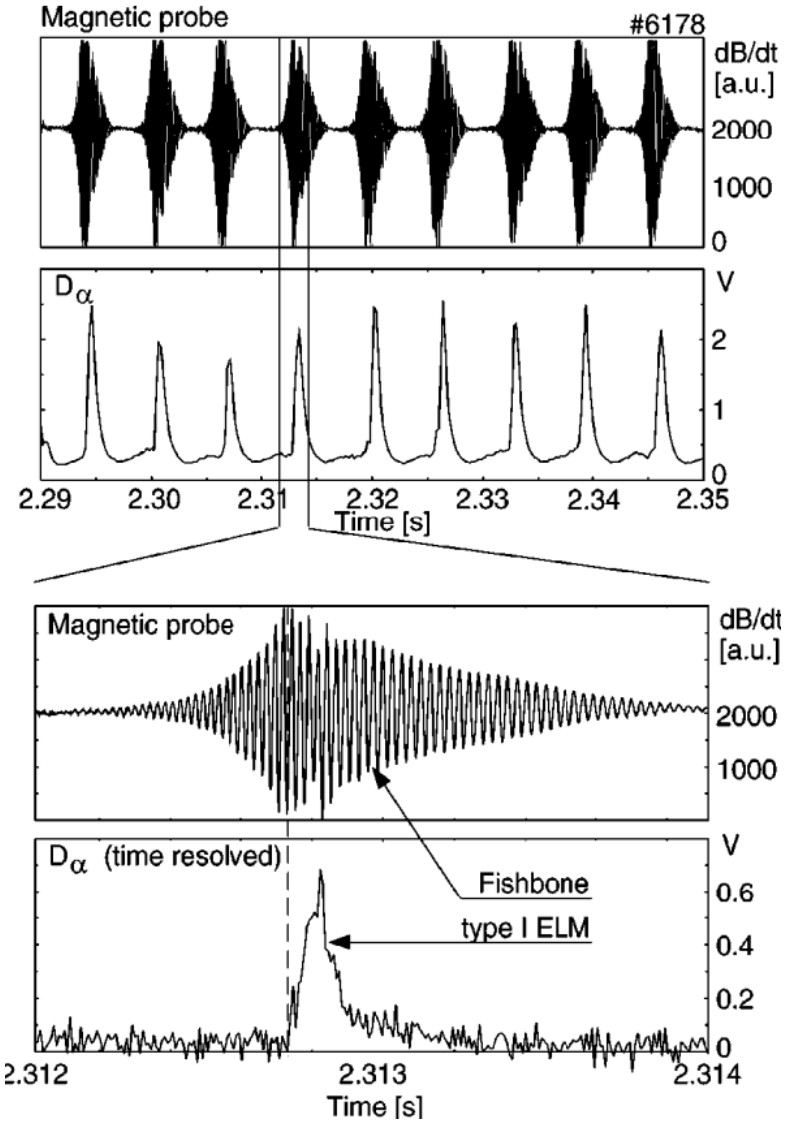

The q=1 fishbone triggered ELM was observed in ASDEX. Usually, fishbone is driven by trapped EP as q_0 is close to unity. resonance with marginal m/n=1/1 internal kink

Fishbone can
- Induce EP outward transport,
- Eject EPs outside plasma.
- Change edge pressure gradient?
- Fishbone structure directly affect?

This phenomena was observed in high beta plasmas (beta_N~2.5)

T. Kass, et al., NF 38, 807 (1998).

ELM triggered by EP instabilities

Fishbones seem to pace ELMs in high beta plasmas

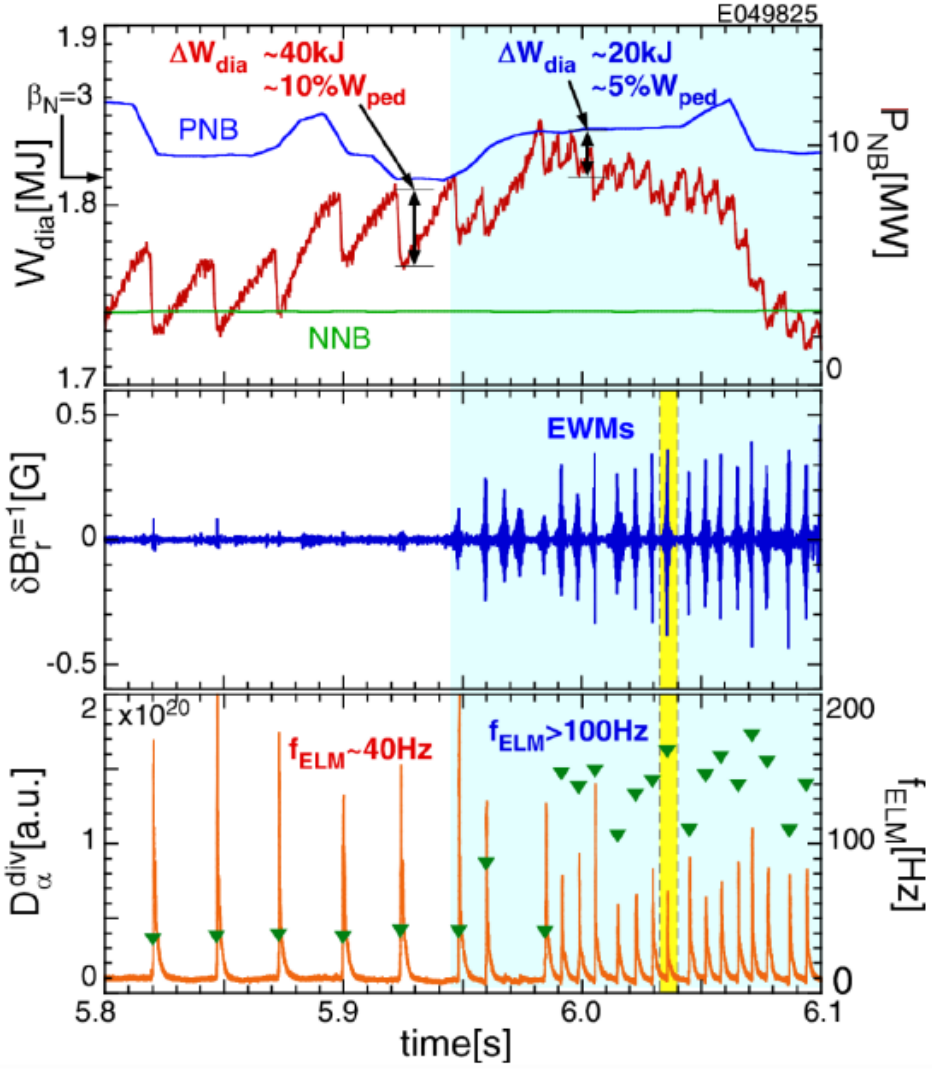

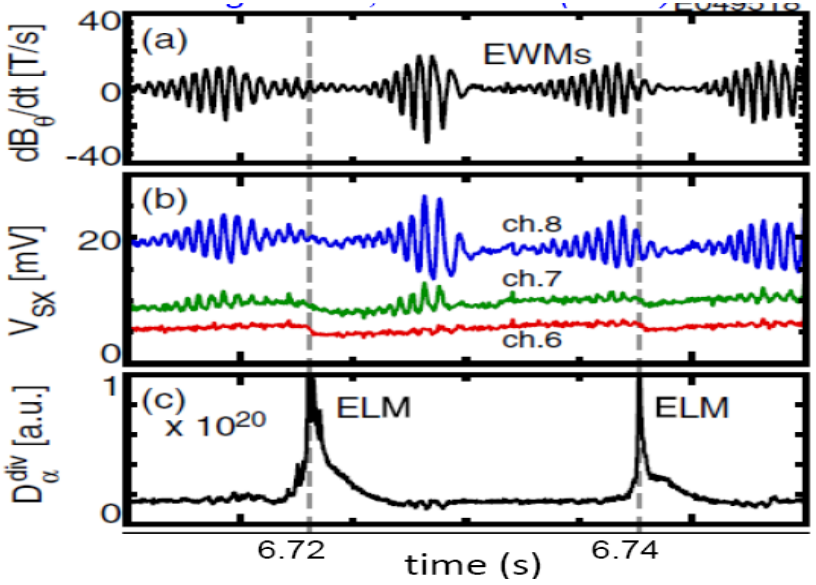

EP instability in high-beta plasma can trigger ELM. ELM frequency becomes higher and energy drop becomes smaller

M. Garcia-Munoz , 12th IAEA TM on EPs Austin, Texas USA (2011), O-11

ELM triggered by EP instabilities

Matsunaga, IAEA2012, EX/5-1.

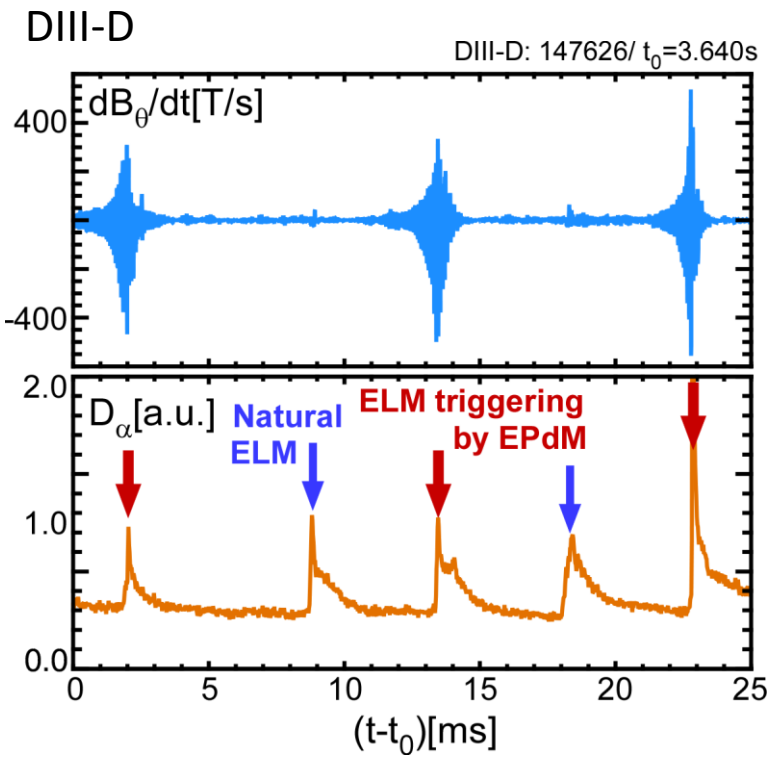

Partially synchronized

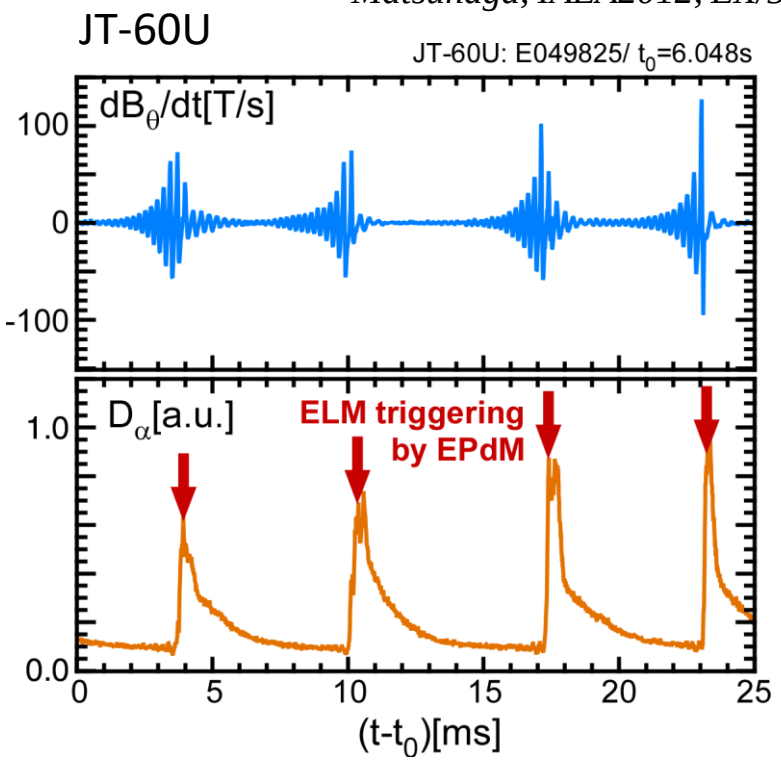

Fully synchronized

- Frequent EP instability cycle can pace ELM,
- Pacing frequency is determined by balance between pedestal recovery and EP transport.

Pedestal collapse triggered by nonlinear dynamics of AEs

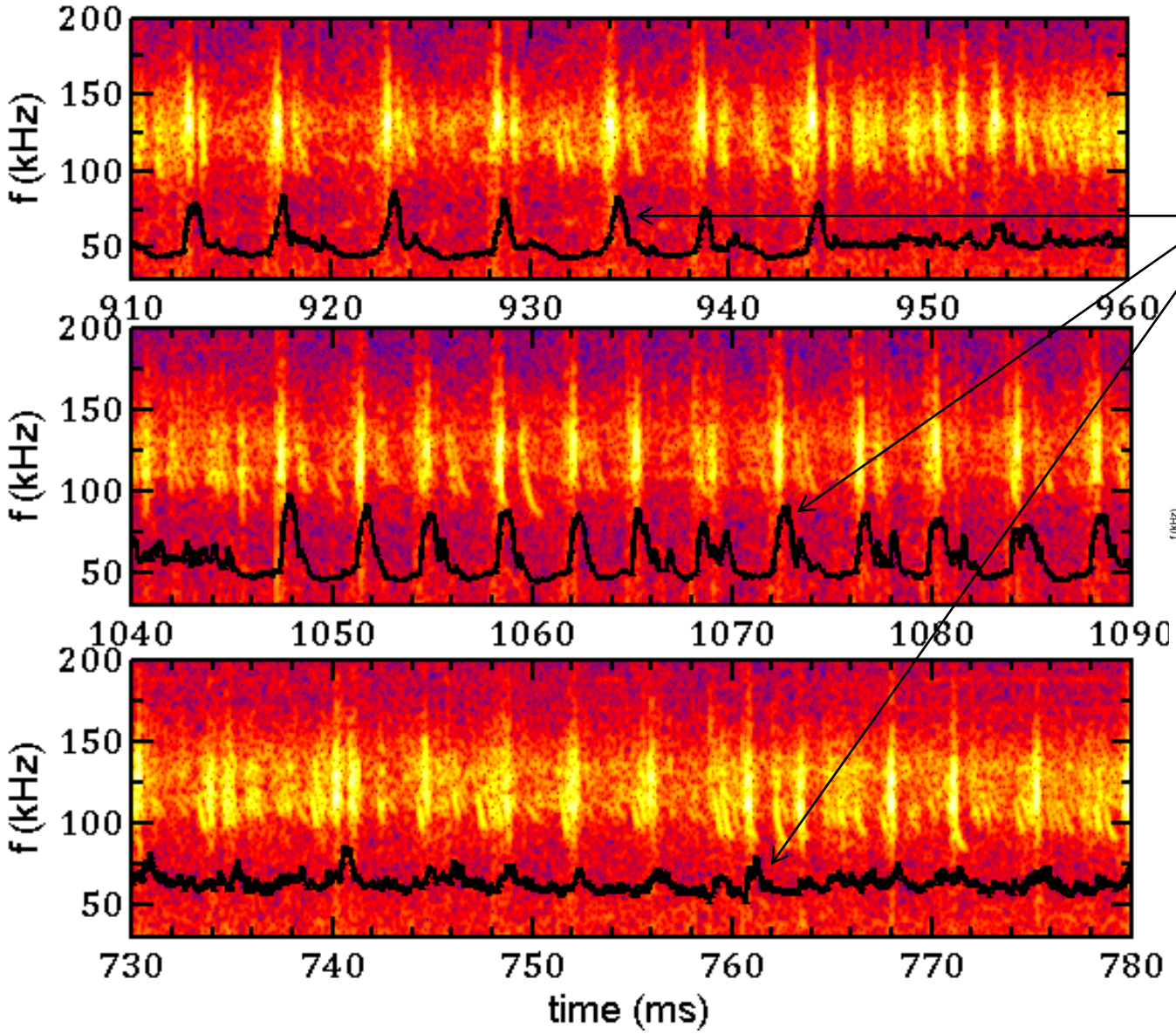

This explosive event triggers the onset of ELMs.

ELMs

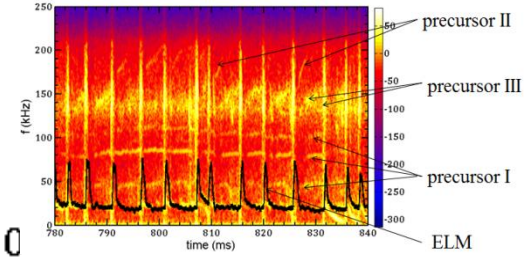

At least, there are three type high-frequency coherent modes during inter-ELM period.

Pedestal collapse triggered by nonlinear dynamics of AEs

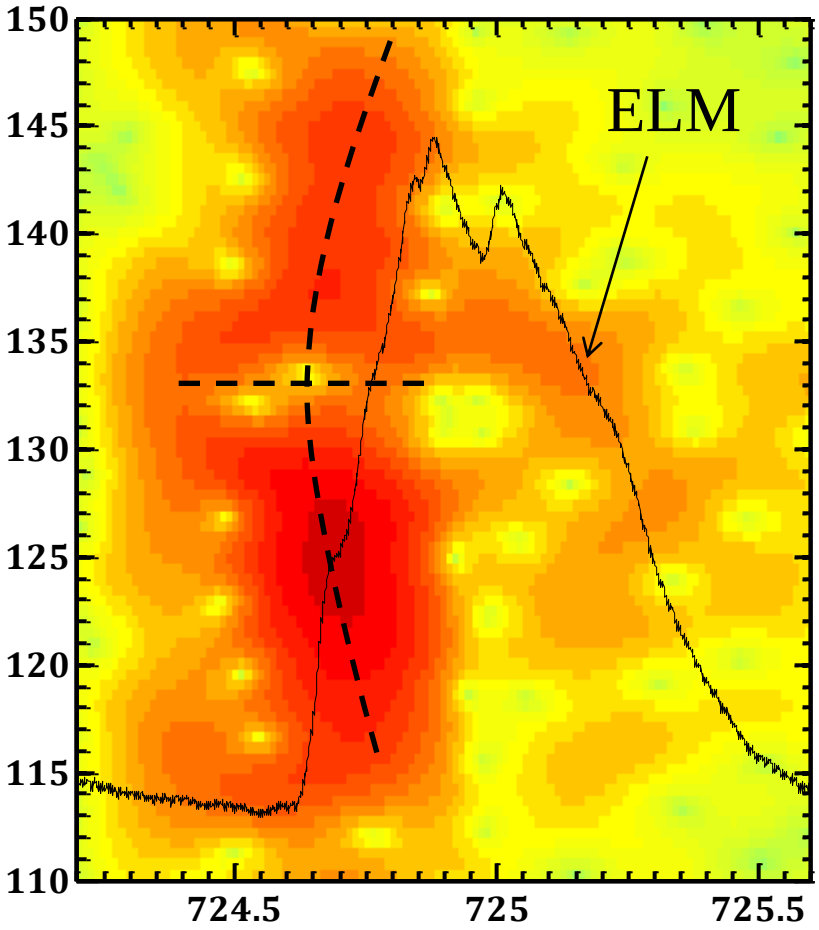

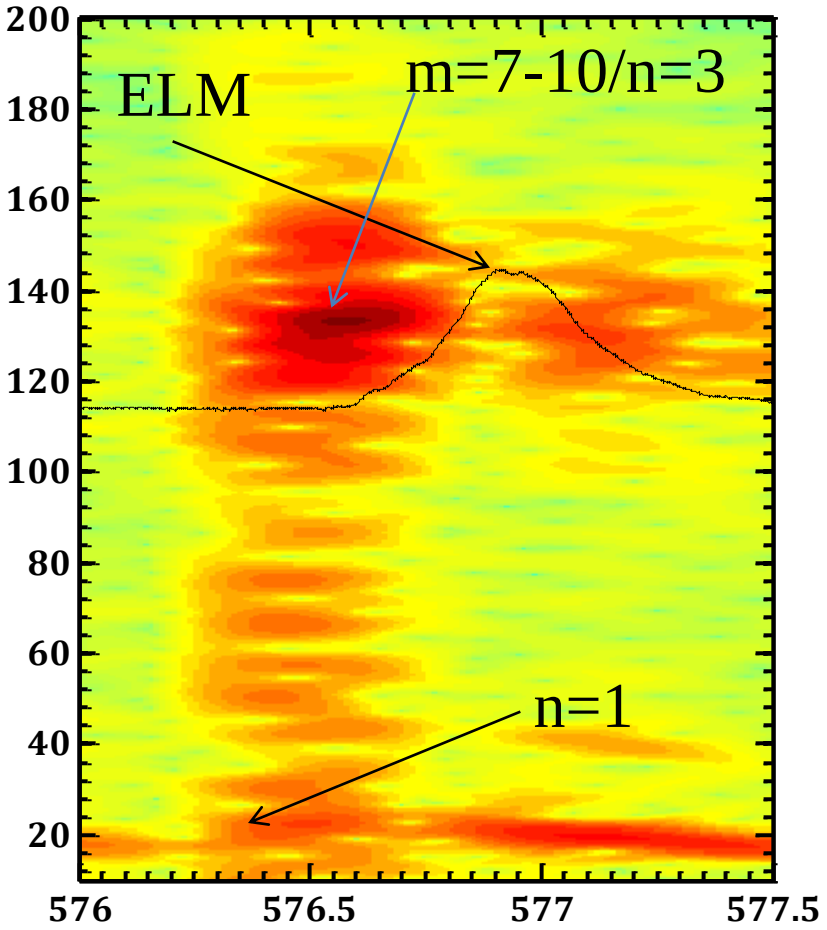

The explosive events have two kind fine structures, i.e., multi-modes and pitch-fork. The two kind structures can coexist, but the strong nonlinear mode coupling induces that the pitch-fork weakens or vanishes (the NMC may redistribute energetic-ions and destroy hole-clump pairs in the phase-space).

Pedestal collapse triggered by nonlinear dynamics of AEs

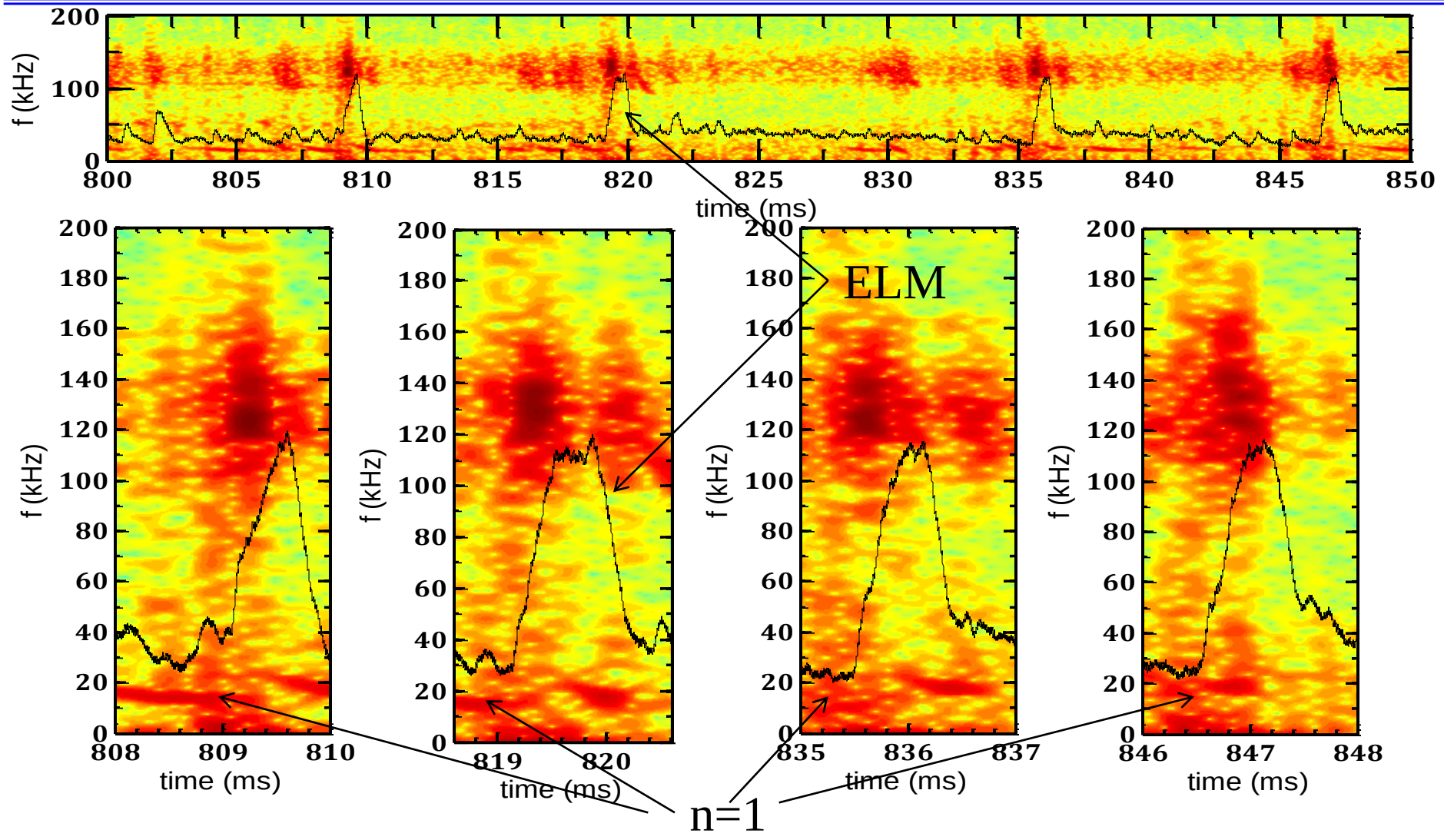

The nonlinear mode coupling triggers the onset of ELMs.

Pedestal collapse triggered by nonlinear dynamics of AEs

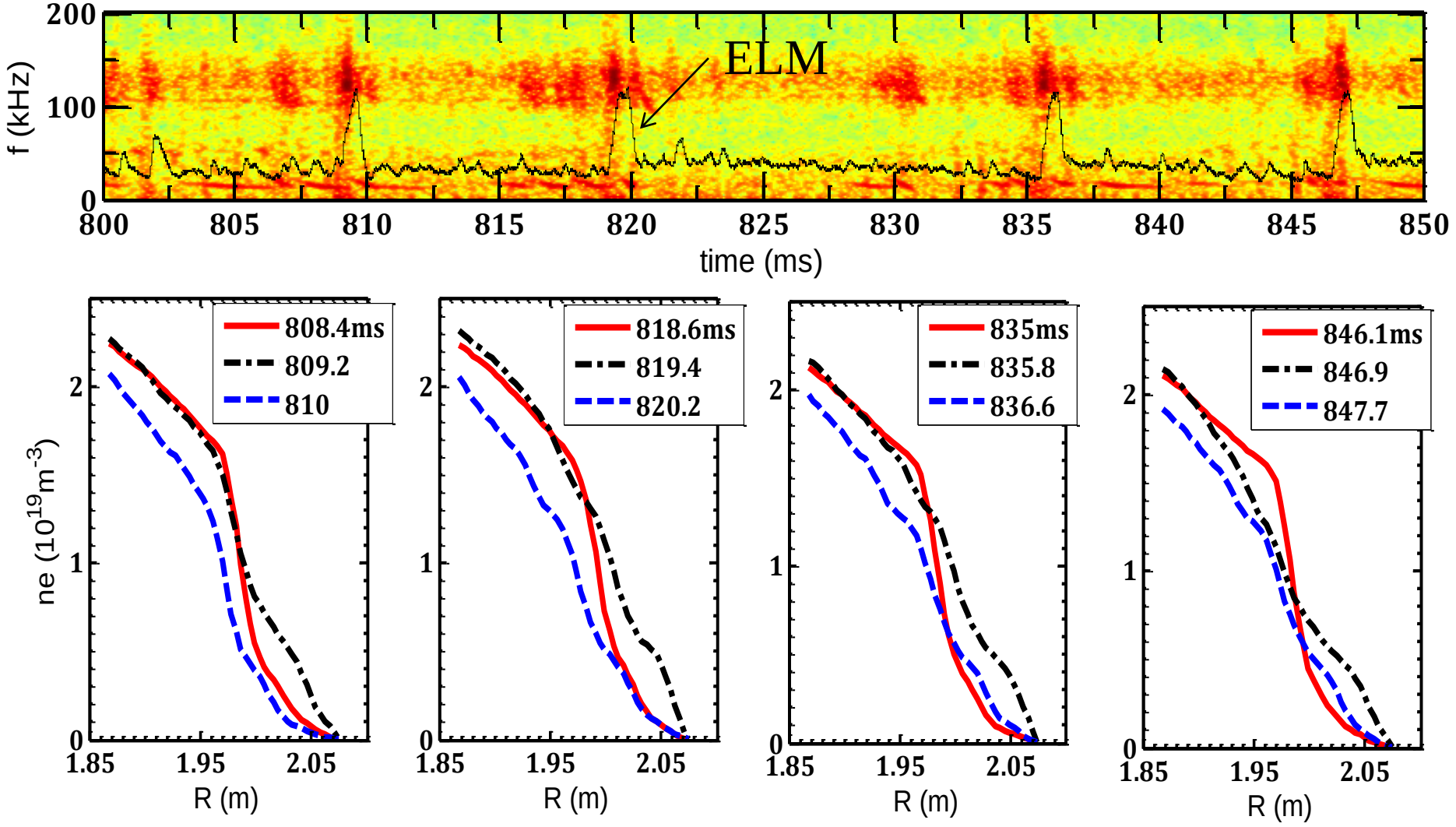

The nonlinear mode coupling triggers the H-mode pedestal collapse (δt=200-400 us).

Pedestal collapse triggered by nonlinear dynamics of AEs:

Possible Interpretation

$$P=P_{th}+\delta P_{th}+\delta P_{EP}$$

The n=1 mode has important effects on ELM trigger. The NMC among AEs and low-n mode may enhance EP transport (avalanche?), and it is more severer than pitch-fork, and it can furnish an additional pressure δP_{EP} in the pedestal. δP_{EP} can move closer to MHD limit. ELM trigger is determined by NMC and edge stability.

Toroidal coupling:

- m/n->m$\pm$1/n =>m/n=1/1, 2/1, 3/1, 4/1=>core-edge coupling;
- long-distance ballistic transport;

Nonlinear mode coupling:

- Low-frequency n=1 mode+High-frequency AE=> avalanche transport=>ELM trigger & pedestal collapse.

Global transport or local transport?

I-phase triggered by sawtooth crash

■ Typical I-phase phenomenon triggered by sawtooth crash on HL-2A.

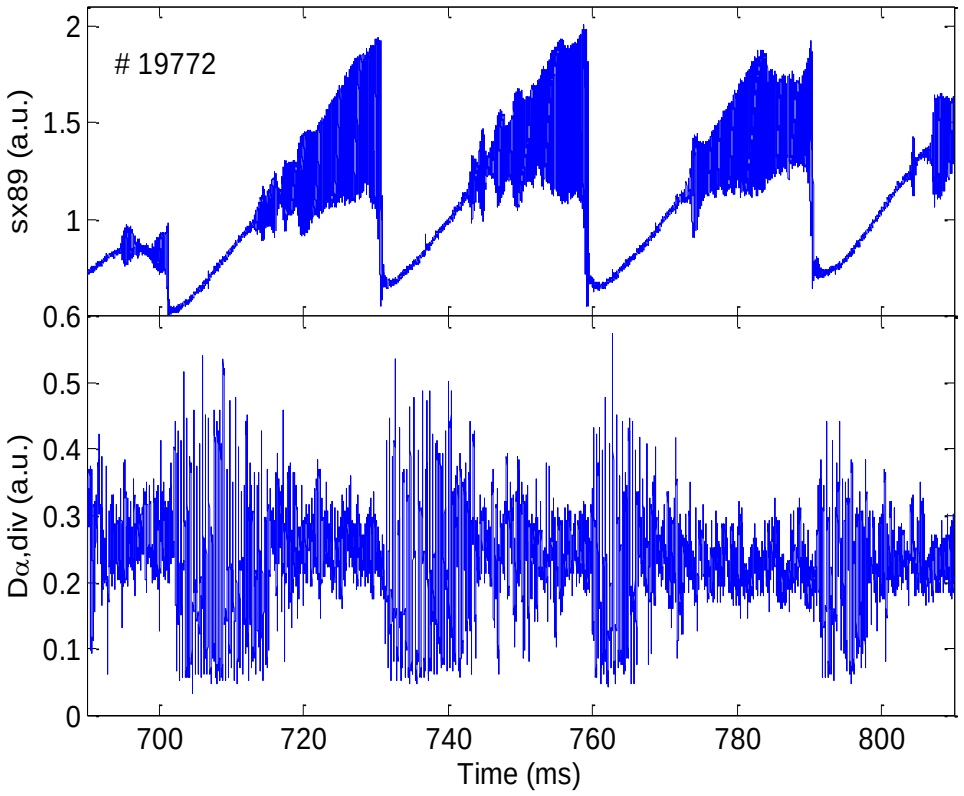

What is the effect of the orbit loss/redistribution of energetic-particles during I-phase?

✓Generate the electric field shear structure due to ion orbit loss?

✓Ion orbit loss current induced by the interaction between energetic-particles and MHD mode?

✓Generate zonal flow, but not via the turbulent Reynolds stress?

K. C. Shiang, PRL1989, 2369

K. L. Wong, NF2005, 30

MHD spectroscopy

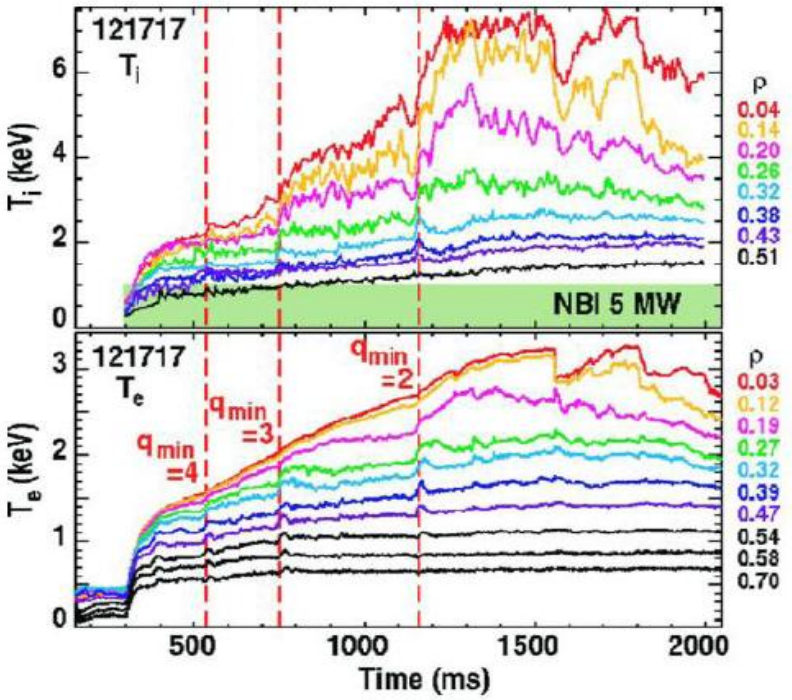

Integer values of q_{min} can be identified by looking at "grand cascade" of RSAEs.

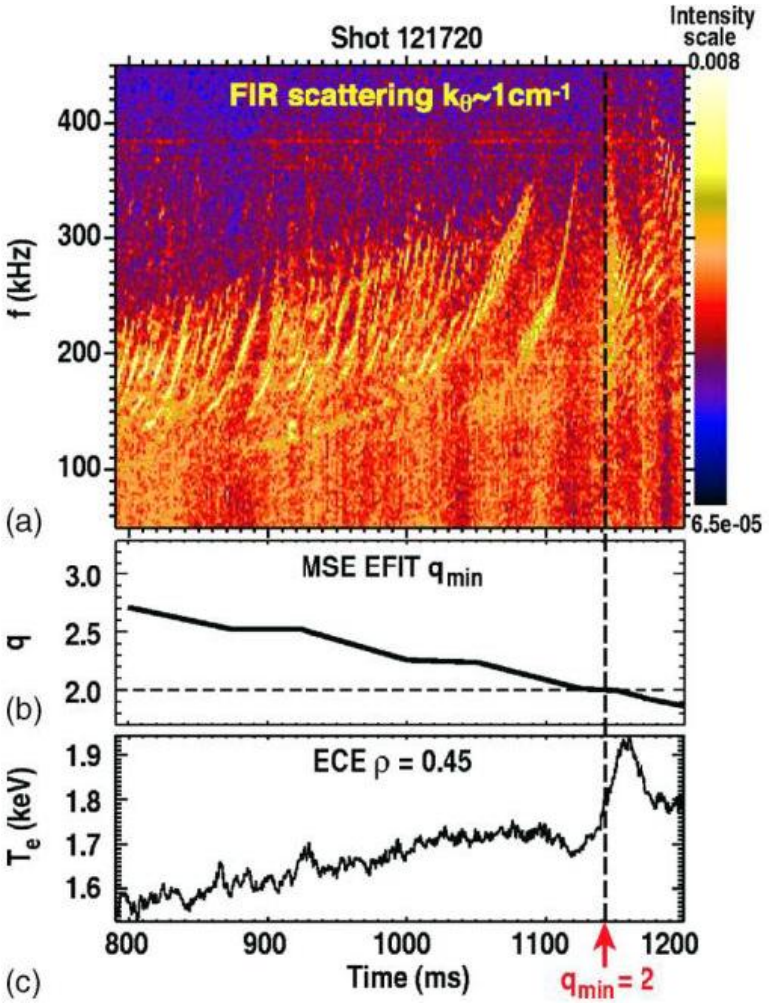

M. E. Austin, et al, PoP 13, 082502 (2006).

MHD spectroscopy

MHD spectroscopy to identify timing of q_{min}=integer

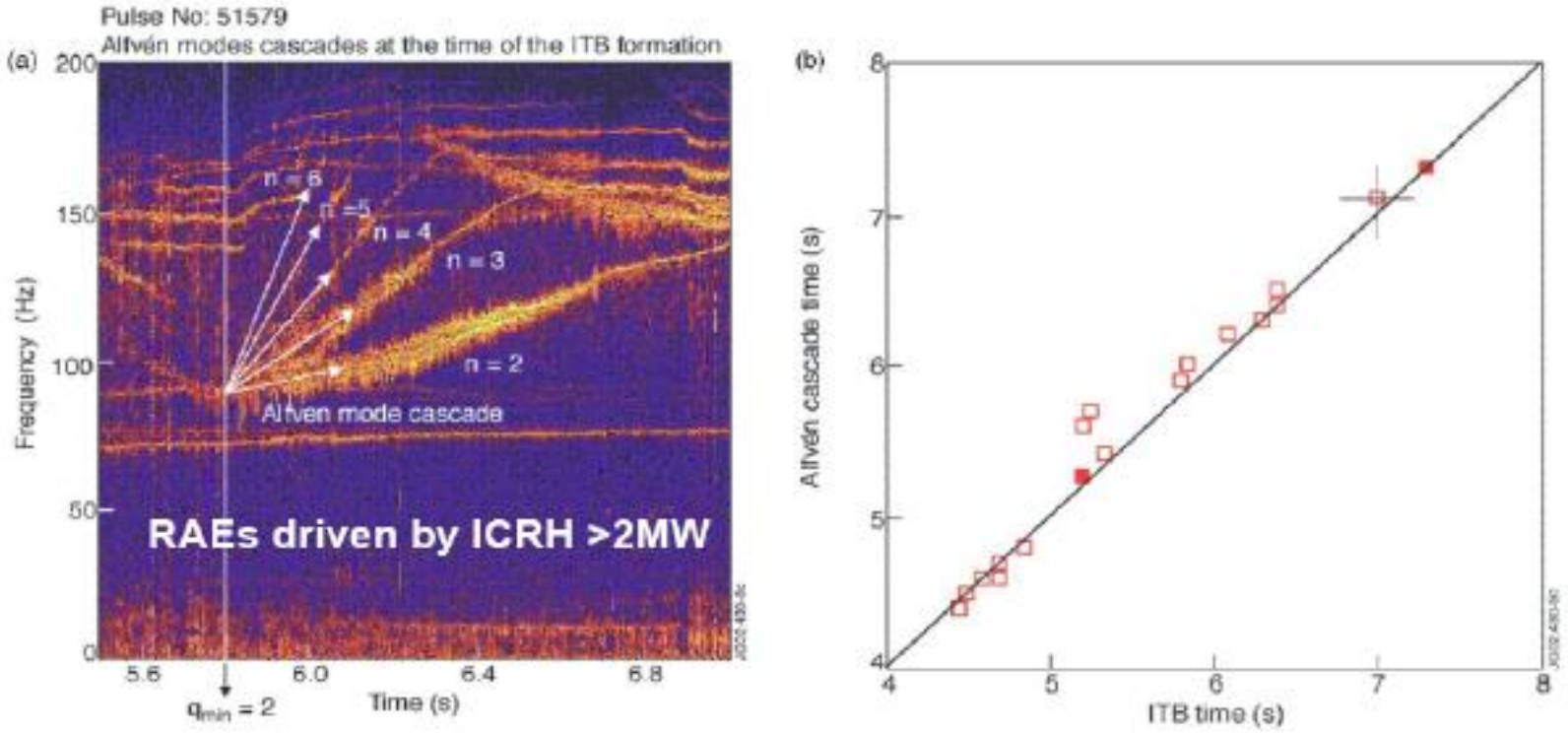

❖Time of cascade onset is correlated with the emergence time of the ITB.

❖This can be used as a very efficient diagnostic for **determination of q_{min}** at the time the ITB is formed.

❖This can be useful tool to identify q_{min} for ITB physics.

E. Joffrin, et al., NF 43, 1167(2003).

Fast Ion Induced Shearing of 2D AEs

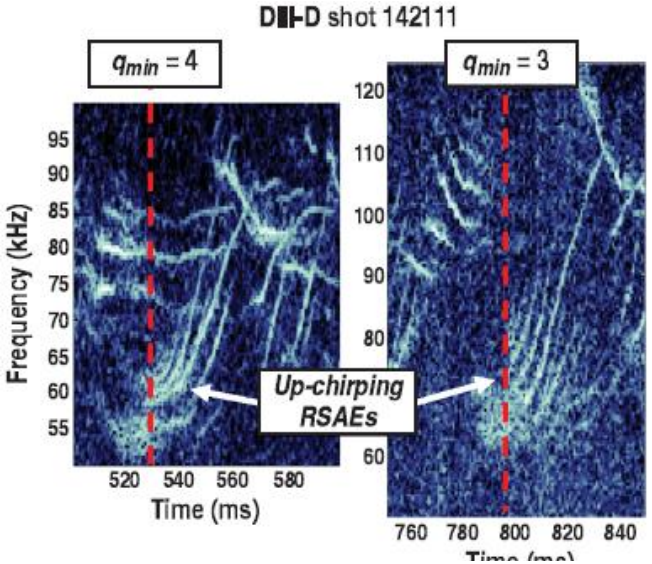

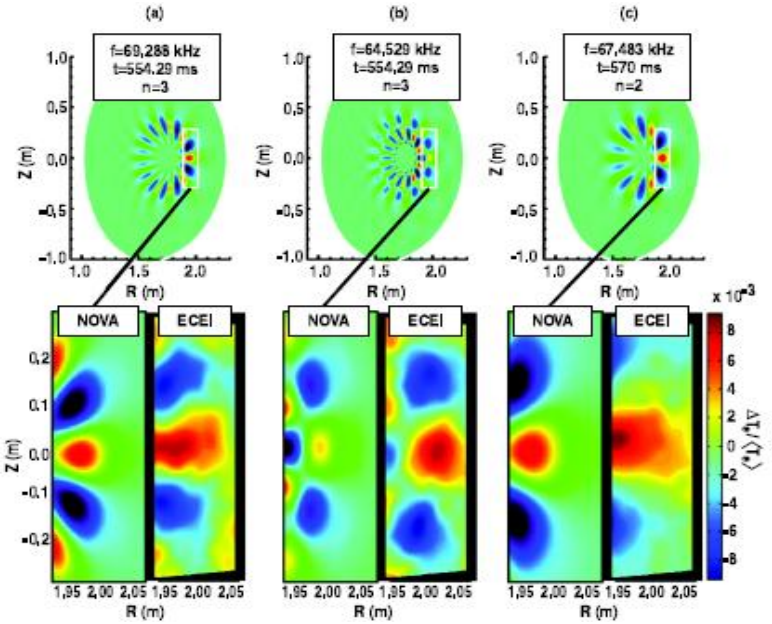

Two-dimensional images of electron temperature perturbations are obtained with electron cyclotron emission imaging (ECEI) on the DIII-D tokamak and compared to Alfvén eigenmode structures obtained by numerical modeling using both ideal MHD and hybrid MHD-gyrofluid codes. While many features of the observations are found to be in excellent agreement with simulations using an ideal MHD code (NOVA), other characteristics distinctly reveal the influence of fast ions on the mode structures. These features are found to be well described by the nonperturbative hybrid MHD-gyrofluid model TAEFL.

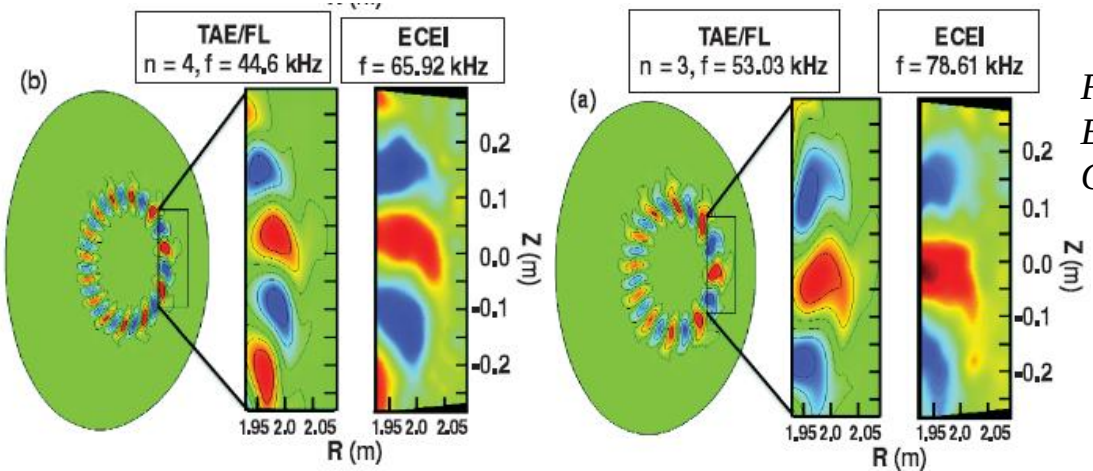

Fast Ion Induced Shearing of 2D Alfven Eigenmodes Measured by Electron Cyclotron Emission Imaging

Tobias, et.al. PRL 106, 075003 (2011)

Enhanced energy transport by radially curved AE wavefronts

$$\xi_0(\psi,\theta,\zeta,t) = \sum_{m=-\infty}^{\infty} \xi_m(\psi)\exp\left(\mathrm{i}(m\theta - n\zeta - \omega t)\right)$$

$$\xi_c = \xi_0\, e^{\mathrm{i}\phi(\psi)}$$

$$\begin{aligned}\tilde{\mathbf{S}}_c &= \frac{1}{2\mu_0}\mathrm{Re}\left(\tilde{\mathbf{E}}_c \times \tilde{\mathbf{B}}_c^*\right)\\ &= \frac{1}{2\mu_0}\mathrm{Re}\left(\tilde{\mathbf{E}}_0 \times \tilde{\mathbf{B}}_0^* - \tilde{\mathbf{E}}_c \times \mathbf{B}_{eq}\left(\tilde{\xi}_0^* \cdot \nabla e^{-\mathrm{i}\phi(\psi)}\right)\right)\\ &= \tilde{\mathbf{S}}_0 + \frac{1}{2\mu_0}\mathrm{Re}\left(\tilde{\mathbf{E}}_0 \times \mathbf{B}_{eq}\left(i\tilde{\xi}_0^* \cdot \nabla\phi(\psi)\right)\right)\end{aligned}$$

G.J. Kramer, et al., NF 59, 094001(2019).

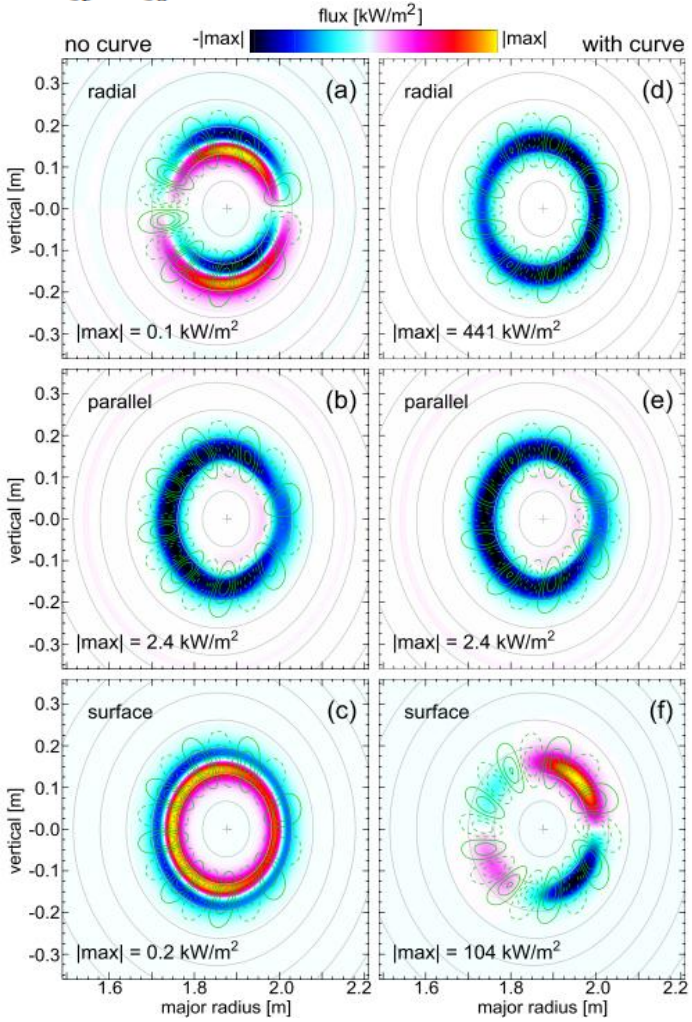

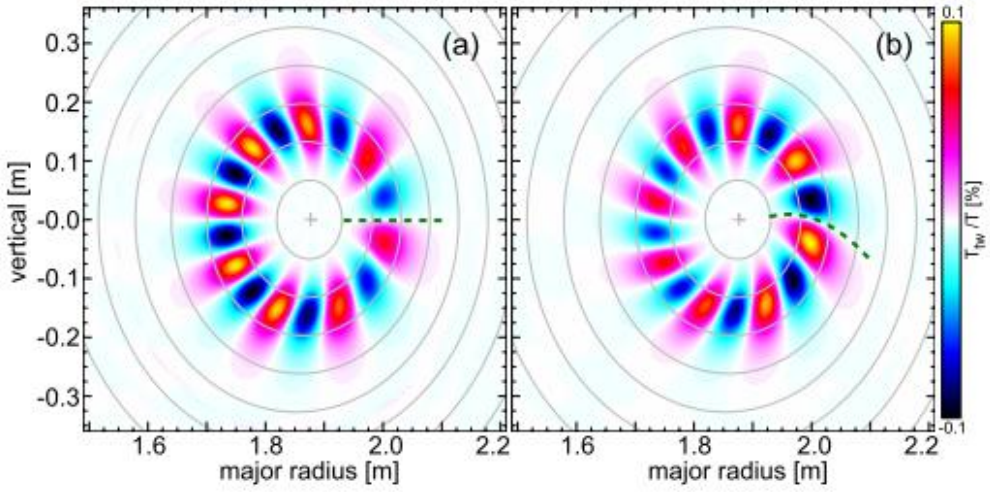

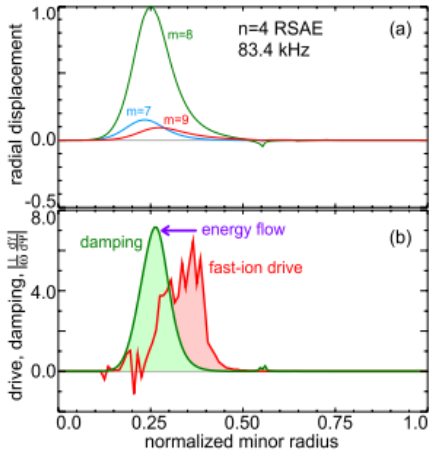

Energy flow: due to radial mismatch in the location of drive and damping.

Energy transport: by enhanced parallel fluctuating magnetic field that is generated by the radial wavefront curvature.

Beam-Ion Acceleration during ELMs

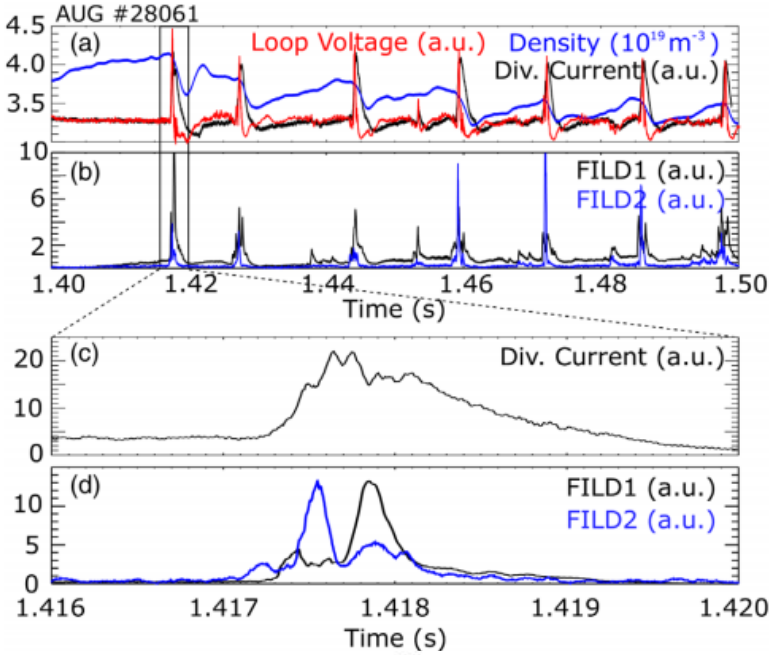

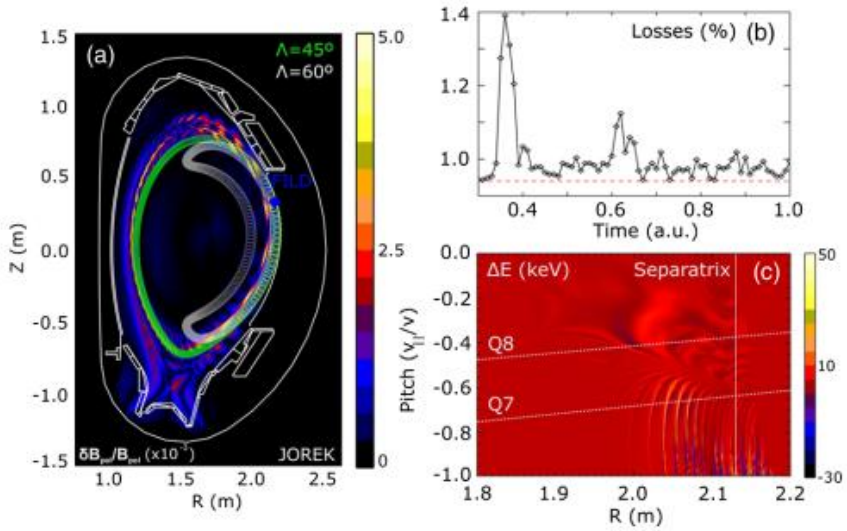

- The acceleration of beam ions during ELMs in a tokamak is observed for the first time through direct measurements of fast-ion losses in low collisionality plasmas.
- The accelerated beam ion population exhibits well-localized velocity-space structures which are revealed by means of tomographic inversion of the measurement, showing energy gains of the order of tens of keV.

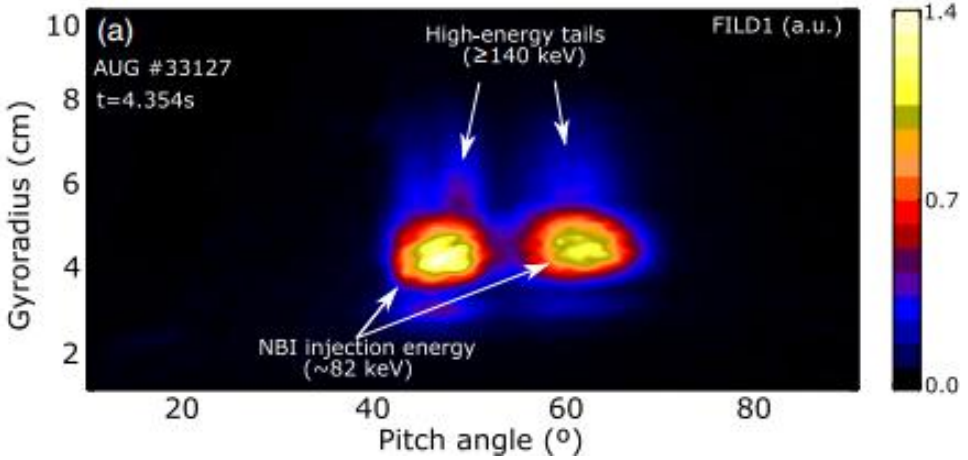

J. Galdon-Quiroga , et al, PRL, 121, 025002,2018

Core-edge coupling physics: an example

Enhanced fast ion losses due to the coupling between CL-TAE+o-TAE. *F. Nabias, et al, PPCF 2019.*

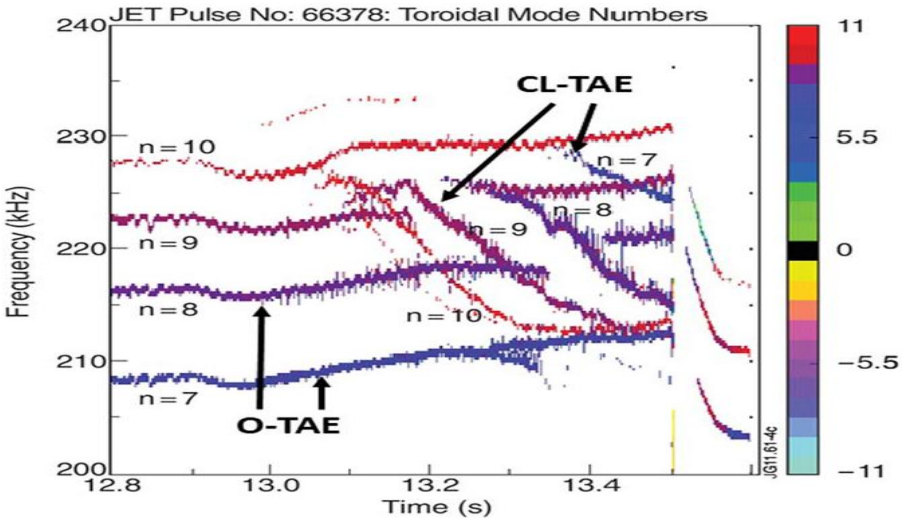

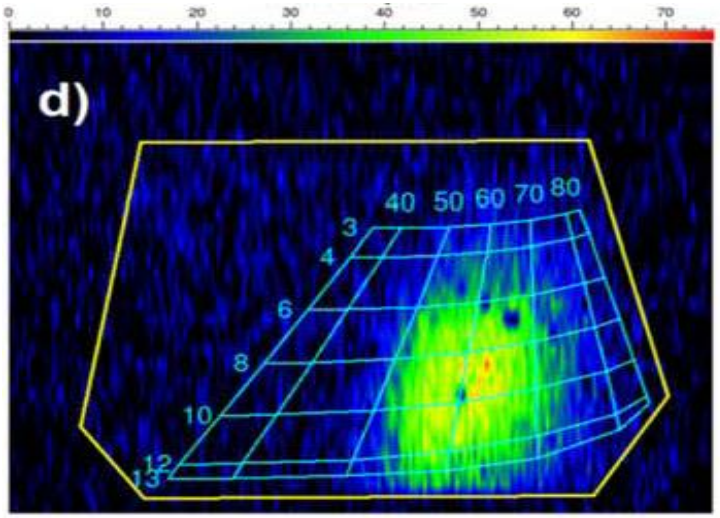

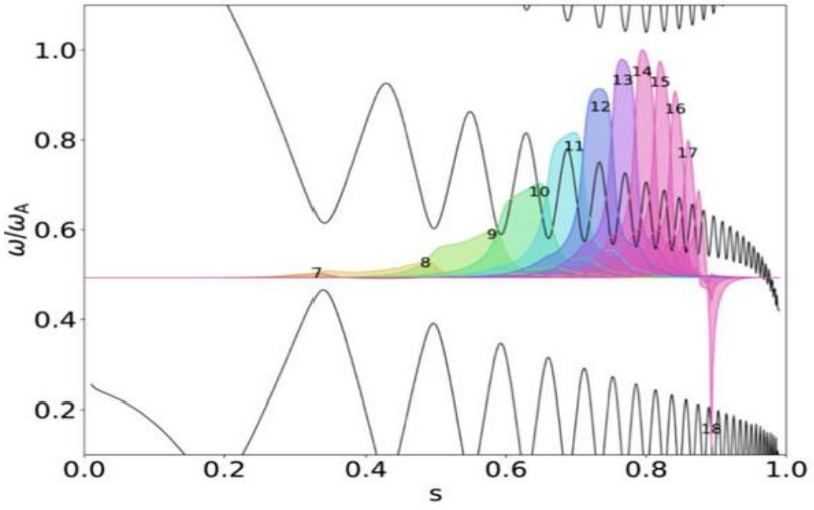

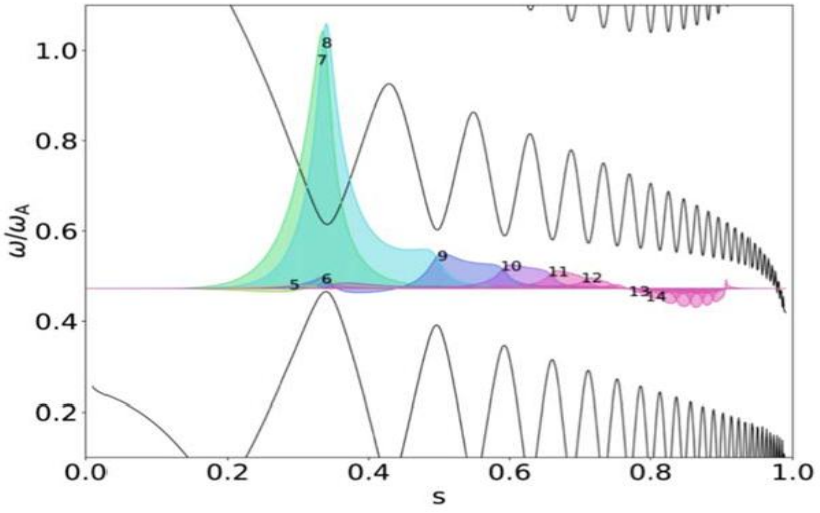

Multi-scale & core-edge coupling & multi-channel

Effects of energetic-particles and related instabilities on the plasma transport.

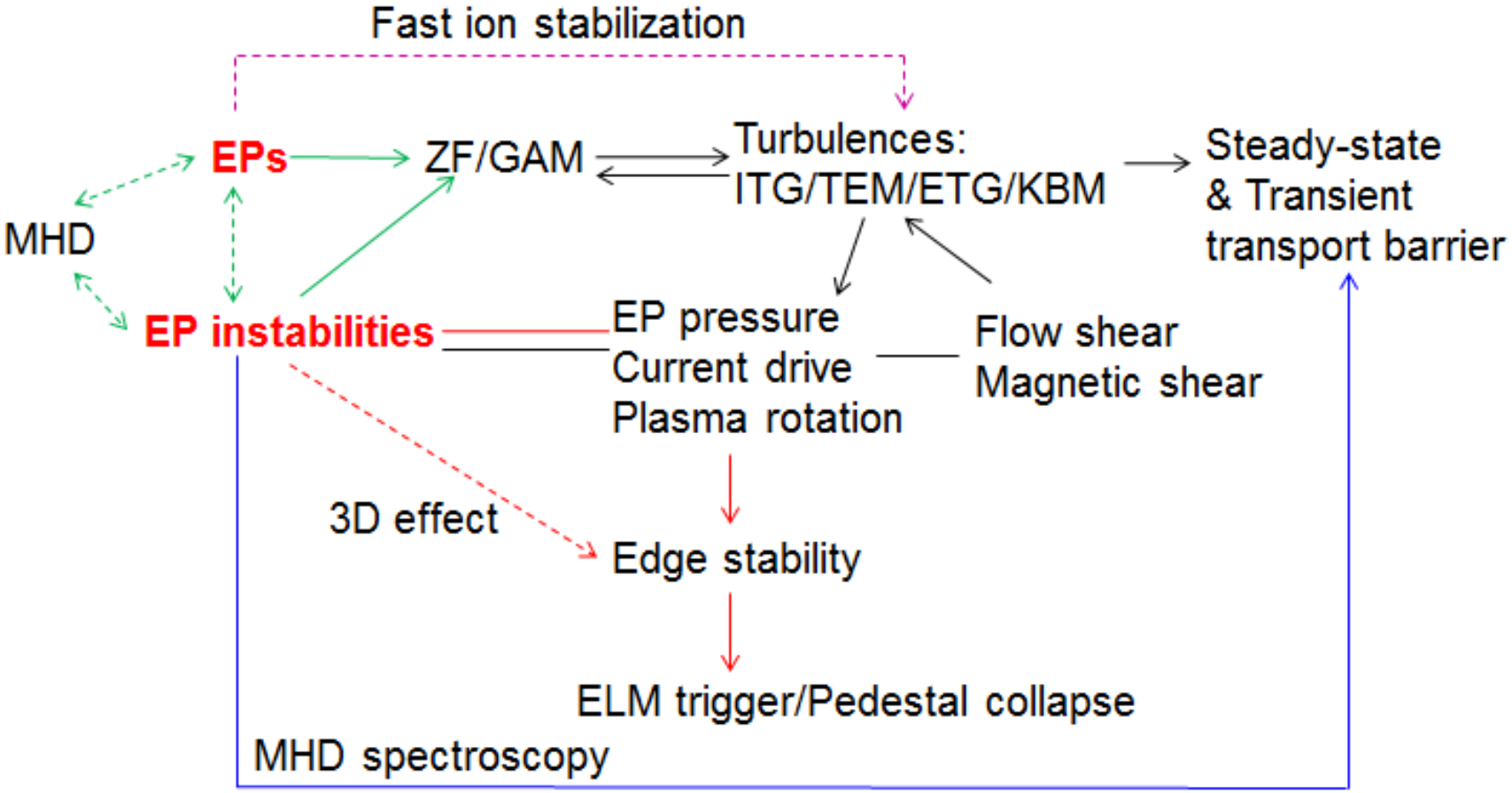

Summary

Many experimental results indicate EPs and related instabilities have important effects on the plasma transport, including H-mode and transport barrier physics.

- EPIs are related to transport channel
- EPs/ EPIs product ZF/ GAM, theory and simulation also predict that AEs nonlinearity can produce ZF and GAM
- EPIs can affect edge stability, EPIs can trigger ELM and pedestal collapse
- EPIs can trigger ITB/ETB and nonlocal transport
- MHD spectroscopy for ITB studies (*MHD activity may be a beacon for some physical studies*)

高能量粒子实验物理

Part-III: Mitigation and control of EP driven instabilities and EP losses

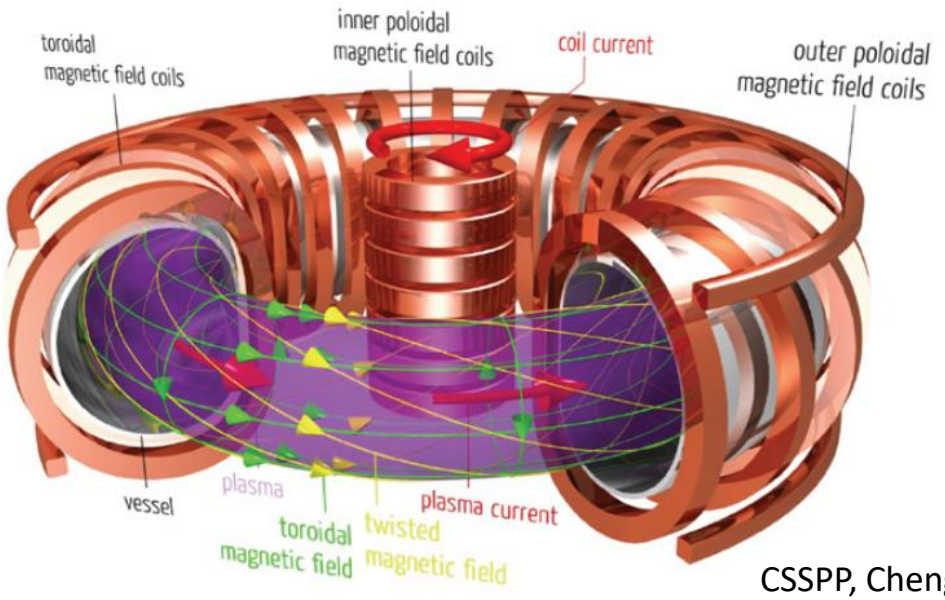

Wei Chen 陳偉

Southwestern Institute of Physics

Mitigation of EPdM by ECRH

- Magnetic dipole experiment CTX
- RF fields suppress rapidly-chirping driven by fast electrons
- Fast electron scattering by rf destroys phase-space structures

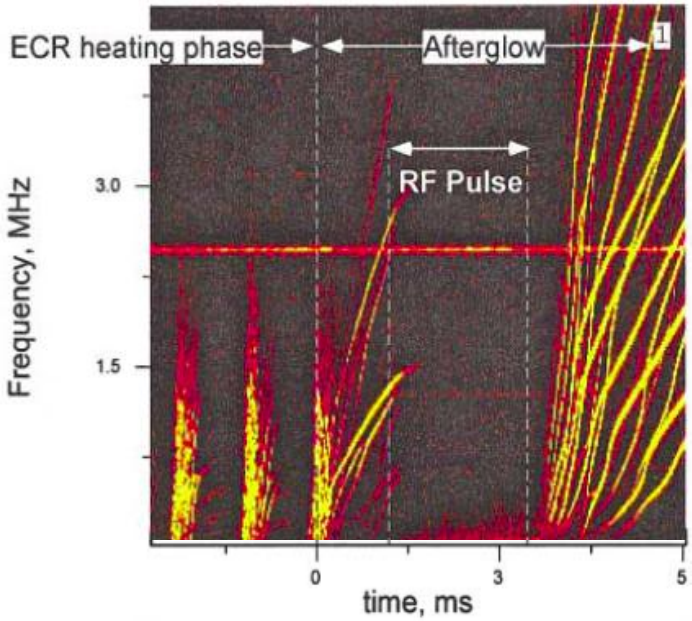

Maslovsky et al. Phys.Rev.Letters 2003

- DIII-D tokamak
- RSAE activity is suppressed when EC heating is deposited near the of the shear reversal radius

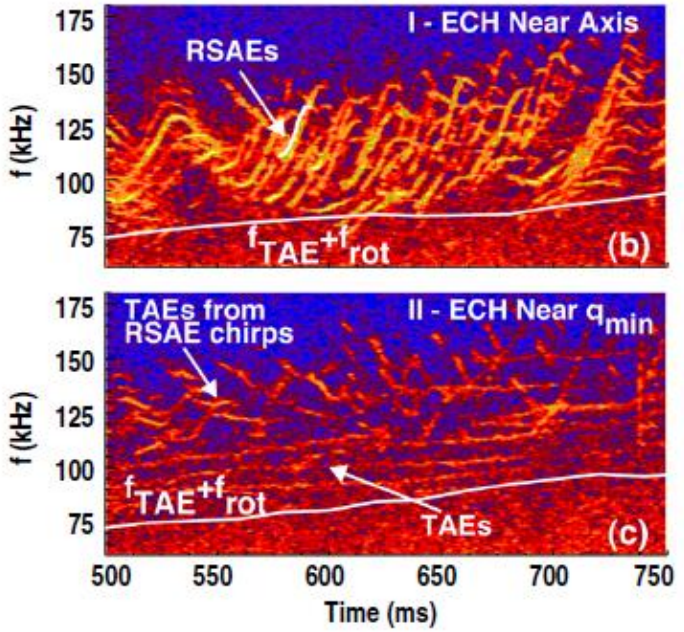

VanZeeland et al. Nucl.Fusion 2009

Mitigation of EPdM by ECCD/ECRH

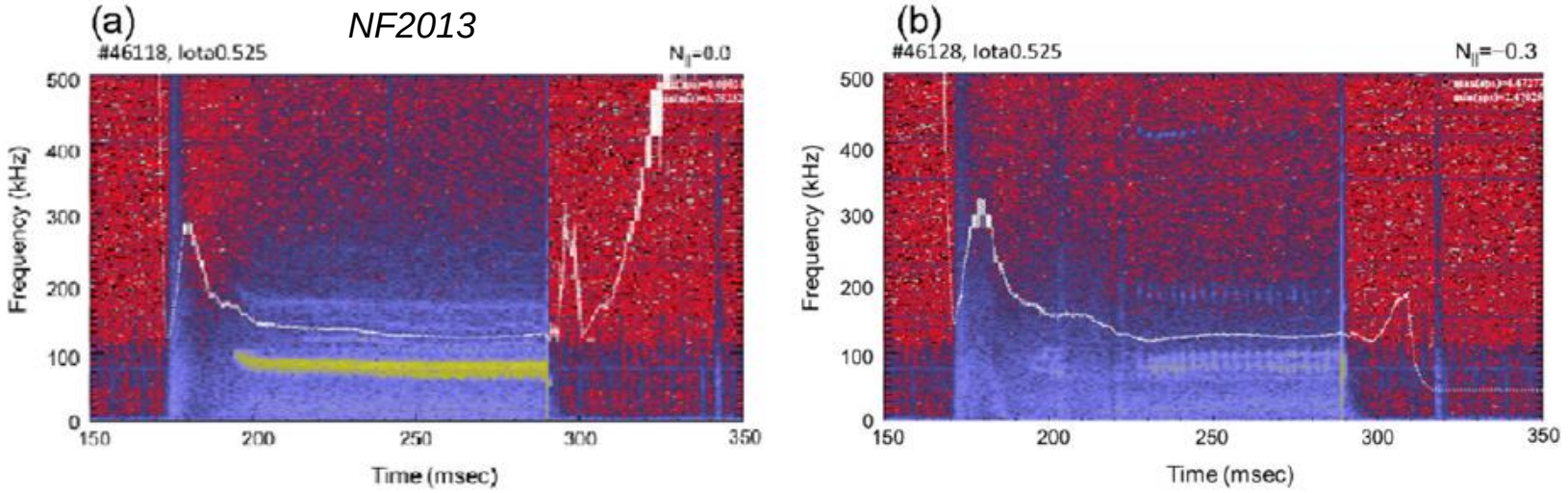

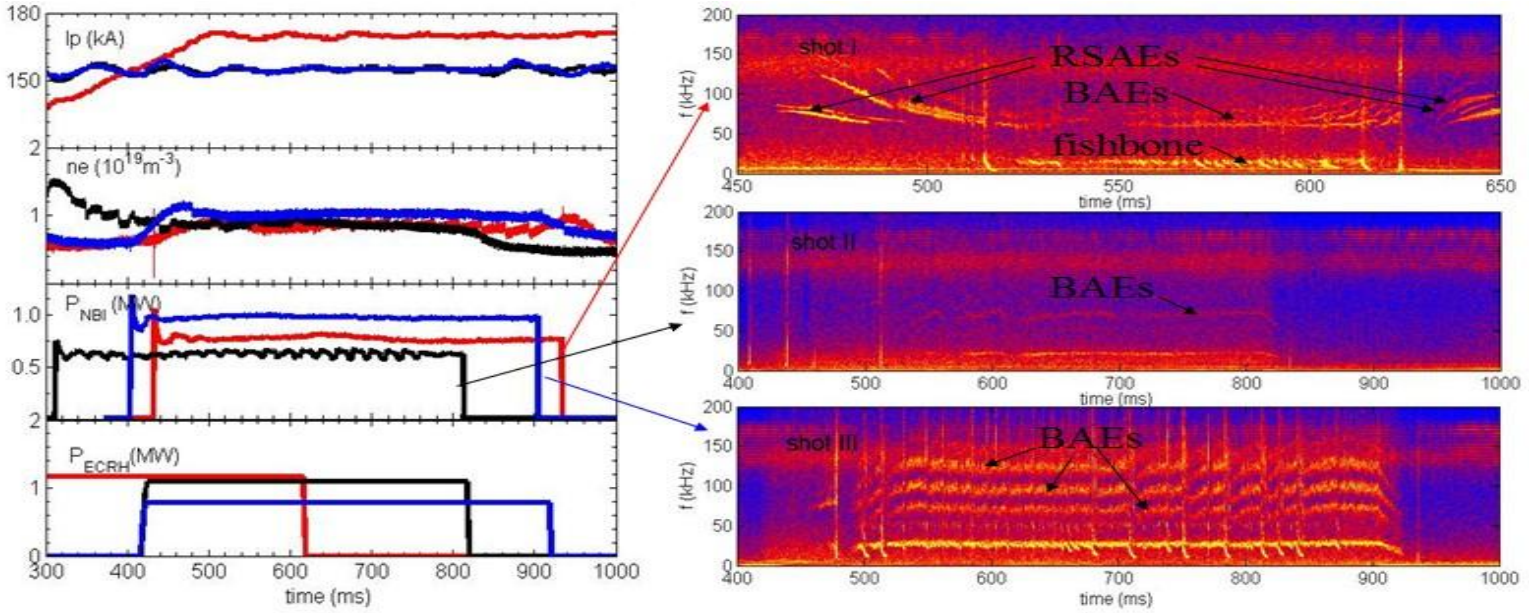

Mitigation of EPdM by ECCD/ECRH

Chen, et al, NF 2018

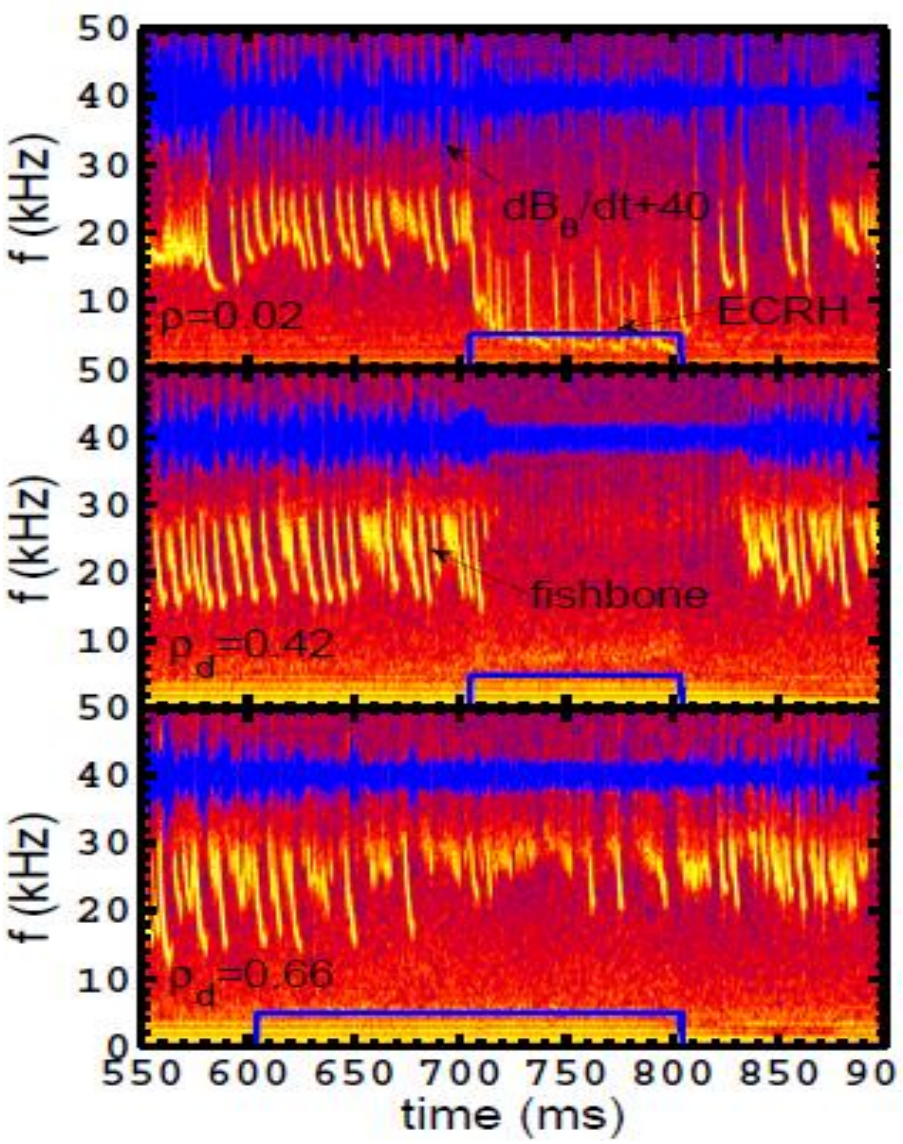

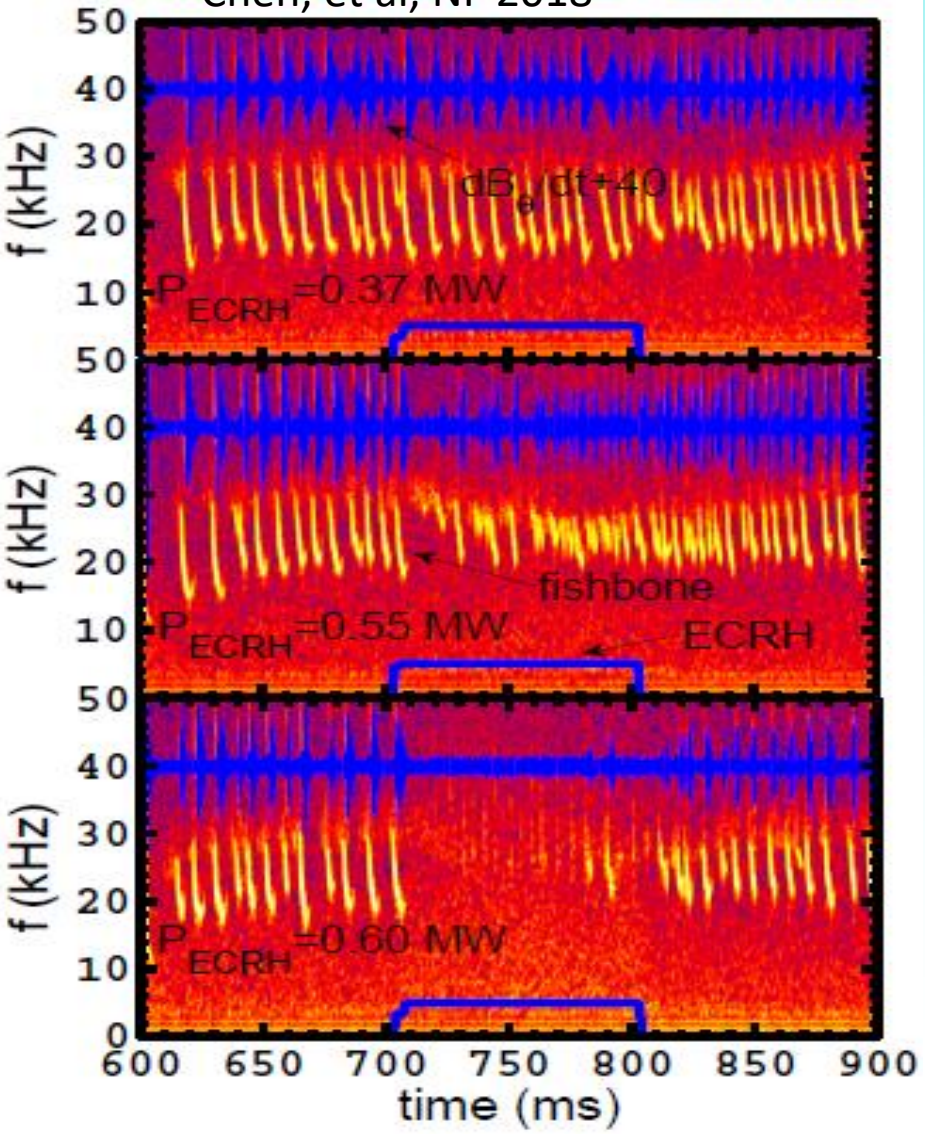

Mitigation of EPdM by RMP

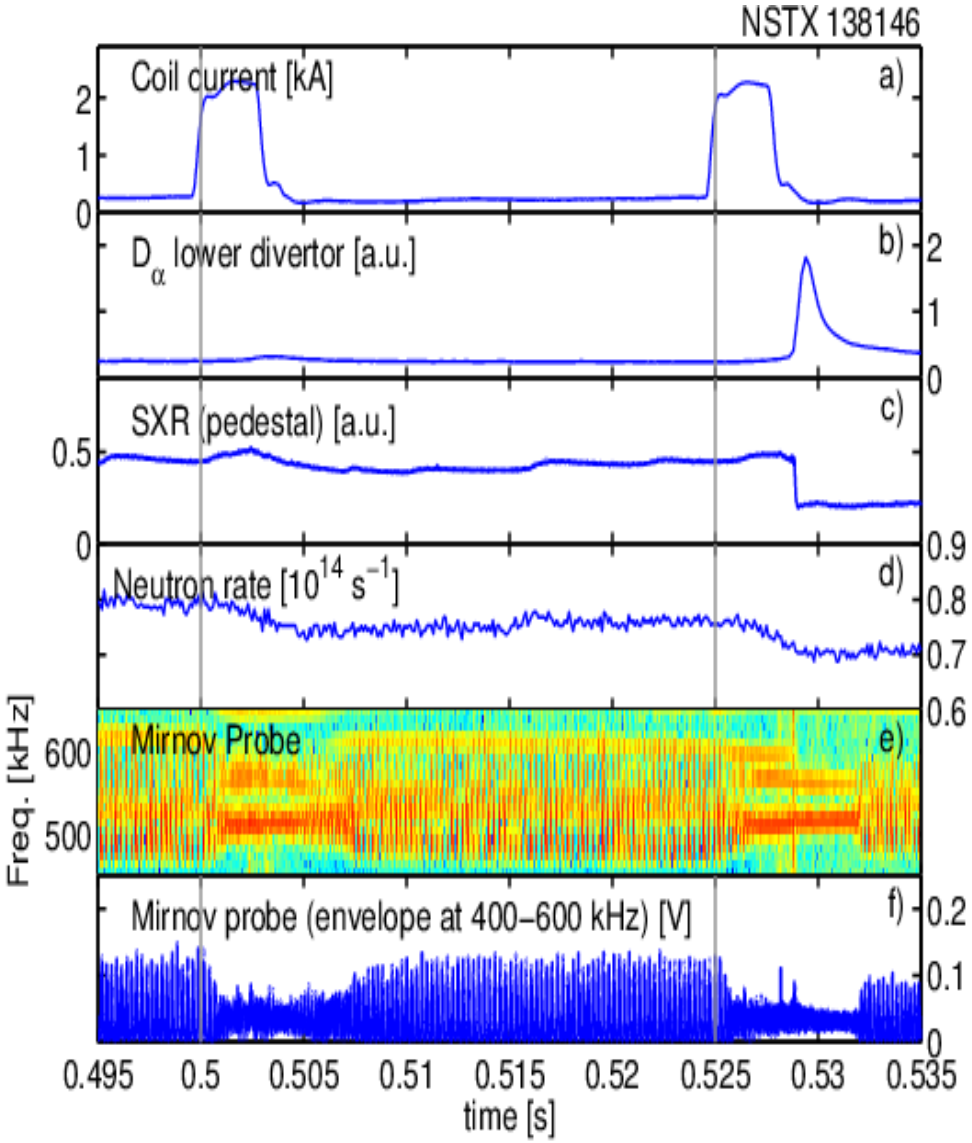

- When n=3 pulse is applied:
  - Burst freq. increased (4→12 kHz)
  - Burst amplitude reduced (x 1/2)
  - Freq. sweep reduced (100 → 40 kHz)
- Fast response (~0.1ms)
  - Precedes neutron drop
  - Effect extends beyond pulse end
- Effect decoupled from ELMs
  - ELM crashes come later
  - Observed in ELM-free phases

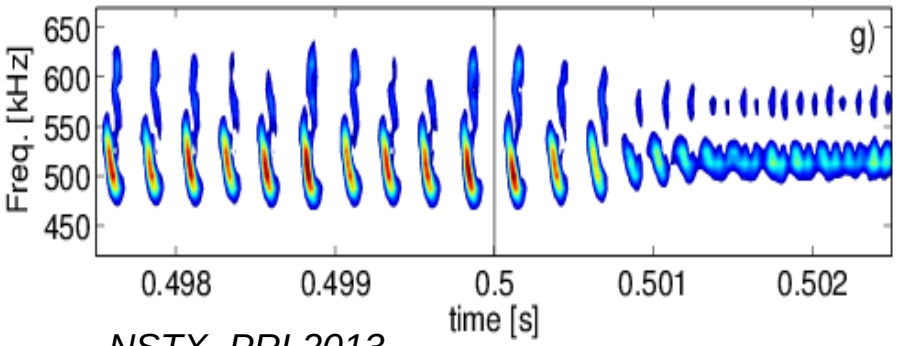

NSTX, PRL2013

MHD control by phase space engineering of EPs

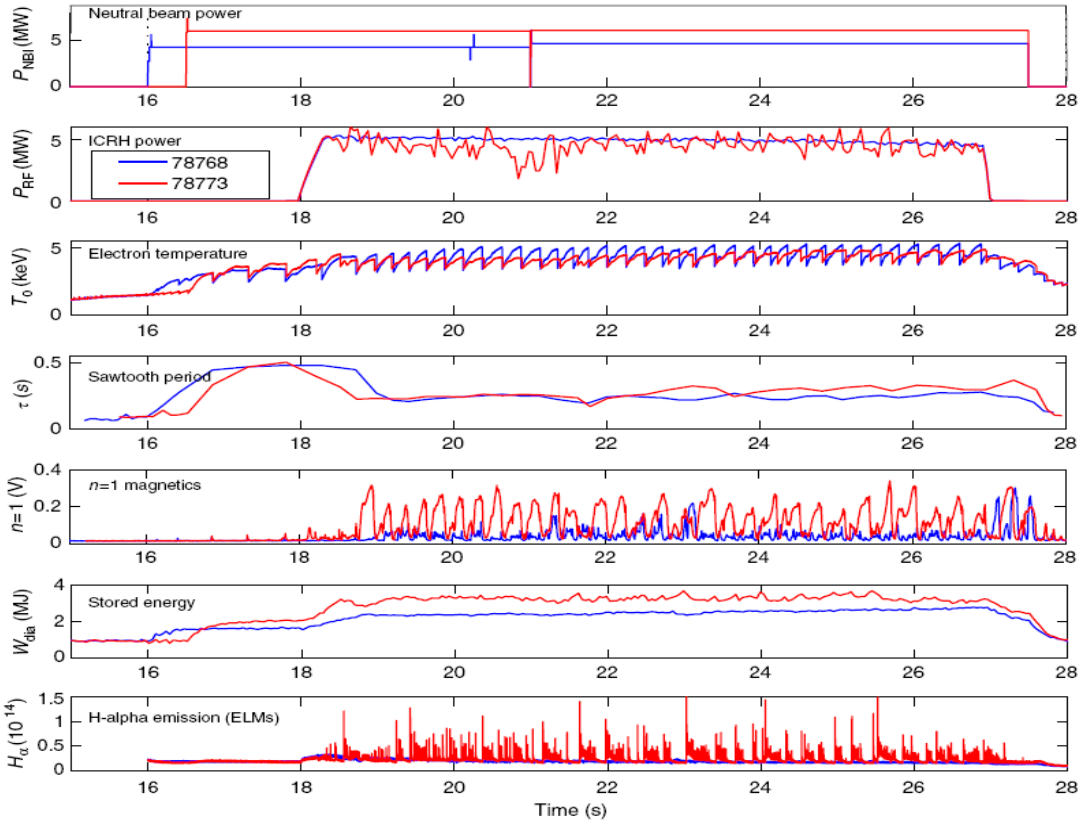

Control of magnetohydrodynamic stability by phase space engineering of energetic ions.

Graves, et.al. Nature Commun. 3:624 (2012)

Demonstration of sawtooth control and NTM avoidance using ICRH in two high-performance JET pulses

The production of energetic ion distribution functions with parallel velocity asymmetry.

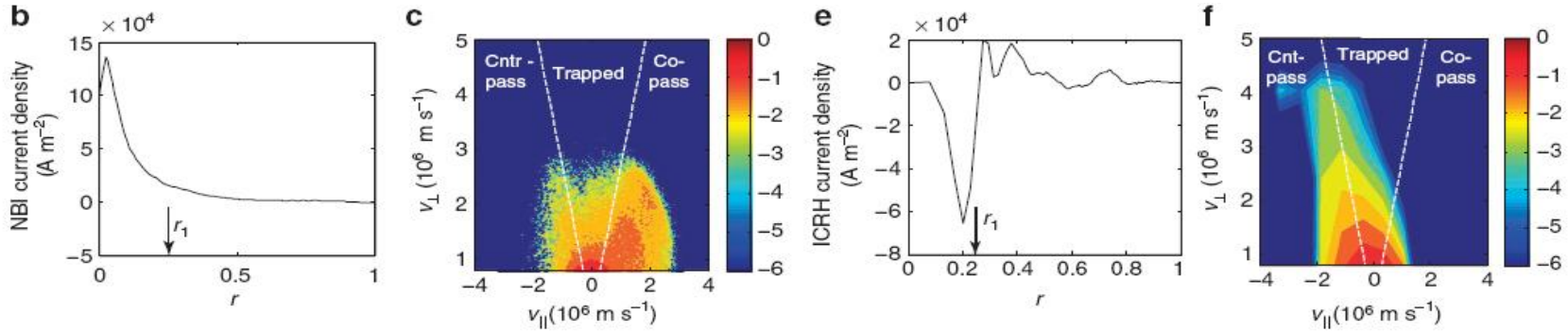

Thank you for your attention!

Your advice and criticism are welcome.

Email: chenw@swip.ac.cn